A NOVEL NF-MBR AND RO FOR WATER RECLAMATION TAY MING FENG 2019

NANYANG TECHNOLOGICAL UNIVERSITY
SINGAPORE

A NOVEL NANOFILTRATION BASED MEMBRANE BIOREACTOR (NF-MBR) AND REVERSE OSMOSIS (RO) FOR WATER RECLAMATION

TAY MING FENG

SCHOOL OF CIVIL AND ENVIRONMENTAL ENGINEERING

2019

A NOVEL NANOFILTRATION BASED MEMBRANE BIOREACTOR (NF-MBR) AND REVERSE OSMOSIS (RO) FOR WATER RECLAMATION

TAY MING FENG

School of Civil and Environmental Engineering

A thesis submitted to the Nanyang Technological University

in partial fulfilment of the requirements for the degree of

Doctor of Philosophy

2019

Statement of Originality

I hereby certify that the work embodied in this thesis is the result of original research, is free of plagiarised materials, and has not been submitted for a higher degree to any other University or Institution.

29/7/2019

Date

Tay Ming Feng

Supervisor Declaration Statement

I have reviewed the content and presentation style of this thesis and declare it is free of plagiarism and of sufficient grammatical clarity to be examined. To the best of my knowledge, the research and writing are those of the candidate except as acknowledged in the Author Attribution Statement. I confirm that the investigations were conducted in accord with the ethics policies and integrity standards of Nanyang Technological University and that the research data are presented honestly and without prejudice.

29/7/2019

.....

Date

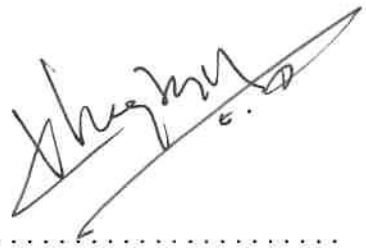

.....

A/Prof Chong Tzyy Haur

Authorship Attribution Statement

This thesis contains material from 2 papers published in the following peer-reviewed journal conferences in which I am listed as an author.

Chapter 4 is published as TAY, M. F., LIU, C., CORNELISSEN, E. R., WU, B. & CHONG, T. H. 2018. The feasibility of nanofiltration membrane bioreactor (NF-MBR)+reverse osmosis (RO) process for water reclamation: Comparison with ultrafiltration membrane bioreactor (UF-MBR)+RO process. *Water Research,* 129, 180-189.

The contributions of the co-authors are as follows:

- A/Prof Chong provided the initial project direction and edited the manuscript drafts.
- I prepared the manuscript drafts. The manuscript was revised by A/Prof Cornelissen and A/Prof Wu.
- I co-designed the study with A/Prof Chong Tzyy Haur and I performed all the laboratory work at the School of Civil and Environmental Engineering and the Singapore Membrane Technology Centre.
- I performed all the experimental work, including bioreactor routine maintenance work, sample preparation, analytical measurement, characterization and system testing.
- Dr Liu Chang prepared the NF membranes for the NF-MBR setup.

Chapter 5 is published as TAY, M. F., LEE, S.K., XU, H.J., JEONG, K.H., LIU, C., CORNELISSEN, E. R., WU, B. & CHONG, T. H. 2018. Impact of Salt Accumulation in the Bioreactor on the Performance of Nanofiltration Membrane Bioreactor (NF-MBR) + Reverse Osmosis (RO) Process for Water Reclamation. *Water Research.*

The contributions of the co-authors are as follows:

- A/Prof Chong provided the initial project direction and edited the manuscript drafts.
- I prepared the manuscript drafts. The manuscript was revised by A/Prof Cornelissen and A/Prof Wu.
- I co-designed the study with A/Prof Chong Tzyy Haur and A/Prof Wu and I performed all the laboratory work at the Singapore Membrane Technology Centre.
- I performed all the experimental work, unless otherwise stated, including bioreactor routine maintenance work, sample preparation, analytical measurement, characterization and system testing.
- Dr Lee Seonki performed the microbial community analysis.
- Dr Xu Huijuan performed the staining procedure for CLSM analysis.
- Dr Jeong Kwanho developed the mathematical model for steady-state salt level prediction.
- Dr Liu Chang prepared the NF membranes for the NF-MBR setup.

29/7/2019

.....

Date

.....

Tay Ming Feng

ACKNOWLEDGEMENTS

First and foremost, I would like to express my deepest gratitude and appreciation to my supervisor, A/Prof. Chong Tzyy Haur. His mentorship, encouragement, patience and support throughout these four years have allowed me to grow both as a researcher and as a person. Thank you for believing in me. I am especially indebted to A/Prof. Wu Bing who have generously shared her immense knowledge and experience in MBR research and carefully guided me throughout the project. I would also like to extend my gratitude to Professor Anthony Fane and A/Prof Cornelissen who have given me invaluable advice for this research project.

My sincere thanks go to Dr. Liu Chang for preparing the tailor-made hollow fiber NF membranes for the NF-MBR project and Dr. Chen Yunfeng for supplying the UF substrate base. Special appreciations go to all the members in the NF-MBR project, Dr. Xu Huijuan, Dr. Lee Seonki, Dr. Jeong Kwanho, Dr. Li xin for the fruitful discussion and productive collaboration. This research work would not be possible without your help, support, and ideas. Special thanks to Dr. Shi Lei, Dr. Ho Jia Shin, Dr. Sim Lee Nuang, Dr. Goh Shuwen, Dr. Stanislaus Suwarno for their help, guidance, and support whenever I ran into difficulties in experiments, analysis and had doubts about my research. Special thanks to my FYP students, Albert Ardy Gunawan, Oh Jia Hao, Neo Puay Lin for their assistance in experimental work. I am glad to have my office and lab mates, Mr Wenqiang Yin, Ms Bao YuePing and Mr Daniel Ng, thanks for the countless lunch-time discussions and encouragement. I would also like to thank all the colleagues, staffs and my friends for their help and providing a great and friendly atmosphere in Singapore Membrane Technology Centre (SMTC).

Finally, I must express my very profound gratitude to my wife and my family for providing me with unfailing support and encouragement throughout my study and through the process of researching and writing this thesis. This accomplishment would not have been possible without you. Thank you.

TABLE OF CONTENTS

SUMMARY

In this study, a novel nanofiltration membrane bioreactor (NF-MBR) was developed and integrated with the reverse osmosis (RO) process for water reclamation. The underlying motivation of using NF-MBR as a pre-treatment to the RO process is to improve the RO feed quality and subsequently increase the RO recovery ratio. However, technological challenges such as low permeate flux, membrane stability, salinity build-up and membrane fouling are the key barriers to the development of NF-MBR. The study focused on addressing the important issues pertaining to membrane performance and evaluating the feasibility of the NF-MBR+RO process.

The use of a glutaraldehyde (GA) crosslinked layer-by-layer polyelectrolyte low-pressure hollow fiber NF membrane has overcome the inherent issues of low permeate flux and membrane stability in the NF-MBR system. It was demonstrated that the membrane could achieve a constant flux of 10 L/m^2h at pressure ~2 bar and produce superior MBR permeate quality consistently in a long term experiment treating real municipal wastewater. Higher organic removal was observed in the NF-MBR than the ultrafiltration MBR (UF-MBR) due to the extended retention time that allows the enhanced biodegradation of the retained organics in the bioreactor. The improved MBR permeate quality has led to ~3.7 times decrease in the RO fouling rates as compared to the UF-MBR+RO process. In addition, it was found that the cake layer fouling that caused the cake-enhanced osmotic pressure (CEOP) effect contributed predominantly to the transmembrane pressure (TMP) increase in the NF-MBR. With the molecular weight cut off (MWCO) of < 500 Da, irreversible pore fouling was marginal for NF membrane fouling, therefore, the membrane permeability was highly reversible by physical cleaning as compared to MF/UF membranes.

The impacts of salt accumulation, through adjusting the solids retention time (SRT), in the bioreactor on the bioprocess as well as membrane performance of a high retention NF-MBR and subsequent RO process for water reclamation was delineated. Salt accumulation as an inherent issue of high-retention MBRs (HR-MBRs) often causes

undesirable consequences to the biological process and membrane operation. In the NF-MBR system applied in this study, the negative impact arisen from the accumulation of NaCl was alleviated by allowing the passage of monovalent ions, particularly NaCl. The build-up of salts (i.e., Ca, Mg, PO_4) is a function of SRT, hydraulic retention time (HRT) and membrane rejection. Despite the accumulation of salts, both NF-MBRs at SRT of 30 and 60 d, achieved (i) similar biodegradation efficiency; (ii) excellent organic removal (>97%); and (iii) ammonia removal (>98%). Extending the SRT could improve the microbial bio-flocculation capability, but did not influence the microbial activity, viability, and community structure. However, more severe membrane fouling was observed in the NF-MBR with elevated salt levels, which was attributed to the greater formation of calcium phosphate scale and Ca-polysaccharides complex (i.e., irreversible fouling layer) as well as the CEOP effect. Although both NF-MBRs produced comparable quality of permeate, a higher RO membrane fouling rate was observed when permeate of NF-MBR with SRT at 60 d was fed to the RO system, implying organic compositions in NF-MBR permeate may influence RO performance.

NF-MBR is an effective pretreatment that improves RO feed qualities (~86% lower dissolved organic matter) and subsequently facilitates the high recovery RO process at 90% recovery ratio. The outcomes of this study showed that the calculated energy consumption of the NF-MBR+RO system at 90% recovery was comparable to that of the UF-MBR+RO at 75% recovery. The thesis substantiated the feasibility of a novel NF-MBR+RO system for high recovery water reclamation.

The findings of this study provide a better understanding of the fouling mechanisms and fouling control strategies in the NF-MBR system and offer useful information for the development of NF-MBR+RO system for high recovery water reclamation.

LIST OF PUBLICATIONS

Journals

1. **Tay, M. F.**, Liu, C., Cornelissen, E. R., Wu, B. & Chong, T. H. 2018. The feasibility of nanofiltration membrane bioreactor (NF-MBR)+reverse osmosis (RO) process for water reclamation: Comparison with ultrafiltration membrane bioreactor (UF-MBR)+RO process. *Water Research*, 129**,** 180-189.
2. **Tay, M. F.**, Lee, S.K., Xu, H.J., Jeong, K.H., Liu, C., Cornelissen, E. R., Wu, B. & Chong, T. H. 2018. Impact of Salt Accumulation in the Bioreactor on the Performance of Nanofiltration Membrane Bioreactor (NF-MBR) + Reverse Osmosis (RO) Process for Water Reclamation. *Water Research*.

Conference

Tay, M. F., Liu, C., Cornelissen, E. R., Wu, B. & Chong, T. H. 2018. A nanofiltration membrane bioreactor (NF-MBR)+reverse osmosis (RO) process for water reuse, Euromembrane 2018, 9 - 13 July 2018, Valencia, Spain (Oral Presentation).

LIST OF TABLES

LIST OF FIGURES

LIST OF ABBREVIATION & SYMBOLS

c_{in}	Influent salt concentration
c_{ml}	Mixed liquor salt concentration
CECP	Cake enhanced concentration polarization
CEOP	Cake enhanced osmotic pressure
CF	Concentration factor
CLSM	Confocal laser scanning microscopy
CP	Concentration polarization
DOC	Dissolved organic carbon
EDX	Energy-dispersive X-ray spectroscopy
EPS	Extracellular polymeric substances
F/M	Food to microorganism ratio
g	Gravitational field strength
H	Water head
HR-MBR	High retention membrane bioreactor
HRT	Hydraulic retention time
J	Flux
LC-OCD	Liquid chromatography – organic carbon detection
LMW	Low molecular weight
ICP	Internal concentration polarization
MBR	Membrane bioreactor
MD	Membrane distillation
MF	Microfiltration
MLSS	Mixed liquor suspended solids
MLVSS	Mixed liquor volatile suspended solids
MWCO	Molecular weight cut-off

NF-MBR	Nanofiltration membrane bioreactor
OLR	Organic loading rate
P	Pressure
P_p	Pump energy demand
Q_{in}	Influent flow rate
Q_{out}	Permeate flow rate
Q_w	Sludge wasting rate
R_c	Hydraulic resistance of the cake layer
R_m	Hydraulic resistance of virgin membrane
R_p	Hydraulic resistance attributed to pore blocking mechanism
R_T	Total hydraulic resistance
SEM	Scanning electron microscopy
SMP	Soluble microbial products
SOUR	Specific oxygen uptake rate
SRT	Solids retention time
T	Temperature
TDS	Total dissolved solids
TOC	Total organic carbon
TrOC	Trace organic contaminant
UF	Ultrafiltration
V	Reactor volume

Greek symbols

d	Thickness
e	Porosity
h	Viscosity
μ	Solvent viscosity
η	Rejection
ρ	Pumped fluid density
ξ	Pump efficiency

Chapter 1

Introduction

1.1 Background

Freshwater is the fundamental resource to ensure public health, food security, economic development and human well-being. The United Nations (UN) has highlighted human right to water in many global events and urged the need to commercialize innovative technology for the provision of safe, clean, accessible, and affordable drinking water for all (UNGA, 2010). Global population growth, rapid urbanization and growing economic activity have put major cities in the world under the pressure of water scarcity. The United Nations claimed that the world would face a 40 percent shortfall in potable water in the coming 15 years and suggested that maximize reuse could be the major contributor to universal access to water (WWAP, 2014). While seawater desalination seems to be a direct and attractive option with the recent advance development and competitive cost of Reverse Osmosis (RO) membrane, water reclamation from wastewater remains to be the more economically viable option mainly due to its lower energy requirement (Bartels et al., 2005a).

The “toilet to tap” concept has long been accepted in Singapore since the Public Utility Board (American Public Health et al.), the Singapore national water agency first introduced it to its citizens in 2001. NEWater, high-quality reclaimed water produced from treated wastewater is the pillar of sustainable water resource management in Singapore as it supplies up to 30 percent of the national water demand (Chew et al., 2011). In the first stage of NEWater process, the treated effluent from activated sludge process is filtered through Microfiltration (MF) or Ultrafiltration (UF) (Wang et al.) membrane to filter out solids and particles in microns such as colloidal particles and pathogens. The filtrate which contains only soluble organics and salts is then subjected

to Reverse Osmosis (RO) membrane that will only allow water molecules and negligible amount of soluble salts and organics to pass. At this stage, the produced water is of high-quality and potable as it is free from bacteria, viruses, heavy metals, sulphate, nitrate, chloride and harmful organics. The third stage of ultra-violet disinfection is to ensure all possible contaminations of pathogens in the water pipeline are eliminated (Kent et al., 2011).

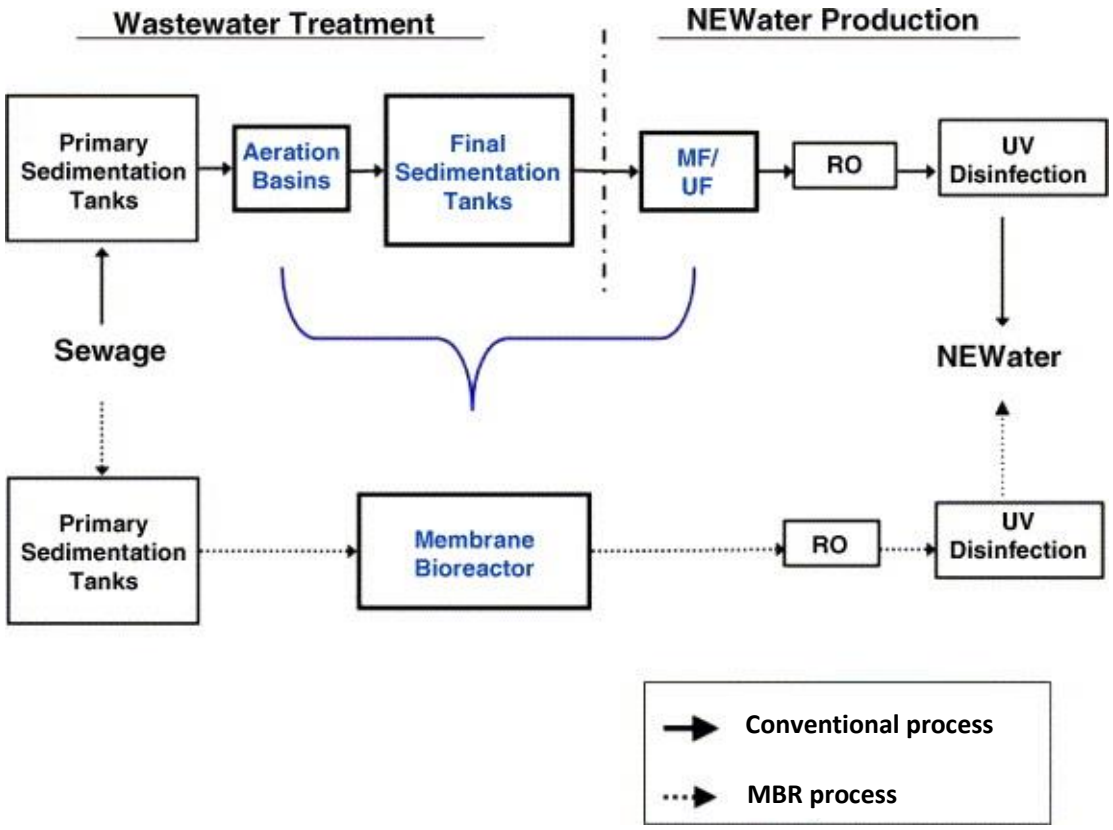

Figure 1-1. Schematic diagram of NEWater process with conventional AS process and MBR process (Qin et al., 2006).

While the activated sludge process (ASP) is commonly adopted in the wastewater secondary treatment prior to the NEWater process, membrane bioreactor (MBR) has been successfully employed in treating municipal wastewater and produce high-quality effluent through membrane filtration (Tam et al., 2007). The MBR technology has become a realistic alternative to replace the conventional ASP due to its advantages in

terms of better effluent quality, smaller footprint, long solids retention time (SRT) that facilitates the proliferation of slow growing bacteria such as nitrifiers, reduced sludge production and the possibility of operating at higher biomass concentrations (Yamamoto, 2001). The replacement of conventional ASP process with the MBR technology as the secondary treatment coupled with RO process results in an integrated MBR-RO process as shown in Figure 1-1. The MBR-RO treatment scheme has been successfully adopted in pilot scale water reclamation plants in Singapore for the production of direct potable water (Qin et al., 2006). MBR plays an important role in the complete removal of biological agents in the mixed liquor through membrane separation and producing high-quality secondary effluents which will be fed to the downstream RO system. However, a typical MBR process has its limitation in removing the inorganic scalants such as calcium phosphate and silica and soluble organics in municipal wastewater. In addition, the availability of carbon source in the RO feed could lead to biofilm development on the membrane surface and result in biofouling which significantly deteriorates the performance of RO process (Ridgway et al., 1985). The presence of these compounds in the MBR permeates causes serious membrane fouling of the downstream RO process which leads to unwanted consequences such as flux decline, increase in the operating pressure, more frequent membrane cleaning, and eventually increase the water production costs.

In view of the challenges in the current MBR-RO process, a novel nanofiltration-based membrane bioreactor (NF-MBR) combining high retention NF membrane and bioreactor was introduced in this thesis to remove low molecular weight organic matter and scale-forming divalent ions in the MBR effluents. NF is a mature membrane process with many pilot and full-scale applications. With the recent development of NF membranes that are fouling resistant, low cost, chemically and biologically stable, and highly permeable, the NF-MBR shows a great potential to replace the conventional MBR as the secondary treatment process to produce high-quality effluent (Mohammad et al., 2015, Luo et al., 2014).

1.2 Problem statement

Membrane fouling in RO is the major obstacle that hindered the widespread application of MBR-RO process for potable water reuse (Greenberg et al., 2005). Complex fouling in the RO process associated soluble organic compounds and calcium phosphate due to poor rejection properties of MF/UF in the MBR towards these compounds has limited the practical recovery level of existing MF/UF-MBR+RO for water reclamation at 75 to 85% (Wetterau et al., 2011). Fouling control and cleaning method is very limited for the thin-film-composite (TFC) RO membrane in spiral wound membrane configuration. Clean-in-place (CIP) which is the common practice for RO cleaning, not only incurs high maintenance cost but also lead to process downtime and higher water production cost. To further improve the quality of the MBR permeates, there is a growing interest in integrating the high retention membrane separation processes, such as membrane distillation (MD), forward osmosis (FO) and nanofiltration (NF) with biological reactor to form MD-MBR, FO-MBR and NF-MBR configurations, respectively (Luo et al., 2017). Such high retention MBRs (HR-MBRs) have enhanced biodegradation of refractory organics due to prolonged residence time as well as the effective rejection of inorganic compounds i.e. Ca^{2+}. However, there remain several technical challenges in HR-MBRs, such as salt accumulation, low permeate flux (i.e. < 10 L/m^2 h), and membrane stability (Luo et al., 2014, Lay et al., 2010, Luo et al., 2016). Specifically, in the FO-MBRs, the setbacks include (i) reversed salt diffusion effect that results in the loss of draw solutes and requires constant topping up of draw solutes to maintain the flux; (ii) both salinity increase in the bioreactor due to accumulation and concentration decrease of the draw solution due to solute diffusion would reduce the net driving force for water permeation, thus causing the flux to decline over time; (iii) elevated salts could increase the soluble microbial products (SMP) and extracellular polymeric substances (EPS) in the mixed liquor that cause greater membrane fouling (Luo et al., 2017); (iv) requires additional steps (i.e. RO or other processes) to separate the draw solution and water. More importantly, the combined FO-MBR and RO process cannot reduce the energy requirement for water production due to the trade-off between FO and RO

processes (Shaffer et al., 2015). While in MD-MBR, the requirement of waste heat and membrane wetting are still the bottleneck.

Compared to MD-MBRs and FO-MBRs, NF-MBRs are more feasible for water reuse purposes. This is attributed to the facts that (i) NF is a pressure driven process similar to MF/UF, which is less complicated compared to FO or MD; (ii) NF has lower monovalent salt rejection, thus lower salt accumulation in the bioreactor; (iii) NF application for surface and groundwater treatment is rather mature with a large number of full-scale installations. Despite the fact that the energy consumption of the NF-MBR is expected to be higher than that of the conventional MBR due to the higher operating pressure required by the NF membrane, with the improved MBR permeates, the RO process could be potentially operated at higher recovery rates with less fouling. Since the RO process is the most energy-intensive unit in the entire water reclamation scheme, the additional energy required for the NF-MBR operation is hypothesized to be offset by the energy saving from the downstream RO process, therefore, resulting in a more sustainable MBR-RO process for potable water reuse.

In spite of the great potential of NF-MBRs, there are only seven existing studies on the NF-MBR (Choi et al., 2002, Choi et al., 2006, Choi et al., 2007b, Golbabaei Kootenaei et al., 2014, Phan et al., 2016). In previous attempts on NF-MBR, low permeate flux of 0.042 L/m^2h or equivalent to 0.5 $L/m^2h \cdot bar$ was attained with a commercial cellulose acetate NF (Choi et al., 2002). The low permeability or high operating pressure required to obtain decent flux has made the NF-MBR less attractive. To bring NF-MBR towards commercialization, it is essential to improve the operating flux up to at least 10 L/m^2h (LMH) so that it is comparable to the conventional MBR (Meng et al., 2009).

In view of the above, the use of a novel low-pressure hollow fiber NF membrane, previously developed by the Singapore Membrane Technology Centre (SMTC) for water softening application, may overcome this challenge. The novel NF membrane possesses a positively charged thin film selective layer with a pure water permeability of ~ 17 $L/m^2h \cdot bar$, molecular weight cut off (MWCO) of < 500 Da, and rejections of Mg^{2+} and Ca^{2+} ~ 90% and Na^{+} < 15% (Rajabzadeh et al., 2014, Liu et al., 2015). Most of the

commercial membranes in the market require operating pressures of > 5 bar, but this membrane only requires < 2 bar to achieve similar performance. The key to achieving such a low operating pressure condition lies in the very low rejection of Na^+ ion while maintaining high rejection of the divalent ions. Indeed, the NF membrane should reduce some degree of burdens faced by the RO membrane as the final treatment for water reuse purposes. However, high rejection of divalent cations through NF membrane may facilitate inorganic fouling and may cause adverse effects on microbial activity in the bulk suspension of NF-MBR. Other technological challenges such as membrane stability and low permeate flux persist and continue to hinder the development of this technology (Choi et al., 2007a, Phan et al., 2016). These technological challenges need to be carefully investigated before NF-MBR can become a mature technology to replace conventional MBR as the secondary treatment process.

1.3 Objectives and scope

The overall objective of this thesis is to incorporate the NF-MBR into the MBR-RO process as the secondary treatment for a more sustainable water reclamation process for potable water reuse. There are some key aspects of the technology mentioned above that need further investigation and optimization. In addition, investigation on the impact of NF-MBR as a pretreatment on the fouling of RO process is mandated in this thesis to provide a more holistic assessment of the whole NF-MBR+RO process. The following presents the specific objectives of this thesis and the breakdown of the thesis structure:

1) Critically review the available literature on the NF-MBRs and MBR-RO process and identify key issues pertaining to NF-MBR+RO process (Chapter 2);
2) Develop general materials and methods for the main body (i.e., Chapter 4, 5, and 6) of the thesis (Chapter 3);
3) The feasibility of a stable-state nanofiltration membrane bioreactor (NF-MBR) in the MBR-RO process for long term operation. The performance of the NF-MBR will be critically assessed with an ultrafiltration membrane bioreactor (UF-MBR) and RO process as a baseline for comparison (Chapter 4);

4) A systemic study of organic fouling in the UF-MBR+RO and NF-MBR+RO process (Chapter 4);
5) Investigate the long-term effect of salt accumulation on the biomass characteristics, membrane fouling potential and foulants properties in the NF-MBR with different SRTs (Chapter 5);
6) The fouling control and cleaning methods for the stable long-term operation of the NF-MBR (Chapter 5);
7) The effect of NF-MBR as a pretreatment on the RO fouling for high recovery water reclamation (Chapter 6).

1.4 Significance of the research

The significant outcomes of this research are enumerated below:

(i) The study demonstrates the feasibility of a novel NF-MBR+RO system for high recovery water reclamation;

(ii) A fundamental understanding is provided on the fouling mechanisms of combined organic, inorganic and biofouling in the NF-MBR system and RO system;

(iii) The study highlights the critical challenges faced by the NF-MBR and offers useful information for the development of NF-MBR technology for water reclamation.

Chapter 2

Literature Review

2.1 MBR technology for water reclamation

2.1.1 Introduction to MBR

MBR is a technology that integrates both biological reaction process and membrane separation process. MBR is a generic term referring to the synergetic coupling of membrane separation with bioreactor systems (fermenter or enzymatic ones) with the aim of selectively separating the biocatalysts (microorganisms, enzymes, or antibodies) from reaction substrates or products. Simultaneous biological reaction and membrane filtration allow selective removal of the desired compounds. The porous membranes such as the MF/UF membranes used by most of the conventional MBRs can be used as barriers to particulate matter i.e., biomass, therefore, the effluent quality is not restricted by the settleability of the biomass.

The maturity of MBR systems in recent decades shows that MBR can be a reliable alternative to the conventional activated sludge (CAS) treatment processes in wastewater treatment technology. Many successful pilot studies have showcased the advantages of MBR technology for water reclamation over conventional treatment methods as presented in the followings (Qin et al., 2006, Yamamoto, 2001):

- Better effluent quality (Effluent is bacteria free and quality no longer depending on the settleability of the activated sludge);
- Smaller footprint of the treatment facility (MBR replaces the aeration basins, final sedimentation tanks and MF-UF filtration prior to RO);
- Proliferation of slow growing bacteria such as nitrifiers (Complete separation of the biomass and long SRT operation);

- Reduced sludge production and the possibility of operating at higher biomass concentrations.

With the decreasing membrane price over the past two decades, MBR technology has become a more attractive solution for water reclamation (Krzeminski et al., 2016). Furthermore, significant progress has been accomplished in the design and process optimization over the past two decades to reduce the capital and operating expenses of MBR plants. According to Krzeminski and co-workers, the global market for MBRs was steadily increasing and registering a compound annual growth rate of 12.8% in the period 2014–2019 due to increasing demand for wastewater treatment.

2.1.2 MBR Configurations

There are typically two configurations for the MBR system: external (recirculated or side-stream) and submerged (immersed or integrated) as shown in Figure 2-1.

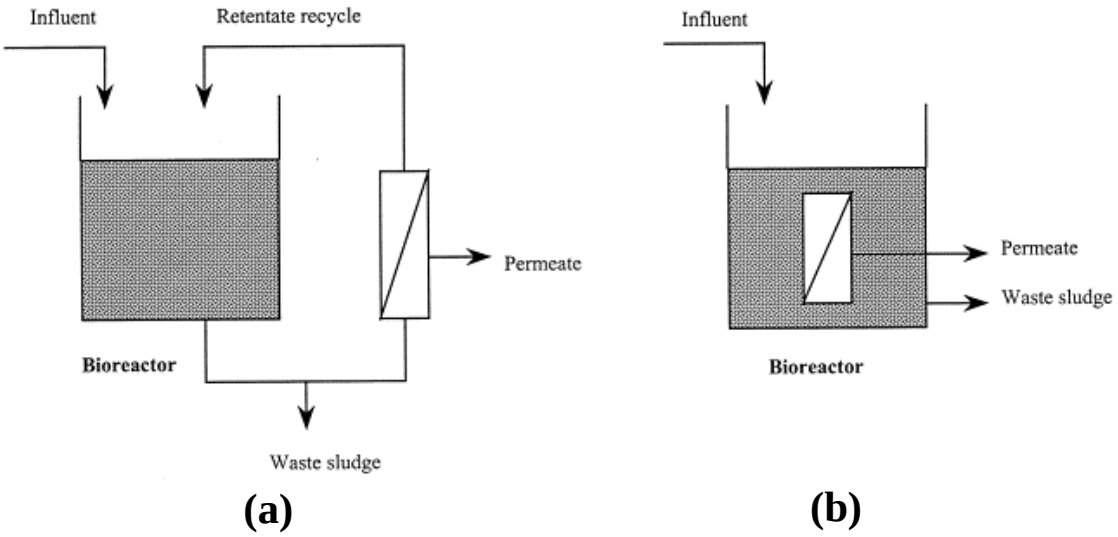

Figure 2-1. MBR configuration:(a) side-stream MBR with external membrane unit with concentrate recirculated back to bioreactor; (b) submerged MBR: membrane unit integrated into the bioreactor.

The side-stream configuration consists of an external membrane connected to the bioreactor. The mixed liquid is channeled through the membrane module with a high crossflow velocity tangentially to the membrane surface and the concentrate is recycled

back to the bioreactor. The high-velocity crossflow creates a shearing force to disturb and reduce the formation of cake layers on the membrane surface, hence, leads to lower membrane fouling.

Submerged MBRs were introduced in 1989 by Professor Yamamoto for water treatment with the idea of reducing energy costs (Yamamoto et al., 1989). He proposed the concept of immersing the hollow fiber membranes either directly into the suspension to be filtered or in a separate membrane filtration tank. The permeation through the membrane was operated at a lower transmembrane pressure (TMP) compared to side-stream configuration. One of the major advantages of this configuration is the compared with its counterpart MBRs due to the elimination of energy required for pumping (Yamamoto et al., 1989). Also, fouling control can be implemented by providing air bubbling to create a scouring effect to the submerged membrane surface. Nevertheless, it has the drawback of being difficult to operate at high operating pressure especially when particles or cells concentrations are high. Additionally, the lower operating pressure of submerged MBR translates to a lower flux operation which implies a higher membrane area is required to achieve targeted water productivity, therefore, results in higher associated membrane investment and maintenance cost (Gander et al., 2000). Although side-stream configuration is more energy intensive, for the more difficult feeds and operation under higher flux, it may be the only option that works reliably (Pearce, 2008).

Despite the fact that the submerged system operates more cost effectively than the side-stream system, previous attempts using the submerged system has shown that the extremely low permeate flux, i.e., 0.042 L/m^2h and large membrane area required by the submerged system has made the NF-MBR less attractive (Choi et al., 2002, Choi et al., 2006). More recent studies on NF-MBR have adopted the side-stream configurations with ceramic multi-tubular membrane module to increase the water productivity of NF-MBR (Zaviska et al., 2013, Phan et al., 2016). In addition, the mixed liquor in the NF-MBR could contain much higher concentrations of organic and inorganic content due to the high rejection properties of the NF membranes used, thus, higher operating pressure

is essential to maintaining a stable-state operation for research purposes. Therefore, side-stream configuration was adopted in the NF-MBR system described in the subsequent chapters.

2.1.3 Moving-bed membrane bioreactor (MBMBR)

The principle of MBMBR is to employ bio-carriers with attached-growth biomass that are able to move freely in the reactor with the agitation provided by aeration or mechanical mixing. With the aid of bio-carriers, washout of the biomass could be reduced, allowing development of specific slow-growing microorganisms such as the nitrifiers. Many studies have reported the advantages of the MBMBR over the conventional MBR especially its positive effect on fouling reduction (Jin et al., 2013, Chen et al., 2016). The following summarizes the reasons MBMBR was adopted in this research work:

(i) Reduced concentration of mixed liquor suspended solids (MLSS) that is compensated by the attached growth biomass (potentially reduce membrane fouling by the biomass)(Palmarin and Young, 2019);

(ii) Cultivation of more diverse and populated microbial community (for nitrification and biodegradation of re calcitrant organics) (Yang et al., 2009, Jamal Khan et al., 2011);

(iii) Simultaneous nitrification and denitrification (as a results of DO level gradient in the attached growth biofilm)(Puznava et al., 2001);

(iv) Improved physio-chemical properties of the mixed liquor suspension for better membrane filtration (reduced biopolymers especially polysaccharides in the membrane foulants) (Chen et al., 2016, Palmarin and Young, 2019).

2.1.4 Fundamentals of membrane fouling in MBR

Membrane fouling is defined as the undesired deposition of EPS, inorganic precipitates, SMP, and microbial cells on the membrane surface which causes a buildup of TMP (constant flux operation mode) or a reduction of permeate flux (constant pressure

operation mode). In addition, membrane fouling can result in lower system efficiency, higher membrane replacement costs, and higher energy requirement for sludge recirculation or gas scouring (Lin et al., 2013). It is one of the major obstacles that hinders the speed of commercialization of MBRs in real world.

2.1.3.1 Fouling mechanisms

Membrane fouling mechanisms are generally characterized into pore blocking by colloidal particles, adsorption of soluble compounds and biofouling, cake layer formation, consolidation of the cake layer and the spatial and temporal changes of the foulants composition during the long-term operation (Hwang et al., 2008). Pore plugging and pore blocking mechanism may occur depending on the sizes of the foulants. Foulants with sizes smaller than the membrane pores such as soluble organics and small colloids cause pore plugging whereas foulants with larger sizes such as sludge flocs, large colloids and particulates tend to block the membrane pores and lead to cake layer formation (Meng et al., 2009). If cake layer formation occurs before pore blocking, it is possible that the cake layer formed on the membrane surface protects the membrane surface and pores from irreversible fouling (Bae and Tak, 2005).

Some empirical models were proposed to explain the relation between sludge characteristics or operating conditions and membrane fouling. These empirical models are helpful for the understanding and mitigation of membrane fouling in MBRs. Filtration resistance model as shown in Figure 2-2 is the basic model to describe the relation among resistance experienced during flux, J with sludge viscosity, μ and transmembrane pressure, ΔP (Shimizu et al., 1993):

$$J = \frac{\Delta P}{\mu}\left(\frac{1}{R_m + R_p + R_c}\right) \qquad \text{Eq. 2-1}$$

where ΔP is the TMP and μ is solvent viscosity, R_m is the hydraulic resistance of virgin membrane, R_p is hydraulic resistance attributed to pore blocking mechanism, and R_c is the hydraulic resistance of the cake layer formed on the membrane surface.

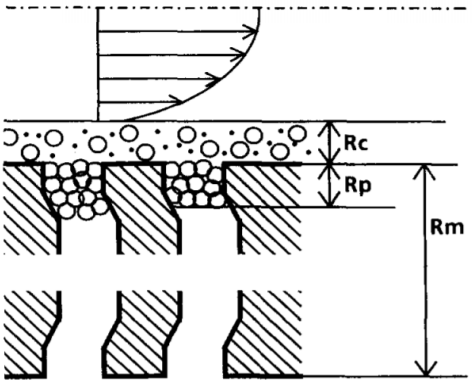

Figure 2-2. Filtration resistance model (Shimizu et al., 1993).

MBR operated under constant flux mode has a three-stage TMP profile consists of the first TMP jump (stage 1) followed by a gradual increase in TMP (stage 2) and a final TMP jump (stage 3) as shown in Figure 2-3 (Cho and Fane, 2002, Zhang et al., 2006).

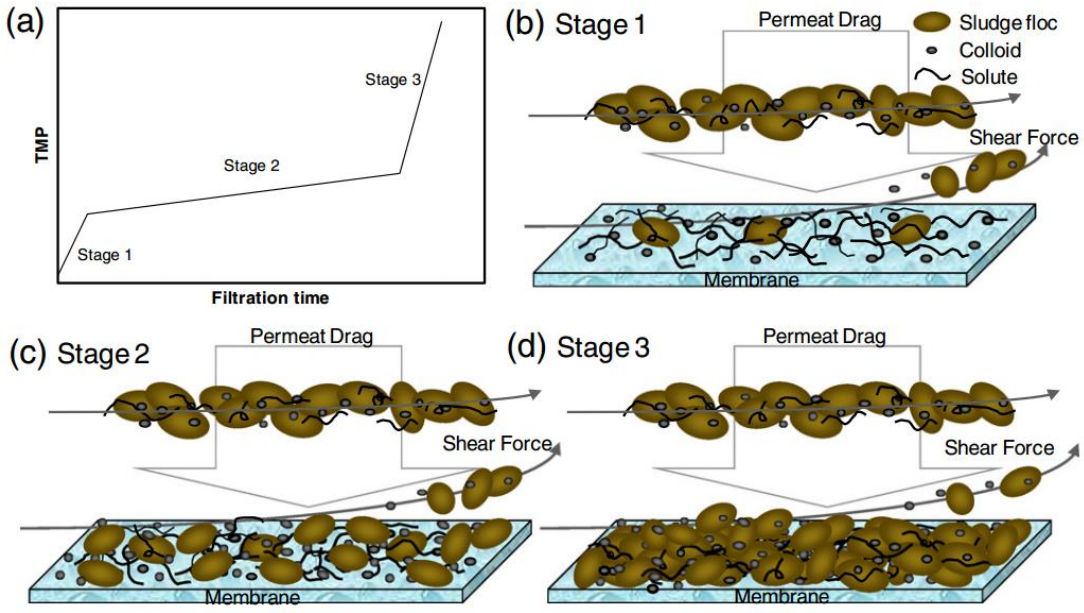

Figure 2-3. Membrane fouling mechanism associated with a three-stage TMP profile (Lin et al., 2013).

During the early stage of the filtration, the colloids and soluble matters are deposited onto the membrane surfaces by permeation drag, and not readily detached by shear force due to its low back transport velocity (Bae and Tak, 2005). The colloids and solutes with

sizes lower than the membrane pore sizes would penetrate and block the membrane pores. Many studies attributed the significant membrane fouling and first TMP jump in Figure 2-4 during early filtration stage to the initial pore blocking phenomenon. Consequently, the gradual increase in TMP is caused by further penetration and pore blocking by the colloids and soluble products that are prevented by the gradient developing sludge cake (Zhang et al., 2006).

There are a few interpretations for the second TMP jump. Cho and Fane (2002) attributed the second TMP jump to the changes in the local flux due to fouling eventually causing local fluxes to be higher than the critical flux, severe fouling may take place with a significant drop in membrane performance. Subsequently, Zhang et al. (2006) revealed that the local flux effect might not be the only explanation for the second TMP jump. He attributed the sudden TMP jump to the collapse of the biofilm or cake layer structure. The collapse of cake layer structure not only increase the membrane resistance but also limits the oxygen transfer rate which eventually causes the death of bacteria in the inner biofilms. As a consequence, more extracellular polymeric substances (EPS) are released and results in a sudden increase in the concentration of EPS at the bottom of the cake layer. The EPS accumulated in the inner of cake layer permanently block the membrane pores, therefore, causes irreversible fouling and (Hwang et al., 2008).

2.1.3.2 Reversible and irreversible membrane fouling

Membrane fouling is a complicated phenomenon that results from the interaction among multiple factors. The mixed liquor physiochemical properties may strongly affect fouling mechanisms in a membrane filtration system, therefore, resulting in reversible and irreversible membrane fouling. Although it can be confusing in the literature regarding the concepts of irreversible fouling and reversible fouling, it is generally agreed that membrane fouling can be classified into reversible and irreversible fouling based on the cleaning practice (Meng et al., 2009). Reversible fouling can be further classified into removable and irremovable fouling. The former is caused by loosely attached foulants while the latter is caused by pore blocking and strongly attached foulants to the membrane surface. The removable fouling refers to the fouling that can be eliminated by

physical means of cleaning such as backwashing or relaxation under crossflow conditions, whereas irremovable fouling refers to fouling that can only be removed by chemical means of cleaning (Meng et al., 2009). The irreversible fouling refers to a permanent fouling which cannot be removed by any approach even chemical cleaning.

2.1.5 Limitations of conventional MBR in water reclamation

In spite of all the advantages of MBR over CAS, conventional MBR has its own limitations in removing a wide range of soluble organics such as pesticides, hormones and trace organic contaminants (TrOCs) (Tadkaew et al., 2011). The MBR system has been increasingly investigated for their performance with respect to TrOCs removal (Radjenović et al., 2009, Wijekoon et al., 2013, Tadkaew et al., 2011). The term trace organic contaminants refers to contaminants present in water and wastewater at very low concentrations as a result of domestic and industrial usage. . They include endocrine disrupting compounds (EDCs), pharmaceutical and personal care products (PPCPs), and disinfection by-products (DBPs). Several studies found that hydrophobic TrOCs can adsorb to the biomass, resulting in longer retention times in the bioreactor (Radjenović et al., 2009, Tadkaew et al., 2011, Wijekoon et al., 2013). The longer retention time in the bioreactor can facilitate better biodegradation, therefore, resulting in higher removal efficiency of these TrOCs. In contrast, hydrophilic TrOCs such as carbamazepine and diclofenac were found to be persistent in both CAS and MBR treatment system as these TrOCs with low MW can pass through the MF and UF membranes employed in the MBR system. Therefore, the retention time of the hydrophilic TrOCs in the bioreactor is almost equal to the hydraulic retention time (HRT) which is insufficient for the biodegradation due to their recalcitrant nature. Therefore, the presence of hydrophilic TrOCs in MBR permeate necessitates a further advanced treatment process to ensure complete elimination of these TrOCs in the final water products.

In water reclamation scheme, the subsequent advanced treatment process mainly consists of a combination of reverse osmosis or nanofiltration and UV oxidation or ozonation. The presence of these dissolved ions and organic matter in the MBR permeates has been

proven to cause serious membrane fouling of the downstream RO process which leads to unwanted consequences such as flux decline, high operating pressure, more frequent membrane cleaning increased plant downtime, and shorter membrane lifespan(Bartels et al., 2005b). Although high water quality is eventually achieved after these multi-stage treatment processes, the overall treatment can be costly and energy intensive due to poor water quality of the RO feed, therefore, compromising the economic and environmental benefits of water reclamation (Luo et al., 2014).

2.2 Nanofiltration membrane process

2.2.1 Fundamentals of NF

NF is a complex process which is highly dependent on the micro-hydrodynamic and interfacial events occurring at the membrane surface and within the membrane nanopores (Mohammad et al., 2015). Unlike the MF/UF membrane, where the mass transport is mainly governed by size exclusion, the separation mechanisms of NF membranes is far more complex and are attributed to a combination of steric (size-based exclusion), Donnan, and dielectric effects. Various predictive models for the transportation through NF membranes have been developed based on the extended Nernst-Planck equation which describes the contributions from diffusion, electromigration and convection as the three terms on the right-hand side of Eq. 2-2 (Schlögl, 1966).

$$j_i = -\frac{c_i D_{i,\infty} K_{i,d}}{RT}\frac{d\mu}{dx} + K_{i,c} c_i V \qquad \text{Eq. 2-2}$$

where j_i is the ionic flux, c_i is the ionic concentration, $D_{i,\infty}$ is the effective diffusion coefficient, R is the gas constant, T is the temperature, V is the solvent velocity and $K_{i,c}$ and $K_{i,d}$ are hindrance factors to account for the convection and diffusion inside a confined space.

The size exclusion mechanism governs the diffusive and convective transportation of neutral solutes across membrane whereas the transportation of charged solutes is

governed by a combination of steric (size-based exclusion), Donnan, and dielectric effects. The classical Donnan effect describes the equilibria and membrane potential interactions between a charged species and the interface of the charged membrane (Donnan, 1995). Electrostatic repulsion or attraction happens based on the ion valence and the zeta potential of the membrane that might vary from time to time depending on the localized ionic environment. However, the mechanisms of dielectric exclusion are not fully understood and debatable. This is attributed to the fact that the dimensions of the NF active layer are at near atomic length scales, coupled with limitations in current measurement technologies have hindered us from getting a detailed information of the physical structure, electrical properties and therefore the true nature of separation mechanisms of NF membranes.

2.2.2 NF membrane applications

The NF membrane process is capable of producing great amounts of high-quality water with its unique membrane characteristics such as high selectivity between multivalent and monovalent ions, the high rejection capacity to retain small organic molecules, longer membrane lifespan, higher flux and lower operating pressure. The excellent removal capacity of contaminants and the decreasing membrane prices have led to the wide acceptance and the applications of NF membrane in many areas including water treatment (Fang et al., 2013), wastewater reclamation (Zaviska et al., 2013, Phan et al., 2016), desalination (Subramanian and Seeram, 2013), food processing industry (Rice et al., 2011), pharmaceutical and biotechnology (Székely et al., 2011, Siew et al., 2013). Recently, NF has gained more attention and been used for novel applications such as for removal of persistent organic pollutants (POPs), arsenic (As), PhACs and hormones (Mohammad et al., 2015). Among these applications, the application of NF membranes in wastewater treatment is discussed in the following section.

2.2.2.1 Wastewater treatment

NF membranes have been tested extensively for their rejection properties in removing pharmaceuticals and personal care products (PPCPs). Both NF90 and NF270 membranes

were examined for their rejection capacities of six PPCPs, namely carbamazepine (CBZ), triclosan (TRI), ibuprofen (IBU), sulfadiazine (DIA), sulfamethoxazole (SMX) and sulfamethazine (SMZ) (Lin et al., 2014). The outcomes showed that size exclusion and electrostatic repulsion worked synergistically for NF 90 whereas electrostatic repulsion was the dominant separation mechanism for NF 270. In addition, the NF membranes were tested for their rejection properties in removing PPCPs in real municipal wastewater.

Andrade et al. (2014) studied the combination of MBR as secondary treatment and nanofiltration as tertiary treatment for the treatment and reuse of dairy wastewater. The results showed that the overall COD removal efficiencies of 99.9 % was achieved. With nanofiltration, excellent effluent quality was achieved. Therefore, an innovative idea to combine MBR process with NF by recirculating NF concentrate to the preceding MBR system was proposed (Rautenbach and Mellis, 1994). Many studies showed successful applications in the MBR-NF process with NF concentrate recirculation for water reuse (Kappel et al., 2014, Woo et al., 2016). The prolonged retention time of the organic micropollutants in the bioreactor caused by the concentrate recirculation enhanced biodegradation. Kappel and co-workers later found that inorganic fouling is the dominant fouling mechanism on the NF membrane, while organics such as humic acids do not contribute much to the NF fouling (Kappel et al., 2014).

To combine the MBR and NF process into a one step process, a study by Choi and co-workers firstly attempted the idea to replace the MF/UF membrane in the conventional MBR system with NF membrane and developed a new type of nanofiltration based MBR (Choi et al., 2002). A more detailed review of the NF-MBR and its development can be found in section 2.3.

2.2.3 Fouling in NF membrane

Fouling is still the major obstacle that limits and slowdowns the prosperous and effective applications of membrane technology. In this section, the fouling in NF is reviewed within the scope of wastewater treatment.

2.2.3.1 Fouling Mechanisms

Generally, there are four basic fouling mechanisms involved simultaneously in the fouling of NF membrane, namely adsorption, pore blocking, cake layer formation, and gel layer formation.

a) Adsorption: It is dependent of the specific interaction between the solutes and the membrane surface. The adsorption may occur on the membrane surface or in pores depends on the size of solutes.

b) Pore blocking: Foulants with sizes smaller than the membrane pores such as soluble organics and small colloids causes pore plugging whereas foulants with larger sizes such as sludge flocs, large colloids and particulates tend to block the membrane pores and lead to cake layer formation

c) Cake layer formation: Deposition of colloids on the membrane surface and eventually form a foulant layer that resist flow.

d) Gel layer formation: The formation of gel layer at the membrane surface is initiated when the solute concentration reaches a maximum value due to concentration polarization.

Unlike the MF/UF membranes, these fouling mechanisms in the NF operation are much closely related to concentration polarization and osmotic pressure. Concentration polarization is a phenomenon where a high solute concentration at the membrane surface compared to the bulk solution, which resulted from the accumulation of retained solutes in the membrane boundary at the feed side during the filtration process. While osmotic pressure is defined as a measure of the tendency of a solution to take in water by osmosis. The accumulation of inorganic or organic solutes increases the osmotic pressure in the bioreactor, therefore, reducing the effective transmembrane driving force. The fouling in NF membrane can be dominated by certain fouling mechanisms which influenced by

both feed properties and membrane properties (Mohammad et al., 2015). For example, Koyuncu et al. (2004) found that the dominant fouling mechanisms of NF treating dye was cake layer formation at low salt condition whereas fouling was dominated by adsorption at high salt condition.

It is customary to assume a single fouling mechanism prevailing throughout the membrane operation. The fouling mechanism revealed by experiment using single-foulant solutions is overly simplified as it may neglect some of the important interactions among multiple foulants types. Therefore, several studies have been conducted to have a better understanding on combined fouling of the NF membranes (Lee et al., 2005, Jarusutthirak et al., 2007, Li et al., 2015). For example, the cake-enhanced osmotic pressure (CEOP) was found to be the dominant fouling mechanism for individual colloidal fouling, however, the combined fouling could be influenced by several fouling mechanisms due to the presence of other natural organic matter (NOM) and inorganic compounds (Mahlangu et al., 2015). Some authors observed that the contributions of the fouling mechanisms for combined fouling are less significant compared to their separate influences on individual colloidal fouling (Lee et al., 2005). In short, the combined fouling may be influenced by the combined effects of 1) CEOP, 2) cake layer resistance, and 3) Surface conditioning (Tang et al., 2011). Despite previous research efforts, the fouling mechanism resulted from the mixed foulants interaction is still not well understood, hence, more investigations in this area are needed.

2.2.3.2 Types of Fouling

Similar to the MF/UF membrane, fouling in NF membrane can be categorized into 4 types based on different types of foulants, namely colloidal fouling, organic fouling, scaling and biofouling. Dependent on the wastewater constituents, different types of fouling, namely colloidal fouling, organic fouling, scaling, and biofouling can occur simultaneously in a NF system.

1) Colloidal fouling

Colloidal fouling is of fundamental important to NF fouling as they are more likely to cause membrane fouling due to their larger sizes. Organic macromolecules such as polysaccharides, proteins, and natural organic matter are often viewed as the major foulants in wastewater reclamation (Mustafa et al., 2016). These organic macromolecules usually present in the form of particulates, and they share many common properties with their inorganic colloids such as aluminum silicate minerals, silica, iron oxides/hydroxides with respect to membranes fouling. The underlying principle for the successful attachment of colloids onto the membrane is mainly governed by the permeate drag force and the various depolarization mechanisms namely shear-induced diffusion, surface interaction, Brownian diffusion and lateral migration (Bacchin et al., 2006). Also, the factors affecting colloidal fouling propensity in the NF membrane operation can be categorized into three groups namely, feed water composition, membrane properties and hydrodynamic conditions as shown in Figure 2-4. Membrane fouling is strongly related to the physiochemical properties and the concentrations of the colloids present in the feedwater. Membrane properties, such surface roughness, charge properties, and hydrophobicity also play an important role in colloidal fouling. Generally, a smooth and hydrophilic membrane with neutral surface charge tend to have lower fouling especially at the initial stage of membrane fouling (Elimelech et al., 1997). Hydrodynamic conditions such as flux, crossflow, temperature and recovery can also have substantial impacts to the colloidal fouling. Lastly, the critical flux and the limiting flux concepts must not be overlooked in the subject of NF colloidal fouling (Tang et al., 2011).

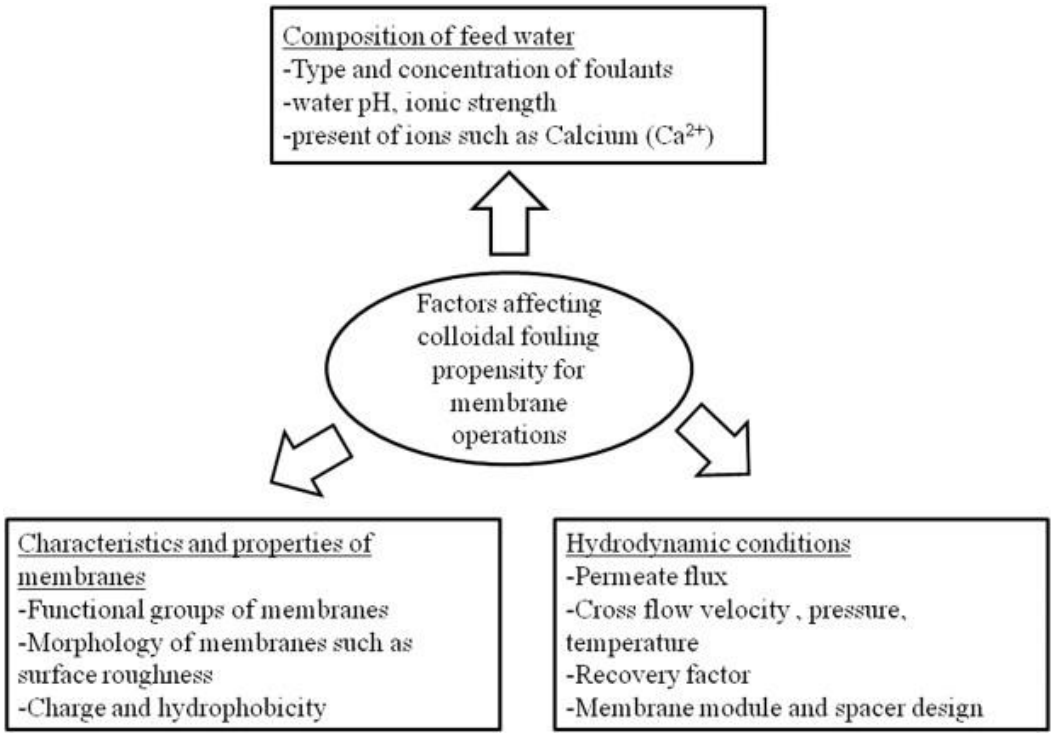

Figure 2-4. Factors affecting colloidal fouling of NF membranes (Tang et al., 2011).

2) Organic fouling

Organic fouling is highly associated with the presence of natural organic matter (NOM) such as humic acids and fluvic acids especially in the context of water reclamation. Humic substance is comprised of both aromatic and aliphatic components with mainly carboxylic and phenolic functional groups (Gong et al., 2017). Similar to colloidal fouling, the factors governing the fouling propensity listed in Figure 2-4 are applicable to organic fouling in NF. In particular, the effect of chemistry parameters such as pH and ionic strength on the morphological and physiochemical changes of both the NOM and membrane surface is of fundamental important to the severity of fouling (Al-Amoudi, 2010). Under low pH condition, humic acids have a smaller molecular configuration due to reduced inter-chain electrostatic repulsion while the surface charge on the membrane tends to be less negative. Given the negatively charged nature of humic acids, the reduction in electrostatic repulsion between the NOM and membrane surface increases the chances of successful attachment to the membrane surface. On the other

hand, the ionic strength of the solution also plays an important role in the organic fouling. At high ionic strength, the membrane pore size was found to exhibit larger pore size compared at low ionic strength (Al-Amoudi, 2010). Ionic strength also has an impact on the secondary and tertiary structure of NOM. A rigid and compact NOM macromolecule is formed under high ionic strength conditions due to higher intermolecular repulsion (Theng, 2012a). As a consequence, a dense, compact and thick fouling layer is formed under low pH and high ionic strength condition whereas a loose and thin fouling layer is formed under high pH and low ionic condition (Elimelech et al., 1997).

3) Inorganic fouling

Scaling occurs when the concentration of one or more inorganic species increases beyond the solubility limits and leads to precipitation of these species on the membrane surface. Salts such as calcium carbonates, gypsum, calcium phosphate, silica, ferric and aluminum hydroxides are the common scaling species found in NF membrane (van de Lisdonk et al., 2000, van de Lisdonk et al., 2001, Vogel et al., 2010). Many studies acknowledged that scaling takes place on the NF membrane surface requires two stages, namely the nucleation stage and crystal growth from supersaturated solution (Al-Amoudi, 2010, Rathinam et al., 2018). Therefore, it is crucial to understand the mechanism of scale formation in order to prevent membrane fouling arise from scaling. Both heterogeneous and homogeneous crystallization are the possible mechanism that causes scaling on the membrane surface. Heterogeneous crystallization occurs when the interfacial energy between the solid substrate and the crystal is smaller than the interfacial energy between the crystal and the solution (Lee et al., 1999, Al-Amoudi, 2010). Subsequently, the nucleation takes place on a solid substrate surface rather than in the bulk solution even at a low saturation point (Rathinam et al., 2018). Concentration polarization is of fundamental important to heterogeneous crystallization because the concentration of scaling species increase exponentially near the vicinity of membrane surface and ultimately lead to precipitation on the membrane. While homogeneous crystallization takes place only when the bulk phase is supersaturated and crystallization takes place in the bulk solution. Additionally, factors such as flux,

crossflow velocity, temperature, pH, concentration polarization, surface roughness of the membrane can influence the scale formation mechanisms as shown in Figure 2-5. For example, in a MBR-NF system treating real municipal wastewater, Kappel and co-workers found that inorganic fouling attributed by calcium phosphate scaling is the dominant fouling mechanism on the NF membrane at high pH, i.e., pH 8, however, no scaling was observed at the lower pH, i.e., pH 6 (Kappel et al., 2014). This implies that scaling could be prevented when the NF system is operated at conditions lower than the critical solubility limits and pH conditions.

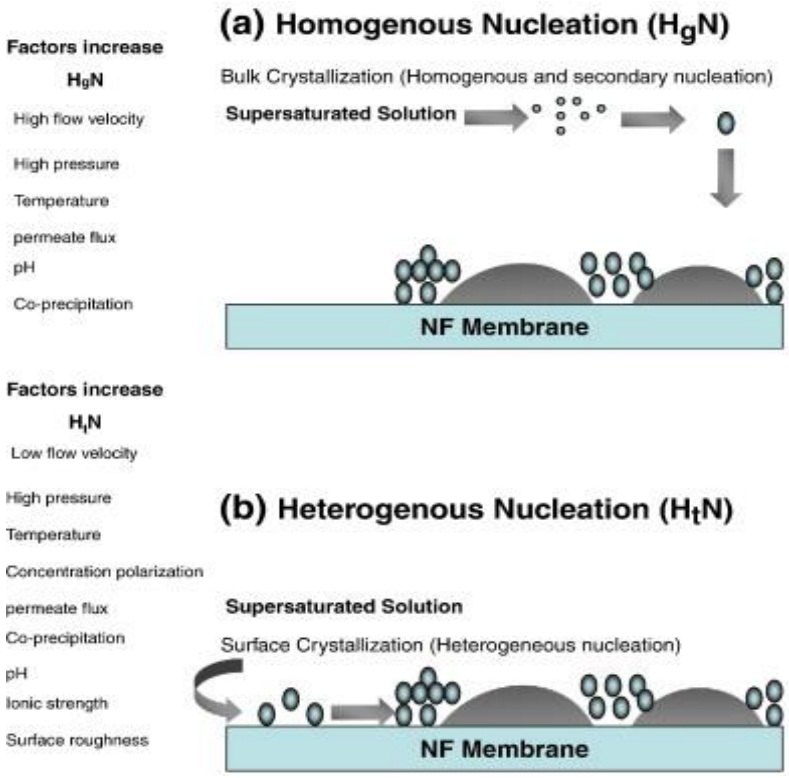

Figure 2-5. Factors affecting scale formation mechanisms in NF operation (Lee et al., 1999).

4) Biofouling

Biofouling is defined as the adhesion, metabolism, and growth of microbial cells in the form of biofilm on the membrane surface which is the main cause of loss of membrane permeability, and therefore, membrane flux and efficiency in the system (Wang et al.,

2005). During the early stage of biofouling, a bacterial cell is transported by the convective water flow to the membrane surface and adheres to the surface reversibly in the first step of cell adhesion. The microbial adhesion to membrane surface is facilitated by several driving factors such as hydrodynamic forces, physiochemical interactions between microorganisms and membrane surface, and adhesive forces as illustrated in Figure 2-6.

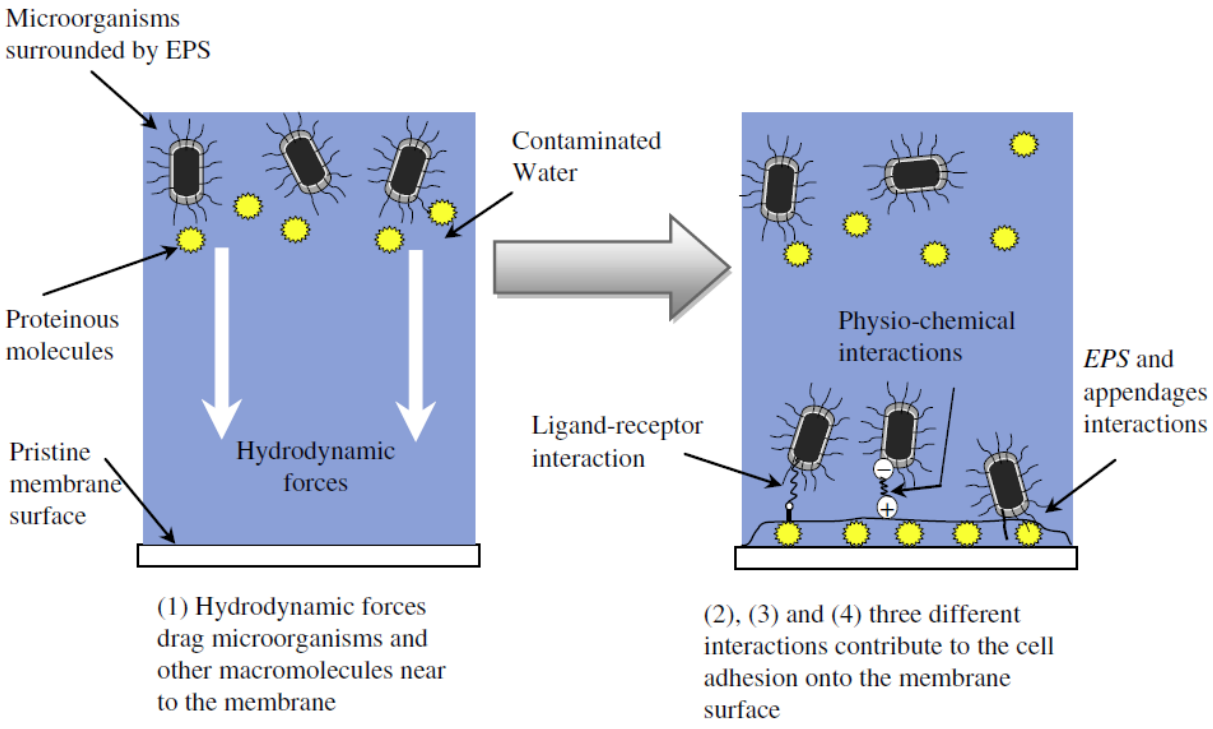

Figure 2-6. Driving forces of microbial adhesion (Al-Juboori and Yusaf, 2012).

Hydrodynamic forces which result from the convective water flow passing an NF membrane are responsible for the transportation of the microorganisms to the vicinity of the membrane surface (Sadr Ghayeni et al., 1998). Physiochemical interactions between microorganisms and the membrane surface are governed by the van der Waals interaction and Coulomb interaction on the electrostatic double layer which described in the classic model based on Derjaguin-Landau-Verwey-Overbeek (DLVO) theory. According to Hori and Matsumoto (2010), the van der Waals attractive force is dominant in the vicinity of a surface whereas the Coulomb interaction becomes dominant at a distance away from

the surface. In addition, hydrophobicity is an important factor that greatly affects bacterial adhesion and the self-agglutination of bacterial cells (Katsikogianni and Missirlis, 2004, Zita and Hermansson, 1997, Gekas et al., 1992). The attractive hydrophobic interactions and repulsive hydration effects are explained in Lewis acid–base interactions between bacteria and membrane surface. According to van Oss (1993), the influence of the acid–base interactions is enormous compared with electrostatic and van der Waals interactions. Therefore, hydrophobic/hydrophilic interactions are then incorporated into the extended DLVO theory. In short, the microbial adhesion to membrane surface can only occur when the total free energy resulted from van der Waals, electrostatic double layer and hydrophobic/hydrophilic interactions between the bacteria and the membrane surface is negative (Brant and Childress, 2002).

After the adhesion, the bacterial cell will then produce exopolymeric substances (EPS), which can pierce the energy barrier for bridging between the cell and surface and eventually form a mature biofilm (Hori and Matsumoto, 2010). Adhesive forces of extracellular polymeric substances (EPSs) and the appendages of bacteria can be very critical to the irreversible microbial adhesion and eventually causing irreversible fouling in RO membrane (Sadr Ghayeni et al., 1998). Transparent exopolymer particles is a subgroup of suspended EPS which are present in the form of discrete particles matrix which is capable of withstanding fluid shear force in the RO system (Meng et al., 2013, Barnes et al., 2014).

The understanding of biofouling can be further built upon the concept of biofilm development. The three general phases of biofilm development are induction phase, logarithmical growth phase, and plateau phase (Flemming, 1997). In the induction phase, the surface is primarily colonized by several groups of pioneer microorganism. Adhesion is substantially proportional to the cell density in the water phase as a result of weak physicochemical interactions. During the logarithmical growth phase, biofilm accumulation mainly due to cell growth on the surface rather than the adhesion of free-moving cells. In the plateau phase, the biofilm growth rate, cell detachment and cellular dying rate are in balance in which the growth rate is independent of the concentration of

cells in the raw water, however, it is governed by other factors such as nutrient concentration, the mechanical stability of the biofilm, and the effective shear forces.

2.3 Novel nanofiltration-based MBR

2.3.1 High retention membrane bioreactor (HR-MBR)

Recent advanced developments in the MBR field have led to the concept of a novel HR-MBR that combines both biological process and high retention membrane separation into one treatment system (Luo et al., 2014). The retention of TrOCs is no longer limited to the hydrophobic TrOCs where the absorption to the biomass is taken place in the bioreactor. The high retention membrane separation process can effectively retain both hydrophobic and hydrophilic TrOCs, therefore, extending their retention time in the bioreactor and potentially enhancing their biodegradation. The HR-MBR is comprised of three major configurations, namely osmosis membrane bioreactor (FO-MBR), membrane distillation membrane bioreactor (MD-MBR) and nanofiltration membrane bioreactor (NF-MBR). The key differences between high retention MBRs and conventional MBRs are summarized in Table 2-1.

Table 2-1. A comparison of conventional and high retention MBRs (adapted from (Luo et al., 2014))

	Conventional MBR	**High retention MBR**		
Type	MF/UF-MBR	MD-MBR	FO-MBR	NF-MBR
Membrane	Hydrophilic MF/UF	Hydrophobic MF	FO	NF
Driving force	Hydraulic pressure	Vapour pressure	Osmotic pressure	Hydraulic pressure
NaCl rejection (%)	Negligible	~ 100	~ 100	40 – 90
TOC in permeate (mg/L)	3 – 10	< 0.8	< 3	1 – 4
Permeate flux (L/m^2h)	10 – 30	1.2 – 15	< 10	< 2.5
Additional step	-	Heat source is required	water/draw solute separation	-
Pros	Simple process design; commercially avaible MF/UF membranes.	Excellent permeate quality; waste heat could be utilised (if available)	Excellent permeate quality; Low energy requirement; Low fouling;	Excellent permeate quality; simple process design; no accumulation of NaCl
Cons	Poor permeate quality	Biological activity affected under thermophilic condition; high energy requirement; membrane wetting	Inconsistent permeate flux; reverse salt transport; internal concentration polarization; Biological activity deteriorated under high NaCl condition	Low permeate flux; high energy requirement (for hydraulic pressure and crossflow); high fouling

2.3.1.1 FO-MBR

The FO-MBR system is a combination of a bioreactor unit and a forward osmosis (Bradford) membrane module which can be incorporated in either submerged or side-stream configuration. FO is an osmotically driven membrane process where only water molecules from a feed solution could pass through the semi-permeable FO membrane to the draw solution. For water reclamation, the FO-MBR is coupled with a draw solute recovery process like RO to reconcentrate the diluted draw solution to obtain the high-quality water product. The FO-MBR system is well known for its potential advantages such as lower fouling propensity (due to the absence of hydraulic pressure), high rejection rate which is comparable to RO and lower energy consumption (Wang et al., 2016). In addition, the integration of the MF/UF membrane unit into the FO-MBRs enables the recovery of nitrogen and phosphorus from wastewater (Qiu et al., 2015). However, low and unstable permeate flux as one of the core challenges of the technology. (Wang et al., 2016). Other challenges such as membrane fouling, internal concentration polarization (ICP) and reverse salt transport (RST) occurs during the FO process continued to hinder its development. Briefly, RST that results in the loss of draw solutes and requires constant topping up of draw solutes to maintain the flux. The elevated salinity condition in the FO-MBR resulted from the accumulation of solutes and RST reduces the net osmotic driving force. ICP phenomenon coupled with membrane fouling causes hindered diffusion of solutes within the membrane support layer and reduces the net osmotic driving force, therefore, resulting in reduction of permeate flux. In addition, elevated salinity also has impacts on the physical and biochemical properties of biomass which could adversely affect the overall microbial activity and population structure (Lay et al., 2010, Wang et al., 2014b). For example, elevated salts could increase the soluble microbial products (SMP) and extracellular polymeric substances (EPS) in the mixed liquor that cause greater membrane fouling (Luo et al., 2017). In short, these inherent issues of the FO process have made the FO-MBR less suitable for water reclamation applications.

2.3.1.2 MD-MBR

MD is a thermally-driven transport of water molecules (in vapor phase) through porous and hydrophobic membranes. When MD is coupled with thermophilic bioprocess, it gives rise to the novel MD-MBR (Phattaranawik et al., 2008a). In the MD-MBR system, the permeate flux can be increased by increasing the temperature difference across the membrane. However, elevated temperature in the bioreactor can have adverse impacts on the biological process. For example, biological activity under thermophilic condition is typically lower than that of the mesophilic condition (Tripathi and Grant Allen, 1999). Moreover, nitrification-denitrification process could not take place due to the absence of nitrifiers under thermophilic condition (Goh et al., 2015). Moreover, severe membrane scaling under high temperature conditions could increase the membrane resistance and therefore result in flux decline (Luo et al., 2014). Like all membrane systems, the MD-MBR faces the challenge of flux decline due to fouling where the fouling layer exerts a mass transfer resistance to flow. Unfortunately, fouling of the MD-MBR has two other unique effects on its flux: thermal resistance and temperature polarization (Schofield et al., 1987, Srisurichan et al., 2006). In addition, the issue of membrane wetting which leads to an increase in TOC transmission and a reduction in organic removal efficiency is unique to MD-MBR (Goh et al., 2013). Also, MD-MBR shares the same challenge faced by FO-MBR related to salts accumulation as discussed above. In view of the high temperature requirement for the MD-MBR, it may find application in industrial wastewater reclamation where waste heat can be harnessed, however, it may not be suitable for municipal wastewater treatment and water reclamation application.

2.3.1.3 NF-MBR

NF-MBR is one type of the HR-MBRs that offers alternatives to produce permeate with high-quality for potable reuse and direct discharge to watercourses (Luo et al., 2014, Choi et al., 2002, Choi et al., 2006). Compared to FO-MBR and MD-MBR, NF-MBRs are more feasible for water reclamation application. The key advantage of NF-MBRs lie in the lower monovalent salts rejection of the NF membrane. This results in lower salts

accumulation in the bioreactor, therefore, lower the negative impacts on the physical and biochemical properties of biomass. In addition, the configuration of NF-MBR is relatively similar to the conventional MBR, implying a minimum alteration or modification required to upgrade the current MBR system. Instead of using the MF/UF membrane as a barrier to biomass, NF-MBR uses an NF membrane to retain both biomass and dissolved organics to produce high quality permeate. Lastly, NF is a mature process with many pilot and full-scale applications, however, most of the commercially available NF membranes were not specifically designed for the separation of activated sludge. Therefore, membrane fouling is expected to be more serious in NF-MBR applications. According to Choi et al. (2002), one approach to minimizing fouling is to operate the NF-MBR system at a very low permeate flux and a high crossflow condition. This approach is found to be effective in controlling cake layer formation on the membrane surface and prolonging membrane lifespan, however, it compromised on the water productivity of the system (Choi et al., 2006). With the advanced development of NF membranes that are fouling resistant, low cost, chemically and biologically stable, and highly permeable, the challenges arise from membrane fouling could be eventually overcome. Therefore, with the use of a novel low-pressure hollow fiber NF membrane described in Chapter 3, the NF-MBR show great potential to replace the conventional MBR as the secondary treatment process for water reclamation application (Luo et al., 2014).

2.3.2 TrOCs removal

The removal of TrOCs has been recently viewed as one of the most challenging tasks in water reclamation process (Luo et al., 2014). Due to the lack of emphasis on TrOCs over the past decades, conventional wastewater treatment technologies were not targeted on removing these TrOCs (Luo et al., 2014). More studies found that TrOCs such as pesticides, pharmaceuticals, antibiotics, personal care products, hormones and endocrine disrupters may pose serious risk on ecosystems and human health (Li et al., 2016). Therefore, water treatment technologies should aim to minimize introduction of critical pollutants into the aquatic environment. With the maturity of MBR technology, advance

treatment targeted on the removal of TrOCs has attracted increasingly attention in the research field of municipal wastewater treatment.

The capacity of the NF membrane to reject TrOCs and macromolecules binding TrOCs is one of the key drivers for the development of NF-MBR. The underlying concept is that the tight NF membrane will be able to retain persistent and low molecular weight organic micro-pollutants more effectively, and thereby facilitate a better biodegradation in the bioreactor (Luo et al., 2014). In order to adequate investigate the removal efficiency of TrOCs in NF-MBR, studies have conducted long-term experiments with NF-MBR in side stream configuration and have provided useful information on the technology (Zaviska et al., 2013, Phan et al., 2016). According to (Phan et al., 2016), TrOCs can be generally classified into hydrophilic and hydrophobic types. The hydrophobic TrOCs exhibit higher removal efficiency due to the fact the they can readily adsorb onto activated sludge, which prolongs their retention in the bioreactor. This phenomenon was also commonly observed in conventional MBR (Tadkaew et al., 2011, Wijekoon et al., 2013). Interestingly, Phan and co-workers also found that small amount of hydrophobic TrOCs can also partition into polymeric membrane and diffuse through the membrane, hence, lowering their removal by NF membrane solely based on size exclusion mechanism (Phan et al., 2016).

In contrast, hydrophilic TrOCs with MW lower than the NF pore sizes were able to escape and end up in the effluents. It is noteworthy that the removal of hydrophilic TrOCs can vary significantly due to the diverse molecular structure and functional groups which directly in relation to their biodegradability. The presence of (electron withdrawing groups) EWGs in their molecular structures was found to be the main reason that hinder the oxidation and biodegradation of these compounds in the reactors (Phan et al., 2016). On the other hand, the hydrophilic or charged organic compounds with molecular weight of higher than the pore sizes of NF membrane can be effectively rejected mainly via size exclusion, electrostatic exclusion, and adsorption to membranes.

2.3.3 Concentration factor

The concentration factor (CF) describes the phenomenon of salt accumulation in an NF-MBR. An ideal condition for the NF-MBR with complete retention is discussed. In this instance, CF simplifies to the ratio SRT/HRT at steady-state operation as follows (Lay et al., 2010):

Based on Figure 2-7, the mixed liquor salt concentration C_{ml} can be determined as a function of time, *t* via solute mass balance in the NF-MBR:

$$V_r \frac{dC_{ml}}{dt} = Q_{in}C_{in} - Q_{out}C_{out} - Q_w C_{ml} \quad \text{Eq. 2-2}$$

where V_r *is the bioreactor volume;* Q_{in} *and* Q_w *are the respective volumetric flow of the influent sewage and the waste sludge*.

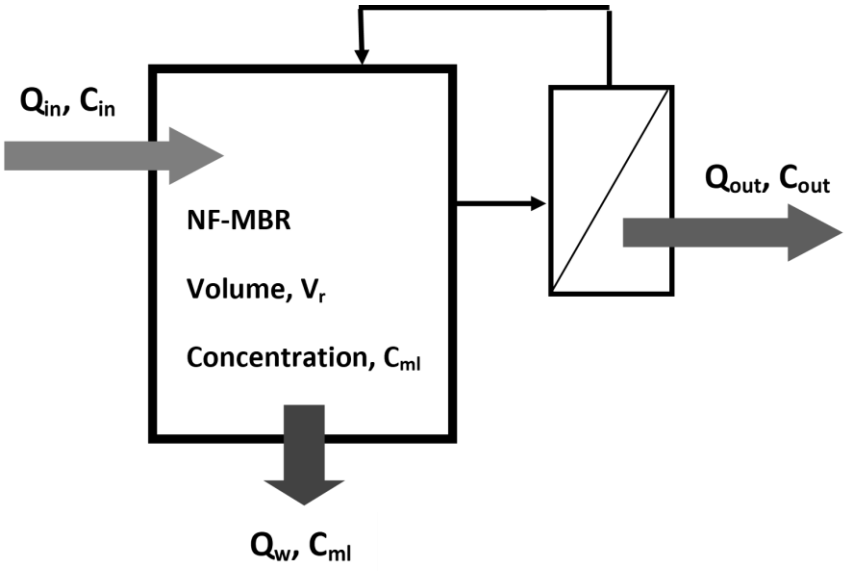

Figure 2-7. Mass balance in a NF-MBR.

$$HRT = \frac{V_r}{Q_w + Q_{out}} = \frac{V_r}{Q_{in}} \quad \text{Eq. 2-3}$$

$$SRT = \frac{V_r}{Q_w} \quad \text{Eq. 2-4}$$

Substituting Eqs. 2-3 and 2-4 into Eq. 2-2, we have:

$$\frac{dC_{ml}}{dt} + \frac{C_{ml}}{SRT} = \frac{1}{HRT}(C_{in} - \frac{Q_{out}C_{out}}{Q_{in}}) \quad \text{Eq. 2-5}$$

At steady state, $\frac{dC_{ml}}{dt} = 0$

Thus, Eq. 2-5 can be re-written as:

$$C_{ml}^{steady} = \frac{SRT}{HRT}(C_{in} - \frac{Q_{out}C_{out}}{Q_{in}}) \quad \text{Eq. 2-6}$$

Under ideal condition with complete retention in the NF-MBR, $C_{out} = 0$

$Q_{out} \approx Q_{in}$ for 100% recovery,

and system rejection, $\theta = \frac{C_{in} - C_{out}}{C_{in}}$

Therefore, CF can be written as:

$$\frac{C_{ml}^{steady}}{C_{in}} = \frac{SRT}{HRT} \times \theta \quad \text{Eq. 2-7}$$

2.3.4 State of the art

To date, there were only seven existing studies on the NF-MBR (Choi et al., 2002, Choi et al., 2006, Choi et al., 2007b, Golbabaei Kootenaei et al., 2014, Phan et al., 2016). The organic removal, nutrient removal, biomass concentration and operating conditions of the NF-MBR in previous studies were summarized in Table 2-2. The first attempt was conducted by Choi et al. (2002), who reported the excellent organic removal capacity of the system. A variety of membranes including cellulose acetate (CA), polyamide (PA), and ceramic membranes were tested for their long-term membrane stability and applicability in the NF-MBR (Choi et al., 2002, Choi et al., 2006). Due to the high rejection capacity of NF membrane, the dissolved organic carbon, total phosphorus, and salt concentrations of the supernatant in the NF-MBR was higher than those in the supernatant of a conventional MBR (Choi et al., 2007b). In consequence, significantly higher effluent quality especially in the removal of TrOCs compared to the conventional MF/UF MBR was achieved by the NF-MBR (Phan et al., 2016).

However, membrane stability has become an issue when degradation of permeate quality in the later stage were observed in the NF-MBR using cellulose acetate NF membranes. The phenomenon might be attributed to the hydrolysis of cellulose acetate membrane over long period of operation (Choi et al., 2007a). To avoid similar biodegradation of membrane, a proper module configuration with intermittent chlorine dosing was proposed to prolong the lifespan of the CA membrane. Alternatively, the performance of PA membranes was also evaluated. However, the permeability of the PA membranes was found to be lower compared to that the CA membrane (Choi et al., 2007b).

The aforementioned studies were adopting the submerged membrane configuration for the NF-MBR. The permeates flux resulted from a submerged NF-MBR were fairly low at between 0.02 and 0.04 LMH (Choi et al., 2002, Choi et al., 2006). Therefore, the side-stream configurations with ceramic multi-tubular membrane module were adopted subsequently to increase the water productivity of NF-MBR (Zaviska et al., 2013, Phan et al., 2016). The attempts have successfully increased the permeate flux to 2.5 LMH and 4.5 LMH respectively without compromising on the permeate quality.

A more detailed review of the challenges faced by the technology of NF-MBR can be found in the following section.

Table 2-2 Performance and operating parameters of NF-MBR.

Reference	Reactor configuration	Membrane	Wastewater	Flux (LMH)	Pressure (bar)	HRT (hr)	SRT (d)	MLSS (mg/L)	Removal efficiency (%)		
									TOC	COD	NH_4^+
Choi et al. (2002)	Submerged	Cellulose acetate (CA) hollow fiber	Synthetic	0.042	0.2-0.4	24	∞	3600	>95	-	-
Choi et al. (2006)	Submerged	CA vs Polyamide (PA) hollow fiber	Synthetic	0.021	0.5-0.8	48	40	510-940	>95	-	>90
Choi et al. (2007a)	Submerged	CA hollow fiber	Municipal wastewater	0.021-0.029	0.6-0.85	48	40, 80	-	>91	-	-
Choi et al. (2007b)	Submerged	PA hollow fiber	Municipal wastewater	0.02	0.65-0.8	48	40, 80	510-940	>95	-	>88.5
Zaviska et al. (2013)	Side-stream	Ceramic multi-tubular membrane	Synthetic	2.5	0.8	15.4	40	2500	-	95	-
Golbabaei Kootenaei et al. (2014)	Submerged	Hollow fiber (material not stated)	Hospital Wastewater	-	-	2	62	6000	-	92	>70
Phan et al. (2016)	Side-stream	Ceramic multi-tubular membrane	Synthetic	4.5	0.7	27	∞	1600-2600	>95	-	>99

2.3.5 Key challenges

Given the potential of NF-MBR in wastewater treatment and water reclamation process, this advanced treatment technology deserved more studies and investigations to scale up and speed up the commercialization process. However, several remaining technological challenges such as salinity build-up, membrane stability, and low permeate flux must be addressed (Figure 2-8).

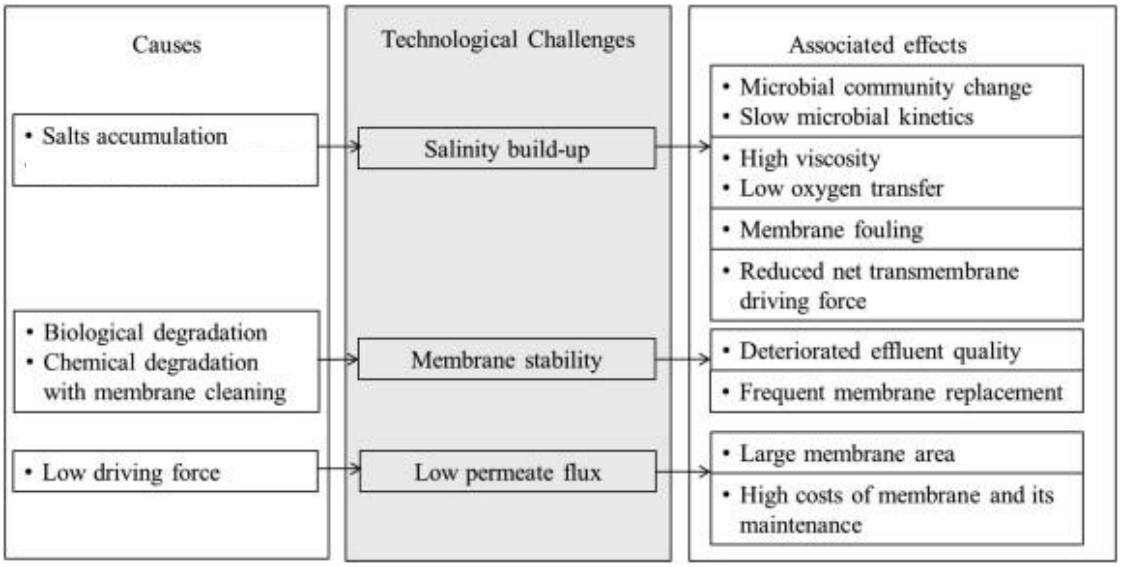

Figure 2-8. Key challenges to further development of NF-MBR (Luo et al., 2014).

2.3.5.1 Salinity buildup

Salinity buildup in the NF-MBR poses several problems to the application of the technology. Recent studies revealed that salts accumulation in the bioreactor could adversely affect the microbial community necessary for the biological treatment and slow down the microbial kinetics of the activated sludge (Reid et al., 2006, Qiu and Ting, 2014). It was reported that the elevated salinity in the bioreactor can be directly co-related to the increase in EPS production, therefore, accelerated membrane fouling (Wang et al., 2014b). In addition, salinity buildup would also bring about considerable osmotic pressures that are normally not experienced in conventional MF/UF MBR (Lay et al., 2010). The effective distribution of oxygen in the bioreactor is governed by the oxygen

transfer rate of the mixed liquor. Under high salinity environment, the solubility of oxygen in the water decreased greatly, hence, lowering the oxygen transfer rates. This is critical to the operation of NF-MBR because aeration is the fundamental requirement for an aerobic biological process for microbial metabolism and contaminant oxidation and also the largest component of the MBR operating cost.

In view of the low monovalent ions rejection properties of the NF membrane, the impact of salinity buildup is expected to be lower in NF-MBR compared to that of the FO-MBR. For example, Choi and co-workers found that the rejection rates of monovalent and divalent ions by the NF membrane ranged between 40-60 % and 70-90% respectively (Choi et al., 2007a). Although the salts accumulation is less severe compared other HR-MBRs, the reduced net transmembrane driving force due to elevated osmotic pressure does make this technology less attractive in term of energy efficiency.

The challenge of salinity build-up necessitated a better comprehension of its effect on the biological and physiochemical properties of the biomass and membrane fouling in the NF-MBR.

2.3.5.2 Membrane stability

Membrane stability is of fundamental importance to the long-term operation of NF-MBR. Chemically and biologically resistant membrane ensures permeates production with consistent quality over a long period of operation. Degradation of membrane not only lead to high membrane replacement cost but also interrupts the smooth operation of the system, therefore, affecting the water productivity and the reliability of the system.

The cellulose membrane is known for its high wettability which could promote high permeability, therefore, higher water flux. Besides, the cellulose membranes are extremely hydrophilic membranes that can alleviate the early attachment of foulants on the membrane surface. Previous study that employed cellulose acetate membrane in the NF-MBR observed a stable filtration performance during the first 80 days (Choi et al., 2007a). However, a deterioration of permeate quality and rejection rates in terms of TOC,

monovalent and divalent ions concentrations was observed. Choi et al. (2007a) later discovered that the deterioration of permeates quality is highly attributed to the bacterial degradation of membrane characteristics including, an increase in pore size and porosity, a decrease in surface charge and hydrophobicity (Choi et al., 2007a). Intermittent introduction of antibacterial reagent to the membrane surface is suggested to overcome the issues of membrane degradation (Choi et al., 2002). However, further investigation to assess the feasibility and effectiveness of this approach is required.

On the other hand, more consistent permeate qualities were obtained in the NF-MBR that employed polyamide (PA) membranes (Choi et al., 2006). The study also showed that PA membrane was sufficiently robust against biological degradation and no chlorine dosing was required for the long-term operation of NF-MBR. In fact, small amount of chlorine can cause structural changes in the active layer. However, PA membranes are more prone to fouling due to their hydrophobic nature. High concentration of organic and inorganic in the mixed liquor and the presence of microorganisms with were expected to cause serious fouling to the PA membrane. Periodic physical or chemical cleaning seems to be the only option to control the formation of cake layer (Choi et al., 2006). Other studies have attempted to use chemically and biologically stable ceramic membrane to ensure the production of permeates with consistent qualities (Zaviska et al., 2013, Phan et al., 2016).

In short, the degradation of membrane could adversely affect the permeate quality. Therefore, it is crucial to evaluate the long-term membrane stability of the NF membranes and develop techniques to control biological and chemical degradation of NF membranes. The development of biologically and chemically resistant membranes has offered a platform with variety of membrane options to overcome the issue of membrane degradation (Li et al., 2019). In this thesis, the membrane stability of NF membranes was evaluated through long-term NF-MBR operation in treating real municipal wastewater.

2.3.5.3 Low permeate flux

Water productivity can be directly related to the permeate flux and membrane area of the MBR system. The low permeate flux at 0.042 L/m^2 h or equivalent to 0.5 L/m^2 h bar was observed in the first NF-MBR employing a cellulose acetate membrane (Choi et al., 2002). The low permeate flux was attributed to the low transmembrane driving force of the system since the maximum pressure difference across the membrane in the submerged configuration was limited to the atmospheric pressure of 1 atm. As discussed earlier in section 2.3.3, side stream configuration was attempted and successfully increased the permeate flux to 4.5 L/m^2 h. However, the permeate flux was still low and not comparable to that of the conventional MF/UF-MBR which usually has a permeate flux of at least 15 L/m^2 h. To achieve a practical water productivity, large membrane area was used, therefore, increasing the initial capital cost and membrane maintenance and replacement cost.

Other than the low-pressure hollow fiber NF membrane (Liu et al., 2015) mentioned earlier, more studies focusing on developing high flux and fouling resistance NF membrane has offered great opportunity in improving the permeate flux in NF-MBR system (Cheng et al., 2015, Li et al., 2019). For example, the thin film composite NF membrane created based on an UF membrane grafted with poly(oxyethylenemethacrylate) was able to yield 10 times higher permeate flux than a cellulose acetate NF membrane (Asatekin et al., 2009). In addition, a hydrophilic thin film composite NF membrane created through the interfacial polymerization (IP) of the hydrophilicity of the PEG-based selective layer i.e., amino-functional polyethylene glycol (PEG) and trimesoyl chloride could yield a permeate flux of 13.2 LMH.bar^{-1} (Cheng et al., 2015). Based on the layer-by layer (LBL) electrostatic assembly method, Li and co-workers has developed a polydopamine (PDA)/polyethylenimine (PEI) modified low-pressure NF membrane that exhibit excellent antifouling performance and membrane stability in a fouling experiment filtering real municipal wastewater (Li et al., 2019). These NF membranes show great potential to be incorporated into the NF-MBR

system. With the proper membrane cleaning protocol in place, the issues pertaining to low permeate flux and membrane fouling were expected to be resolved in near future.

2.4 Implications for MBR-RO process

2.4.1 RO fouling in water reclamation process

Water reclamation from the secondary effluent often requires multiple pretreatments prior to the RO process owing to the high concentration of colloids (macromolecular organics and bacteria), soluble organics present in the secondary effluent (Wilf and Alt, 2000). However, multi-stage pretreatment processes involving MF/UF filtration, disinfection, and flocculation can be ineffective and result in RO feed with high fouling propensity (Qin et al., 2006, Khanzada et al., 2017). Membrane fouling in RO has been the major obstacle that hindered the widespread application of MBR-RO process for potable water reuse (Greenberg et al., 2005). The fouling in RO process possess several consequences in the membrane operation such as flux decline, increase in the operating pressure and the need of frequent membrane cleaning which shorten membrane lifespan and eventually lead to the replacement of new membrane. The cumulative effect of all these factors increases the production cost of potable water reuse significantly.

In view of the similarities shared between the NF and RO filtration, detailed information related to colloidal fouling, organic fouling, scaling and biofouling can be found in section 2.2.3. In the existing MBR-RO process, effluent organic matter (EfoM) which comprises organic compounds ranging from low to high MW, i.e., proteins, polysaccharides, amino-sugars, nucleic acids, humic and fulvic acids present dominantly in the MBR permeates and led to serious organic fouling in the RO process. The pretreatment of MF/UF membrane is usually ineffective in removing these EfoMs owing to their sizes which are mostly smaller than the pore size of MF or UF membranes.

The organic fouling is often escalated in the presence of divalent ions, i.e., Ca, Mg due to its ability to form ionic bridges that resulted in more compact fouling layers (Khanzada et al., 2017). In addition, due to the stronger intermolecular adhesion force between

alginate and BSA molecules in the presence of Ca, the formation of crosslinked alginate–calcium complexes could lead to more severe fouling. In the aspect of biofouling, the availability of carbon source in the RO feed could lead to biofilm development on the membrane surface and result in biofouling which significantly deteriorates the performance of the RO process (Suwarno et al., 2016). Scaling due to saturation of marginally soluble salts i.e., calcium phosphate could be critical especially when RO is operated at high recovery level (Greenberg et al., 2005).

With the NF-MBR as pretreatment, colloidal fouling is expected to be minimal due to the complete removal of colloidal particles and the high rejection properties of the NF membrane. The organic fouling can be potentially reduced to a great extent owing to the high rejection capacity of NF-MBR in removing organics with wide range of MW, including the low MW organics (Choi et al., 2007a). Due to the lower organic content in the NF-MBR permeates, biofouling is expected to reduce due to the depletion in carbon source. More importantly, NF membrane could reject divalent ions that are potential scalants in RO fouling, therefore, could potentially increase the RO recovery level for water reclamation.

2.4.2 Energy requirement

One of the barriers that hinder worldwide application and implementation of water reuse systems has been the insufficient data with respect to energy costs to convince the public and policymakers of the advantages of water reuse. While treatment efficiency of the treatment system is important, energy requirement and footprint of the technology must be considered so that the economic and environmental advantages of water reuse are not compromised. The energy requirements for two different water reclamation schemes, namely the CAS + MF/UF-RO and MBR-RO schemes are compared and summarized in Table 2-3. The total energy requirement for water reclamation under the CAS + MF/UF-RO scheme is 0.8–1.3 kW h/m^3 whereas the energy cost under MBR-RO scheme is slightly higher at 1.0 – 1.5 kW h/m^3. The higher in energy requirement under MBR-RO

scheme is mainly attributed to the air bubbling requirement to control fouling in MBR. However, MBR-RO scheme is more suitable for cities when land area is at a premium.

Table 2-3 Comparison of energy requirement for different water reclamation schemes (Adham et al., 2005, Tao et al., 2010).

Estimated Energy Requirement (kWh/m3)	***Water Reclamation Scheme***		
	CAS + MF/UF-RO	MBR-RO	NF-MBR+RO
Aeration for biological activity	0.3 – 0.6	0.1 – 0.2	0.1 – 0.3
Air bubbling for MBR fouling control	N.A.	0.4 – 0.6	N.A.
Hydraulic pressure for membrane filtration	N.A.	0.1 – 0.2	0.4 – 0.7
MF/UF pretreatment	0.1 – 0.2	N.A.	N.A.
RO process	0.4 – 0.5	0.4 – 0.5	0.2 – 0.4
Total	0.8 – 1.3	1.0 – 1.5	0.7 – 1.4

N.A. represents not applicable.

The energy requirement for RO process can be potentially reduced by system improvements such as development of improved fouling-resistant membranes, optimization of process configuration and brine management schemes, utilization of low-cost renewable energy and more effective pretreatment prior to RO process (Zhu et al., 2009). Here, NF-MBR has the potential to lower the energy cost for the RO process by replacing the conventional MBR process as a more effective pretreatment. Admittedly, the NF-MBR process is indeed a more energy-intensive process compared to conventional MBR process due to the provision of crossflow recirculation and high operating pressure (approximately 2 bar). However, with the improved secondary effluent, fouling associated with the energy intensive RO process can be potentially reduced, therefore, reducing both the energy and the membrane replacement costs for

RO process. By evaluating the reduction in operating energy for the RO process and the additional energy requirement for high operating pressure and crossflow recirculation for the NF-MBR, a better understanding of the overall energy cost for the NF-MBR+RO water reclamation schemes can be established.

2.5 Concluding Remarks

The foregoing literature review reveals research gaps and shed light on issues of relevance to NF-MBR development and the potential of NF-MBR in the MBR-RO process for water reclamation (Section 2.3 and 2.4). With the limited studies available for the NF-MBR, further studies are necessary to address the technological challenges and further develop the technology. In addition, a more holistic assessment on the effect of NF-MBR on the downstream RO process is mandated in this thesis. The following presents research issues of priority which this project seeks to address:

- The feasibility of stable-state nanofiltration membrane bioreactor (NF-MBR) in treating municipal wastewater;
- Long-term membrane stability under biologically active environment;
- Systemic investigation on the membrane fouling in the UF-MBR+RO and NF-MBR+RO process;
- The long-term effect of salinity build-up on the biomass characteristics, membrane fouling potential and foulants properties in the NF-MBR;
- The fouling control and cleaning methods for the sustainable long-term operation of the NF-MBR;
- Overall energy consumption of the NF-MBR+RO system.

Chapter 3

General materials and methodologies

3.1 Introduction

The purpose of this chapter is to describe the general materials and methods that are applied to the following chapters (chapter 4 to 6) in the thesis. The information pertaining to the NF-MBR system and the RO system which employed for the following experiments was provided. Analytical methods involved in determining the water qualities and membrane characterization were elaborated in detail. Additional descriptions were provided in subsequent chapters to address specific experimental design and methodology used, where necessary.

3.2 The lab-scale NF-MBR setup

The lab-scale NF-MBR setup was a moving bed biofilm reactor employing side-stream nanofiltration membrane modules respectively were set up as shown in Figure 3-1. The bioreactor had a total effective working volume of 7.0 L and was filled with K3 bio-carriers (physiochemical characteristics are presented in Table 3-1) to achieve the desired filling ratio according the experimental design. The dimension of a bio-carrier is 12 × Ø 25 (mm, W × D) with a surface area of 500 m^2/m^3 (Ping Yin Chemical Packing, China). The hydraulic retention time (HRT), pH and temperature of bioreactors were kept at 22 h, 6.8 ± 0.5, 20 ± 0.5^oC respectively. The permeate flux of the NF-MBRs was maintained by a mass flow controller (Brooks, USA) installed on the permeate stream. The pressures of feed, retentate and permeate were recorded by digital pressure transducers (Ashcroft, USA) connected to a data logging system (LabVIEW, National Instrument, USA).

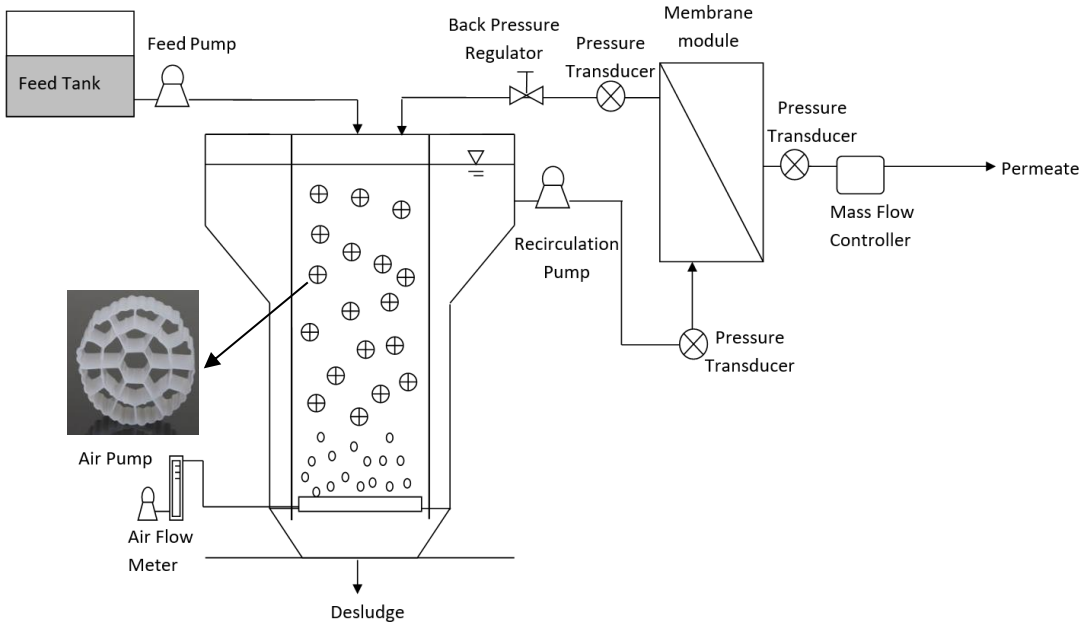

Figure 3-1. Schematic diagram of lab-scale MBRs.

Table 3-1 Properties of K3 bio-carriers

	NF membrane
Material	High-density polyethylene (HPDE)
Surface area (m^2/m^3)	500
Specify Gravity (g/cm^3)	0.98
Dimension (mm, W × D)	12 × Ø 25
Void Volume (%)	90.0
Applicable temperature (^oC)	5-40

3.3 NF and RO membrane

In this thesis, a novel low-pressure hollow fiber NF membrane developed by the Singapore Membrane Technology Centre (SMTC) was used to incorporate into the NF-MBR system. The highly permeable NF membrane was developed by using layer-by-layer electrostatic assembly method in combination with glutaraldehyde (GA) crosslinking (Liu et al., 2015). The layer-by-layer electrostatic assembly method has been increasingly used to synthesize high performance NF membranes due to its

simplicity and flexibility in modifying the charged skin layer without compromising the pure water permeability (Rajabzadeh et al., 2014). However, the LBL-based NF membrane was found drastically deteriorated in the presence of SO_4^{2-} in the feed water. Therefore, the GA crosslinking was adopted to improve the long-term stability of the LBL-based NF membranes and enhance the size exclusion ability by tightening the membrane surface pores (Liu et al., 2015). In addition, the crosslinking could tighten membrane surface pores and increase the hydrophilicity of the membrane. The membrane exhibits excellent divalent ions rejection of more than 90% and could achieve pure water permeability of ~ 17 $L/m^2h \cdot bar$. The properties of the NF membrane are summarized in Table 3-2.

Table 3-2. Properties of NF membranes (Liu et al., 2015)

	NF membrane
Material	Glutaraldehyde (GA) crosslinked layer-by-layer polyelectrolyte with PES UF membrane as substrate base
Pore size (MWCO, Da)	200-300
Active Layer	Lumen side
ID/OD (mm)	0.9/1.4
Ca^{2+} Rejection (%)	91.8
Mg^{2+} Rejection (%)	98.4
Pure water permeability ($L/m^2h \cdot bar$)	17

Note: MWCO: Molecular weight cut-off; ID: inner diameter; OD: outer diameter. The single salt rejection tests were conducted using 1000 ppm CaCl2 and MgSO4 solutions, respectively, based on the conductivity measurements.

3.4 The lab-scale RO system

Two identical RO systems were used to study the fouling potential of the permeates from the conventional MBR and NF-MBRs. The schematic diagram of the RO system is illustrated in Figure 3-2. Briefly, the RO setup comprised of a feed tank, a high-pressure pump (Hydra Cell D-03-S, USA), a chiller equipped with temperature controller (PolyScience 9106, USA), a stainless steel RO test cell. The chiller was used to maintain

constant temperature of 25 ± 1 ^{o}C in the feed stream. The stainless steel RO test cell was designed for flat sheet membrane with a flow channel of 310 x 60 x 0.8 mm with an effective area of 0.0186 m^2. The feed pressure and crossflow rate of the system were controlled by a back pressure regulator (SS-4R3A, Swagelok) and a flow control valve (Cole Palmer, USA). Mass flow controllers (LIQUI-FLOW L30, Bronkhorst, Netherlands) was installed in the permeate stream to maintain constant flux operation. The pressure and conductivity of the feed and permeate stream were continuously monitored by pressure transducers (EUTECH Instruments, USA) and conductivity meters (EUTECH Instruments, USA) respectively throughout the fouling experiment.

For the RO fouling experiment, RO flat sheet membranes (BW30, DOW FilmTec, USA) with an effective membrane area of 0.0186 m^2 were used. Properties of the RO membrane were shown in Table 3-3. The RO concentrate and RO permeate were recirculated to feed tank during the fouling experiment. The test solution in the feed tanks was replenished subsequently depends on the experimental protocol. Prior to each experiment, the RO system was cleaned with 0.1 M HCl (Merck, USA) for 1h, followed by 0.1 M NaOH (Merck, USA) for another 1h, and rinsed thoroughly with ultrapure water.

Table 3-3. Properties of RO membrane

	RO membrane (BW30)
Membrane Type	Polyamide Thin-Film Composite
Stabilized Salt Rejection (%)	99.5%
Maximum operating pressure (bar)	41
Maximum Temperature (^{o}C)	45
Free Chlorine Tolerance (ppm)	< 0.1
pH range	2-11

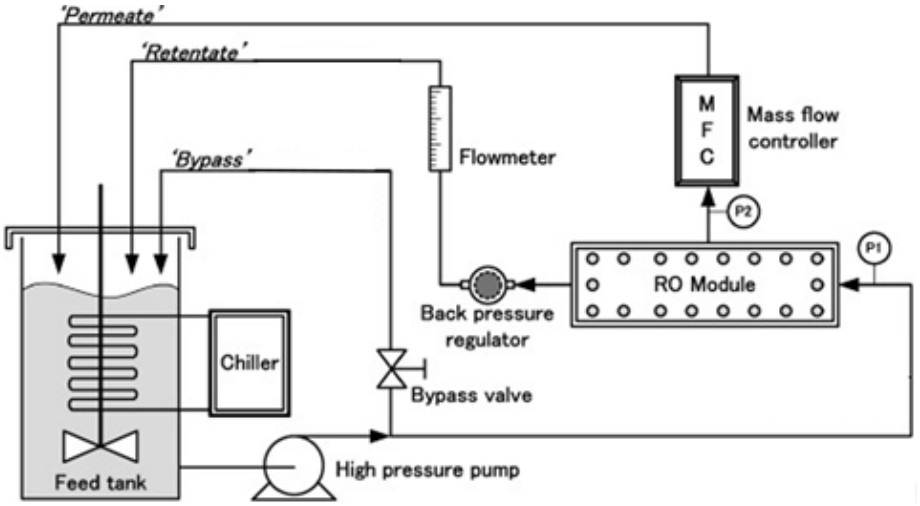

Figure 3-2. Schematic diagram of the lab-scale RO system.

3.5 General analytical methods

3.5.1 Water quality parameters

The feedwater, mixed liquor and permeate of the MBRs were sampled twice weekly for analysis. The supernatant of the feedwater and mixed liquor was obtained by centrifuging for 10 min at 4000 ×g and filtering through 0.45 µm membrane filter before analysis. The analyses included:

(i) Total organic carbon (TOC) (DOC is measured for the feedwater and the mixed liquor) and total nitrogen (Barnes et al.) were determined by a TOC/TN-V analyzer (Shimadzu, Japan);

(ii) Chemical oxygen demand (COD), ammonia, nitrite, nitrate and total phosphorus (Jarusutthirak et al.) were measured using the colorimetric method with a spectrophotometer (DR 3900, HACH, USA);

(iii) Concentrations of ions (i.e. Na, K, Ca, Mg, P, Si, and Fe) were determined by an inductively coupled plasma optical emission spectrometry (ICP-OES, Optima 8000, Perkin Elmer, USA);

(iv) The extracellular polymeric substances (EPS) content were determined by analyzing the concentrations of polysaccharides and proteins in the MBR permeates. The polysaccharides concentration was determined according to the phenol-sulfuric acid method with glucose as a standard and absorbance measurement at 490 nm using a spectrometer (HACH, USA) (Dubois et al., 1956). The protein concentration was determined by Bradford method with bovine serum albumin (BSA) as standard and absorbance measurement at 595 nm (Bradford, 1976).

(v) The conductivity and total dissolved solids (TDS) of feed, mixed liquor and permeate were measured using a multi-function meter (Eutech Instruments, USA).

3.5.2 Biomass Characterization

(1) Total biomass concentration

Total solid amount in the bioreactor was defined as the sum of mixed liquor suspended solids (MLSS) and total attached solids on the bio-carriers. Similarly, total biomass amount in the bioreactor was defined as the sum of mixed liquor volatile suspended solids (MLVSS) and total attached growth biomass on the bio-carriers. The attached samples on the bio-carrier was extracted by sonication (10 min) and vortex (1 min). The total attached solids/biomass was estimated by multiplying the attached solids/biomass amount extracted per bio-carrier and the total number of bio-carriers in the bioreactor. The total solids/biomass concentration was calculated by dividing the total solids/biomass amount by the effective reactor volume. The MLSS and mixed liquor volatile suspended solids (MLVSS) were measured according to Standard Methods (American Public Health et al., 2005). Briefly, the mixed liquor was filtered by glass fiber filter papers (47mm) before putting them into the 100 oC oven for drying overnight. The weight difference between the filter paper before sampling and the total weight of the dry solids plus filter paper was measured as the MLSS. Then, the samples were placed

inside the 550°C furnace for 30 min to burn off the volatile solids. The weight difference of the sample before and after burning was recorded as the MLVSS.

(2) ATP analysis

The intracellular ATP (i.e., live cells) and extracellular ATP (i.e., dead cells) concentrations were measured according to manufacturer's specifications (Kikkoman, Japan). In brief, the diluted mixed liquor sample were added and mixed with eliminating reagent for 30 min. Subsequently, 100 μL of ATP releasing agent solution was added for 20 s followed by the addition of 100 μL luciferin–luciferase reagent prior to fluorescence measurement by a luminometer (Lumitester C-110, Kikkoman, Japan). The intracellular ATP concentration was calculated using the conversion factor for the linear relationship between RLU values and concentrations of ATP standard solutions. The total ATP concentration was measured following the same procedure without adding the eliminating reagent. The extracellular ATP concentration was obtained by subtracting the intracellular ATP concentration from the total ATP concentration. The viability of the activated sludge was determined by the ratio of intracellular ATP concentrations to the total ATP concentrations.

(3) Specific oxygen uptake rate (SOUR)

The microbial activity was assessed by measuring the specific oxygen uptake rate (SOUR) of the activated sludge according to Standard Method 1683 (American Public Health et al., 2005). Briefly, the sample was well mixed and aerated until DO reached saturation level in a BOD bottle. Thereafter, DO was recorded periodically over a 15-minute period using a DO-sensing probe (Mettler Toledo, USA) and plotted against time. Oxygen uptake rate was defined as the gradient of the linear portion of the DO versus time curve. SOUR was calculated by the ratio of oxygen uptake rate over total biomass solids as shown below:

$$SOUR_T = \frac{OUR}{VS} \times \frac{60\ min}{h}$$

Where:
$SOUR_T$ = specific oxygen uptake rate at temperature (T), (mg/g)/h
OUR = oxygen uptake rate in the mixed liquor, (mg/L)/min
VS = total volatile solids in the mixed liquor, (g/L)

$$SOUR_{20} = SOUR_T \times \emptyset^{(20-T)}$$

Where:
$SOUR_{20}$ = specific oxygen uptake rate at 20 ^oC,
$\emptyset$ = 1.05 above 20 ^oC; 1.07 below 20 ^oC

(4) EPS extraction method

The separation of bound EPS and soluble EPS in the mixed liquor and foulant solution was done by centrifuging the foulant solution at 4000 ×g for 10 min at 4 °C. The supernatant was collected for soluble EPS measurement. The bound EPS was extracted by formaldehyde–NaOH method (Liu and Fang, 2002, Zhang et al., 2006). Briefly, the solid fraction was re-suspended in 10 ml of ultrapure water, followed by adding 12 μL of formaldehyde (36.5%; Sigma Aldrich, USA) and keeping for 1 h at 4 °C. After that, 0.8 mL of 1M NaOH was added and kept for 3 h at 4 °C. Subsequently, the solution was

centrifuged at 13200 ×g for 20 min and the supernatant was collected for bound EPS measurement. The EPS contents were determined by analyzing polysaccharides and proteins. The polysaccharides concentration was determined according to the phenol-sulfuric acid method with glucose as a standard and absorbance measurement at 490 nm using a spectrometer (HACH, USA) (Dubois et al., 1956). The protein concentration was determined by Bradford method with bovine serum albumin (BSA) as standard and absorbance measurement at 595 nm (Bradford, 1976).

(5) Particle size and zeta potential

Particle size of the activated sludge was measured by a Mastersizer (MS-2000, Malvern, UK). Zeta potential of the bioflocs was analyzed by a Zetasizer (ZEN3600, Malvern, UK).

(6) Microbial community analysis

To examine microbial community compositions, the suspended activated sludge samples in the NF-MBRs were collected during steady operation period and the cake layer foulants on the NF2 membranes were collected at Day 86 (i.e., at the end of filtration experiment). The genomic DNA of the microbial community was extracted from the samples by PowerSoil® DNA isolation kit (MO bio, USA). The 16S rRNA genes were sequenced by Illumina MiSeq platform using primers 357wF (CCTACGGGGNGGCWGCAG) and 785R (GACTACHVGGGTATCTAATCC). The sequencing results were analyzed by QIIME using the standard de novo operational taxonomic unit (OTU)-based approach.

3.5.3. Membrane autopsy

At the end of the experiment, membrane modules were removed for autopsy studies. To detach the foulant from the UF, NF or RO membrane surface, the hollow fibers (UF/NF) and membrane coupon (RO) were first soaked in 30 ml of ultra-pure water and followed by ultrasonication (Fisher Scientific, model FB15068) for 30 min and vortex for 1 min. The foulant solution was centrifuged for 10 min at 4000 ×g and filtered through 0.45 μm

membrane filter prior to analysis. In addition, to quantify the inorganic compositions of the foulants, the membrane samples were submerged in 10 mL of 2% nitric acid for acid digestion. The digested foulant solution was centrifuged at 4000 ×g for 10 min and then filtered through a 0.45 µm membrane filter. Finally, the supernatant was collected for inorganic element analysis by ICP-OES.

3.5.4 Foulants characterization

(1) Liquid chromatography-organic carbon detector

Dissolved organic carbon characterization (i.e. note that all samples were filtered with a 0.45 µm filter prior measurement) by liquid chromatography-organic carbon detector (LC-OCD) analyzer (LC-OCD Model 8, DOC-LABOR, Germany). LC-OCD is a size-exclusion based technique which is able to separate natural organic matter (NOM) into major fractions based on their molecular weight and assign them into different fraction group such as biopolymers, humic substances, low molecular weight organics acids and neutrals (Huber et al., 2011). In the OC chromatogram, peak A is known as the bypass peak which represents the total DOC concentration. Peak B, at retention time ~ 30 min, is known as the biopolymer peak. It usually refers to the organic fractions with a molecular weight (MW) of higher than 10 k Da (Chen et al., 2016). The biopolymer fraction is composed of polysaccharides and proteins that can be differentiated by the corresponding UV peak, in which, polysaccharides are not detectable with UV, thus the UV peak is caused by absorption through the associated proteins or by light scattering through the colloids (Rosenberger et al. (2006). Peak C, at retention time ~ 43 min, is known as the humic substance peak which corresponds with a UV peak, represents organic fraction with MW of ~500 Da. Peak D, at retention time ~ 46 min, represents the organic fraction with MW of ~ 300 Da, which is known as the building blocks. The organic fraction with MW of ~ 200-250 Da is known as the low molecular weight (LMW) acids which is represented by Peak E, at the retention time of ~ 43 min. All other peaks beyond retention time ~ 55 min represent the LMW neutrals and acids with MW

less than 200 Da. The concentration of each organic fraction was calculated by ChromCALC (LC-OCD Model 8, DOC-LABOR, Germany).

(2) Excitation-emission matrix fluorescence spectroscopy

Organic compounds characterization by excitation-emission matrix (EEM) (Vogel et al.) fluorescence spectroscopy using a fluorescence spectrophotometer (LS 55, Perkin Elmer Company, USA). The excitation wavelength was set from 200 to 400 nm whereas the emission wavelength increased from 280 to 550 nm with a 5 nm increment. Excitation and emission slits were set at 10 nm with a scanning speed of 1000 nm/min. The EEM fluorescence spectroscopy analysis was carried out to characterize the organics and SMP compositions of mixed liquor, permeate and foulant solution. The compositions of five fluorescence organic components were delineated based on their fluorescence in different range of emission and excitation wavelength suggested by Chen et al. (2003), namely aromatic protein I (tyrosine) (Region I), aromatic protein II (tryptophan) (Region II), fulvic acid-like substances (Region III), soluble microbial by-product-like substances (Region IV), and humic acid-like substances (Region V).

(3) Confocal laser scanning microscopy (CLSM)

CLSM (Leica, German) was employed to record the biofilm morphology after the membrane sample (1.3 mm × 0.45 mm) was stained with dyes. In detail, the biofilm on membrane surface were stained with LIVE/DEAD BacLight™ Bacterial Viability kits (Molecular Probes, USA) according to manufacturer's instruction. The live and dead cells in the biofilm were analyzed and the biovolume was calculated using IMARIS software (version 7.1.3, Bitplane, Switzerland).

The EPS staining procedure was conducted as follows (Adav et al., 2008). Briefly, 100 µl of 0.1M sodium bicarbonate buffer was added to the sample to maintain the amino groups in non-protonated status. Then 10 µl of 10 g/L fluorescein isothiocyanate (FITC, Molecular Probes, USA) solution was added to bind with proteins. The stained sample was placed on a shaker for 1 h. After that, 100 µl of 250 mg/L concanavalin A (Con A)

conjugated with tetramethyl rhodamine (Molecular Probes, USA) was added to the sample to bind with α-d-glucopyranose-D polysaccharides and incubated at room temperature for 30 min. The stained sample was then washed twice with PBS to remove unbound dye. After that, 100 µl of 300 mg/L Calcofluor white (Sigma-Aldrich, USA) was added to the sample for 30 min to stain the β-polysaccharides and subsequently the sample was washed twice with PBS to remove excess dye. Lastly, 60 µl of 100 mg/L of Nile red (Molecular Probes, USA) was employed to bind with the intracellular lipids, followed by washing twice with PBS prior to CLSM analysis.

(4) SEM-EDX

Surface morphological features and elemental composition of the clean and fouled membranes were analyzed by a scanning electron microscope (SEM) (FE-SEM, JEOL, Japan) equipped with an energy dispersive X-ray (EDX) spectrometer (ISIS, Oxford Instruments, UK). The membrane samples were stored in a -40 degree Celsius freezer before drying in a freeze drier overnight. Platinum sputter coating was done prior to the SEM-EDX scanning.

Chapter 4

The feasibility of NF-MBR+RO Process for water reclamation

4.1 Introduction

This chapter describes a feasibility study that aim to develop a high-flux NF-MBR (i.e., 10 L/m^{2}h) using the SMTC's in-house fabricated low-pressure hollow fiber NF membrane (with inside-out configuration) and integrate the NF-MBR with the RO process for high recovery water reclamation. The main objectives of this study are:

(1) to evaluate the performance of a NF-MBR+RO for high recovery water reclamation;

(2) to illustrate the membrane fouling mechanisms and examine foulant characteristics in the NF-MBR;

(3) to examine foulant characteristics in the RO and investigate the relationship between organic fractions in MBRs permeate and RO fouling.

(4) to estimate the energy consumption of the NF-MBR+RO at different recovery levels.

An UF-MBR+ RO system was used as a baseline for comparison. This study provides meaningful information for further improvement and scale-up of the NF-MBR+RO system.

4.2 Materials and methods

4.2.1 Experimental protocol

The general materials and methods were described in Chapter 3. Two identical lab-scale moving bed biofilm reactors employing side-stream ultrafiltration (defined as UF-MBR) and nanofiltration (defined as NF-MBR) membrane modules respectively were set up. Each bioreactor was filled with 117 pieces of K3 bio-carriers (i.e., filling ratio of 10%). No activated sludge was inoculated in the bioreactors. The aeration rate of bioreactors

was set at 3 L/min. The sludge retention time (SRT), hydraulic retention time (HRT), pH and temperature of bioreactors were kept at 30 d, 22 h, 6.8 ± 0.5, 20 ± 0.5°C respectively. The bioreactors were fed continuously with municipal wastewater collected from Ulu Pandan wastewater treatment plant of Singapore (after sieving with a 1 mm opening mesh). The operating parameters of UF-MBR and NF-MBR and the characteristics of the municipal wastewater are summarized in Tables 4-1 and 4-2, respectively.

Table 4-1. Operating parameters of UF-MBR and NF-MBR

Parameter	MBRs
HRT (h)	22
SRT (d)	30
Flux (L/m^2h)	10
Organic loading Rate (g COD/L.day)	0.43
F/M Ratio (g COD/g MLSS.d)	0.43
Crossflow velocity (m/s) of side stream membrane unit	0.20
pH	6.3 – 7.3
Aeration (L/min)	3.0
Dissolved oxygen level (mg/L)	5.5 – 6.5
Biocarrier filling ratio (%)	10

Table 4-2. Characteristics of the municipal wastewater (n=25)

Parameter	Concentration (mg/L)
tCOD	389.8 ± 169.9
sCOD	124.9 ± 45.1
DOC	48.3 ± 13.9
Ca^{2+}	28.9 ± 3.5
Mg^{2+}	7.9 ± 1.2
TN	40.7 ± 6.1
NH_4-N	40.9 ± 4.5
NO_3^--N	0.3 ± 0.2
NO_2^--N	N.D.
TP	8.2 ± 1.1
Conductivity (µs/cm)	859.5 ± 18.9

Note: tCOD: total chemical oxygen demand; sCOD: soluble chemical oxygen demand; DOC: dissolved organic carbon; TN: total nitrogen; TP: total phosphorus; N.D.: not detectable.

In this study, SMTC's in-house fabricated polyethersulfone (PES) hollow fiber UF membrane and low-pressure hollow fiber NF membrane with PES as substrate were used and their characteristics are summarized in Table 4-3. Each membrane module consisted of 25 pieces of hollow fibers (0.46 m in length; a total effective area of 0.031 m^2) and filtration was performed in an inside (lumen)-out (shell) configuration.

4.2.2 Membrane cleaning protocol

Periodic membrane cleaning was performed when the transmembrane pressure (TMP) reached the pre-set upper limit due to membrane fouling. The filtration process was stopped, membrane modules were removed and cleaned externally. After flushing the lumen side of the hollow fiber membrane with tap water at 500 mL/min for 2 mins, backwashing was performed (15 mins) by using distilled water at pressures of 0.5 and 2 bar for UF and NF membrane, respectively. When the membrane cleaning was no longer able to restore the TMP to the desired level, the fouled membrane module was replaced with a new module. In the NF-MBR, three new NF membrane modules were used, hereinafter, defined as NF1, NF2, and NF3; while in the UF-MBR, two new UF membrane modules were used, hereinafter defined as UF1 and UF2.

Table 4-3. Properties of UF and NF membranes (Liu et al., 2015)

	UF membrane	NF membrane
Material	PES	Glutaraldehyde (GA) crosslinked layer-by-layer polyelectrolyte with PES UF as substrate
Pore size (MWCO, Da)	50,000	200-300
Active Layer	N.A.	Lumen side
ID/OD (mm)	0.9/1.4	0.9/1.4
Ca^{2+} Rejection (%)	N.A.	91.8
Mg^{2+} Rejection (%)	N.A.	98.4

Note: MWCO: Molecular weight cut-off; ID: inner diameter; OD: outer diameter; N.A.: not applicable.

Two identical RO systems were used to study the fouling potential of the permeates from the two MBRs. The details of the RO system were described in Chapter 3. The RO flat sheet membrane (BW-30, DOW FilmTec, USA) with an effective membrane area of

0.0186 m^2 was employed in the RO test cell. The crossflow rate of the RO system was maintained at 18 L/h (i.e., equivalent to a crossflow velocity of 0.10 m/s) and the permeate flux was kept at 20 L/m^2h by the mass flow controller. In this study, the RO concentrate and RO permeate were recirculated to feed tank and the test solution in the feed tanks was replenished daily.

4.3 Results and discussion

4.3.1 Overall MBRs performance

Both NF-MBR and UF-MBR were operated for 60-80 days. The accumulation of dissolved organics and divalent ions was observed in the NF-MBR (Figure 4-1). For example, after 60 days of operation (i.e., both reactors tended to be stable based on the constant total organic removals as shown in Figure 4-2), the concentrations of DOC (~116 mg/L), conductivity (~ 2212 µs/cm), Ca^{2+} (~267 mg/L), Mg^{2+} (~108 mg/L) and PO_4^{3-} (~71 mg/L) in the NF-MBR were approximately 5.3, 2.4, 8.3, 13.5, and 2.8 times of that in the UF-MBR (DOC at ~22 mg/L, conductivity at ~ 930 µs/cm, Ca^{2+} at ~32 mg/L, Mg^{2+} at ~8 mg/L, and PO_4^{3-}at ~25 mg/L), respectively. The concentration of Ca^{2+}, Mg^{2+}, and PO_4^{3-} increased gradually and reached an equilibrium level at around day 10 due to high rejection properties of the NF membranes (NF1 and NF2). On day 52, a new NF membrane with higher rejection properties, NF3, was used. This has resulted in a further build-up of Ca^{2+}, Mg^{2+}, and PO_4^{3-} concentrations in the NF-MBR. The retention and accumulation of slowly-biodegradable and non-biodegradable organic compounds were inevitable in the high retention NF-MBRs (Figure 4-1). This finding was similar to the reported studies in the NF-MBR, FO-MBR and MD-MBR (Choi et al., 2007b, Qiu et al., 2016, Phattaranawik et al., 2008b).

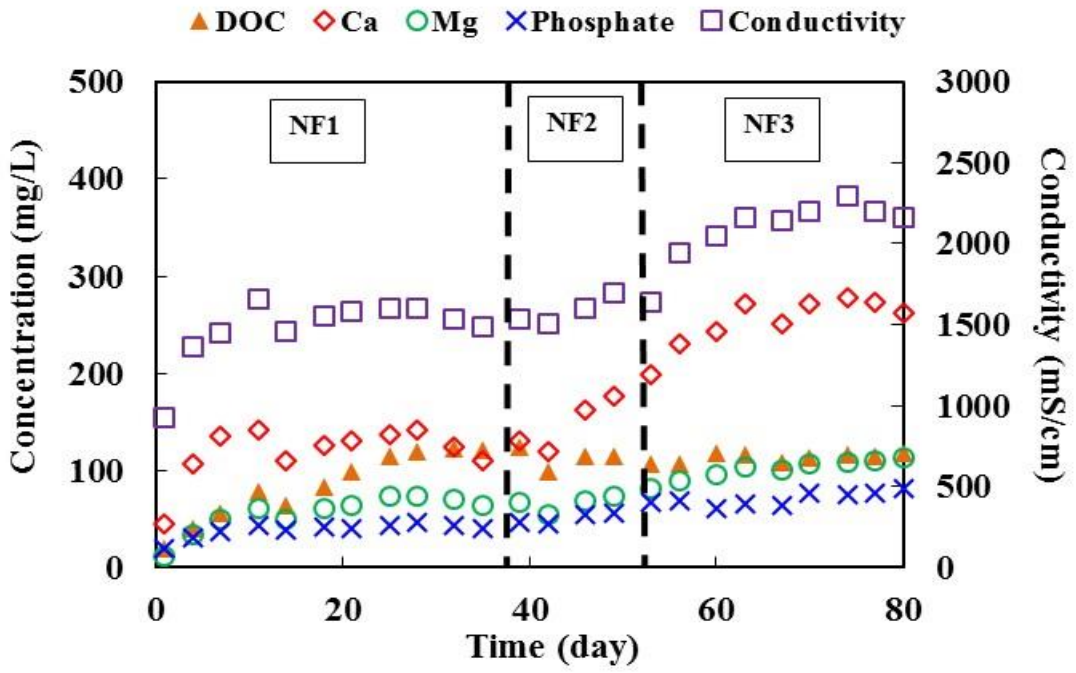

Figure 4-1. DOC, Conductivity, Ca^{2+}, Mg^{2+}, and phosphate concentrations in the NF-MBR.

Note: NF1 (Day 0-38), Physical cleaning performed when TMP increase 50%
NF2 (Day 39-50), NF3 (Day 50-80), Physical cleaning performed when TMP reached 2 bars.

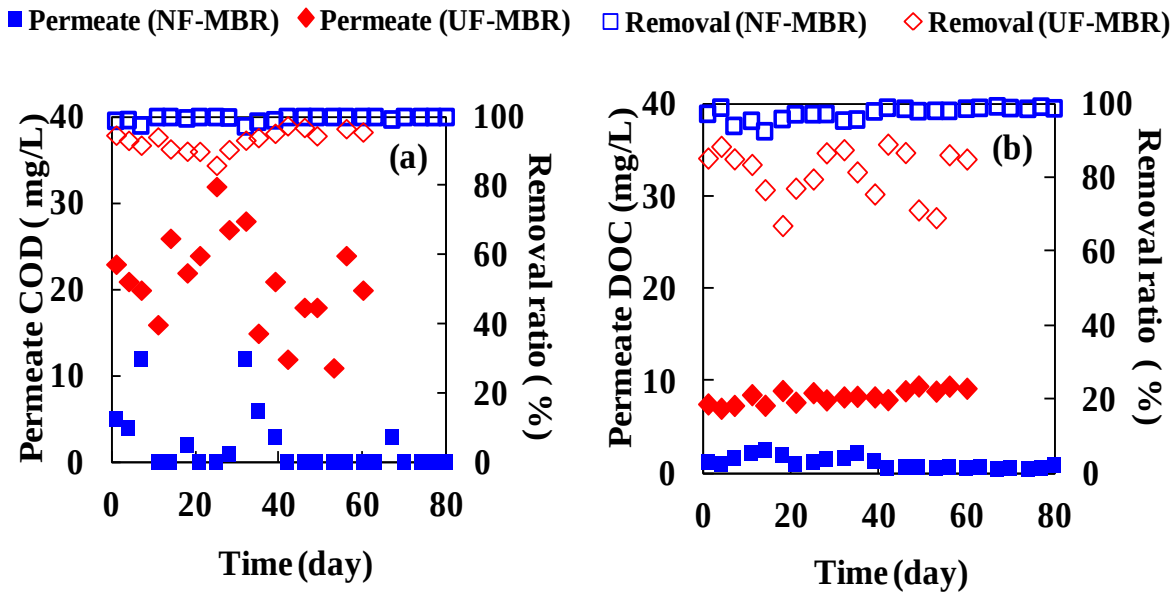

Figure 4-2. COD (a) and DOC (b) in the permeate of NF-MBR and UF-MBR.

The total attached growth biomass on the bio-carriers in NF-MBR and UF-MBR were maintained at 17.1 ± 4.1 g/m^2 and 17.4 ± 3.4 g/m^2, respectively; whereas the MLSS in the reactors were kept at 503 ± 69 and 513 ± 96 mg/L, respectively (Figure 4-3a and 4-3b). Despite the total biomass was relatively low (~1 g/L), NF-MBR and UF-MBR achieved excellent biodegradation of DOC of 80.5±8.2% and 76.7±9.5%, respectively (detailed mass balance calculation was presented in Supplementary Data). This implied that the elevated salts level (i.e., Ca^{2+}, Mg^{2+}) in the NF-MBR did not show significant negative impact on the biodegradation of organics; instead slightly greater biodegradation rate was observed. This could be attributed to two factors. Previous studies had pointed out the microorganisms derived from municipal wastewater could tolerate high salt concentration of up to 10 g/L without acclimation (Jang et al., 2013). Interestingly, the presence of additional salt (<10 g/L) could improve the biodegradability of organic carbon due to stimulatory effect on microorganisms (Ng et al., 2005). Furthermore, a longer retention time of the slowly-biodegradable organic substances could enhance their degradation.

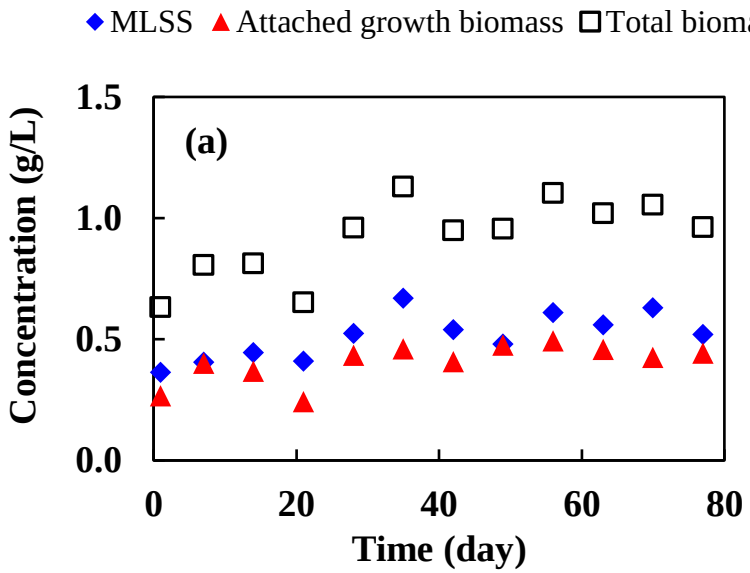

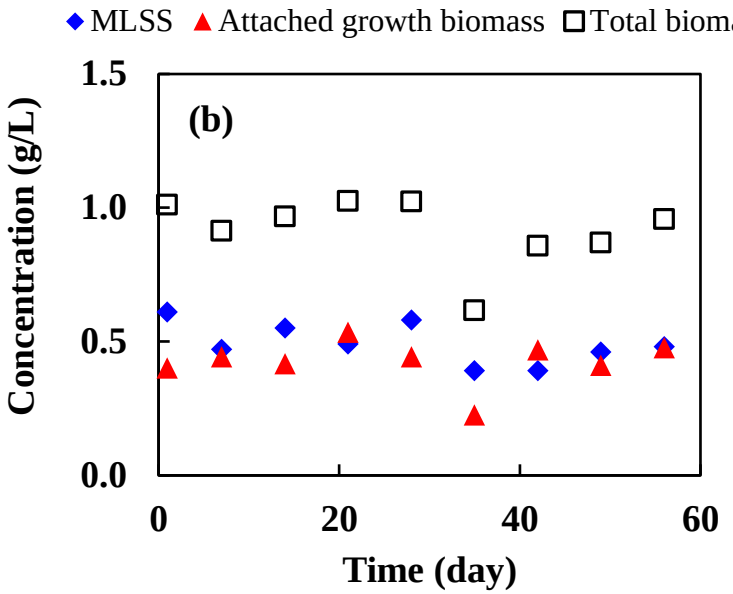

Figure 4-3. Total biomass in the (a) NF-MBR and (b) UF-MBR.

The sufficient oxygen supply (DO of 5.5-6.5 mg/L) in the bioreactor had resulted in low NH_3-N and high NO_3-N concentrations in the mixed liquors of both bioreactors. The ammonia removal of above 80 % was achieved through nitrification in UF-MBR whereas ammonia removal of above 90 % was achieved in NF-MBR. The concentrations of phosphate in the mixed liquor of NF-MBR were more than doubled the concentrations in UF-MBR due to the rejection properties of the NF membrane. Without the provision of anoxic condition in the MBR systems, the denitrification process could not take place to convert nitrate to nitrogen gas, therefore, no noticeable TN removal was observed throughout the operation. Similarly, TP removal through biological process was also negligible due to the absence of anaerobic environment that was essential for the growth of phosphorus accumulating organisms (PAO).

Figure 4-2 shows the COD and DOC levels in the permeates and removals of both MBRs, respectively. The NF-MBR produced permeate with DOC concentrations in the range between 0.5 to 2.5 mg/L, much lower than the permeate of UF-MBR, i.e., in the range between 7.0 to 9.5 mg/L. The overall COD and DOC removal rates in the NF-MBR were

99.6±0.8% and 97.5±1.8%, significantly higher than the UF-MBR (93.4±3.0% and 81.3±6.9%, respectively).

In addition, the permeate qualities of NF-MBR and UF-MBR were compared as shown in Figure 4-4. In general, the permeate of NF-MBR had lower concentrations of proteins (~12 times lower), polysaccharides (~1.6 times lower), Ca^{2+} (~2.3 times lower), Mg^{2+} (~5.2 times lower) and PO_4^{3-} (~1.4 times lower) compared to permeate of UF-MBR. The improved quality of the MBR permeate (i.e., RO feed water) due to better retention property of the NF membrane would contribute to less fouling in the subsequent RO process.

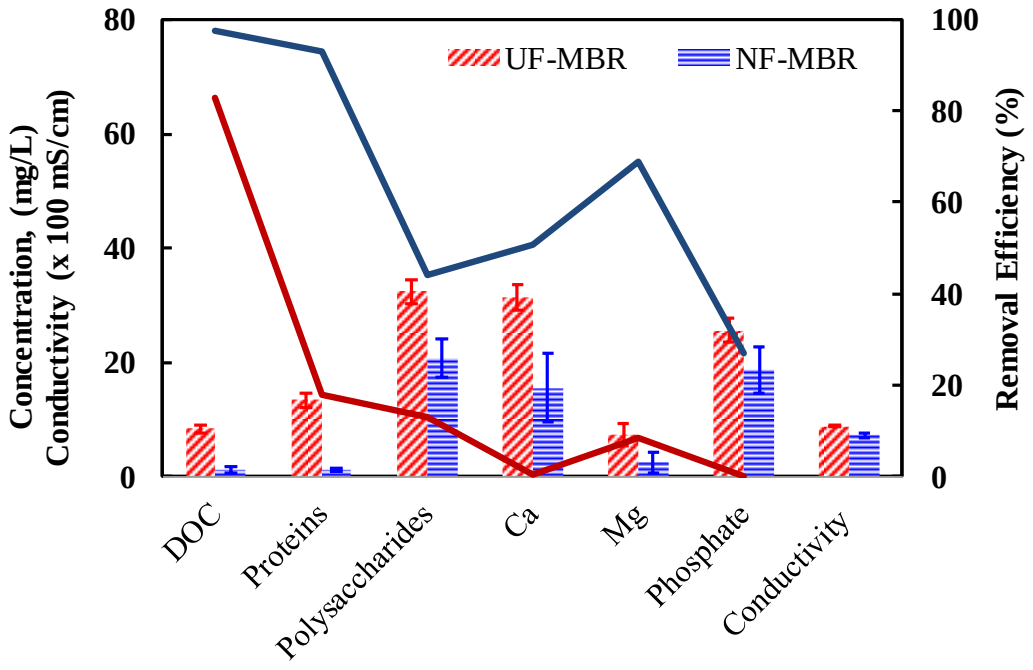

Figure 4-4. Comparison of permeate quality of NF-MBR and UF-MBR.

4.3.2 Membrane performance

4.3.2.1 Membrane stability

The stable membrane performance as evidenced by the stable organic matter and divalent ions rejection throughout the experimental period indicated that the PES based NF

membrane was sufficiently robust against biological degradation and no antibacterial reagent, i.e., chlorine dosing was required for the operation of NF-MBR. The NF membrane, NF1 was exposed to the mixed liquor for almost 40 days and no deterioration in the permeates quality was observed. The LBL-GA crosslinked NF membrane exhibited excellent biological and chemical stability in the biologically active environment, therefore, it is suitable to be incorporated into the NF-MBR system. The robust structure and chemical stability of the LBL deposition layer was mainly attributed to the GA crosslinking (Liu et al., 2015). However, the structural stability of the LBL-based NF membrane could be compromised under alkaline conditions, i.e. pH > 8, therefore, alkaline chemical cleaning agents such as NaOH is not suitable to be used for this membrane.

4.3.2.2 TMP profile

Figure 4-5a and 4-5b illustrate the TMP profiles of NF-MBR and UF-MBR, respectively. To control membrane fouling, periodic water flushing and backwashing were performed when the TMP had risen to the pre-set TMP levels. In the NF-MBR, from Day 0 to 38, the periodical cleaning of NF membrane (i.e., NF1) was performed when the TMP reached to 1.5 times of the initial TMP. During the early stage of operation (Day 0-12), a gradual increase in TMP was observed. This could be attributed to (i) the increase in osmotic pressure due to the build-up of rejected inorganic ions (Ca^{2+}, Mg^{2+}, PO_4^{3-}, etc.) and organic molecules in the bioreactor (Figure 4-1); and (Hori et al.) the cake formation due to the deposition of suspended and colloidal particles, soluble microbial products and microorganisms on the membrane surface that increased the overall resistance and possibly the cake enhanced osmotic pressure (CEOP) effect (Tang et al., 2011).

After first backwashing of NF1 on Day 7, the TMP could not return to the original value of ~150 kPa, mainly due to a continuous increase in osmotic pressure (i.e., as indicated by the increase of conductivity, Figure 4-1). After 6 days of filtration, the second backwashing was performed when the TMP reached ~220 kPa, the TMP could not return to its original value and was even higher than the value after first backwashing. In the

third cycle which lasted ~ 7 days, the TMP rise was more notable, hence, pure water flushing was performed to remove the loosely bound cake layer before backwashing. Nevertheless, a rapid fouling rate of ~ 150 kPa/day was observed in the 4th cycle and the TMP reached the upper limit of ~ 350 kPa, where the constant flux operation could not be attained and dropped from 10 L/m^{2}h to 8.5 L/m^{2}h. The duration of 2 subsequent cycles became shorter (3-4 days). Also, it was observed that when the TMP exceeded ~250 kPa, the fouling rates increased exponentially (for the last 3 cycles). This could be attributed to the formation of a more compressed cake layer at a high operating pressure of ~ 400 kPa (Teychene et al., 2011), which was not effectively removed by the employed cleaning method.

A new cleaning protocol in an attempt to prolong the NF membrane lifespan was adopted in the operation of NF2. It was hypothesized that more frequent physical cleaning was beneficial in removing the loose cake layer by shear and uplift forces when the TMP rise was low. To prevent the cake compression or collapse under a high-pressure condition, a combination of water flushing and backwashing was performed when the TMP reached an upper limit of 200 kPa. After implementing the new cleaning protocol, the cycle duration was reduced to around ~1.5-2.5 days. Unexpectedly, a sudden jump in TMP to ~320 kPa at Day 12 occurred due to unattended operation over the weekend. Thus, the membrane was replaced.

In NF3, frequent physical cleaning was performed, i.e., cycle duration of 1 to 3 days (when TMP reached an upper limit of 200 kPa). The lifespan of NF3 could be prolonged to ~26 days without any chemical cleaning.

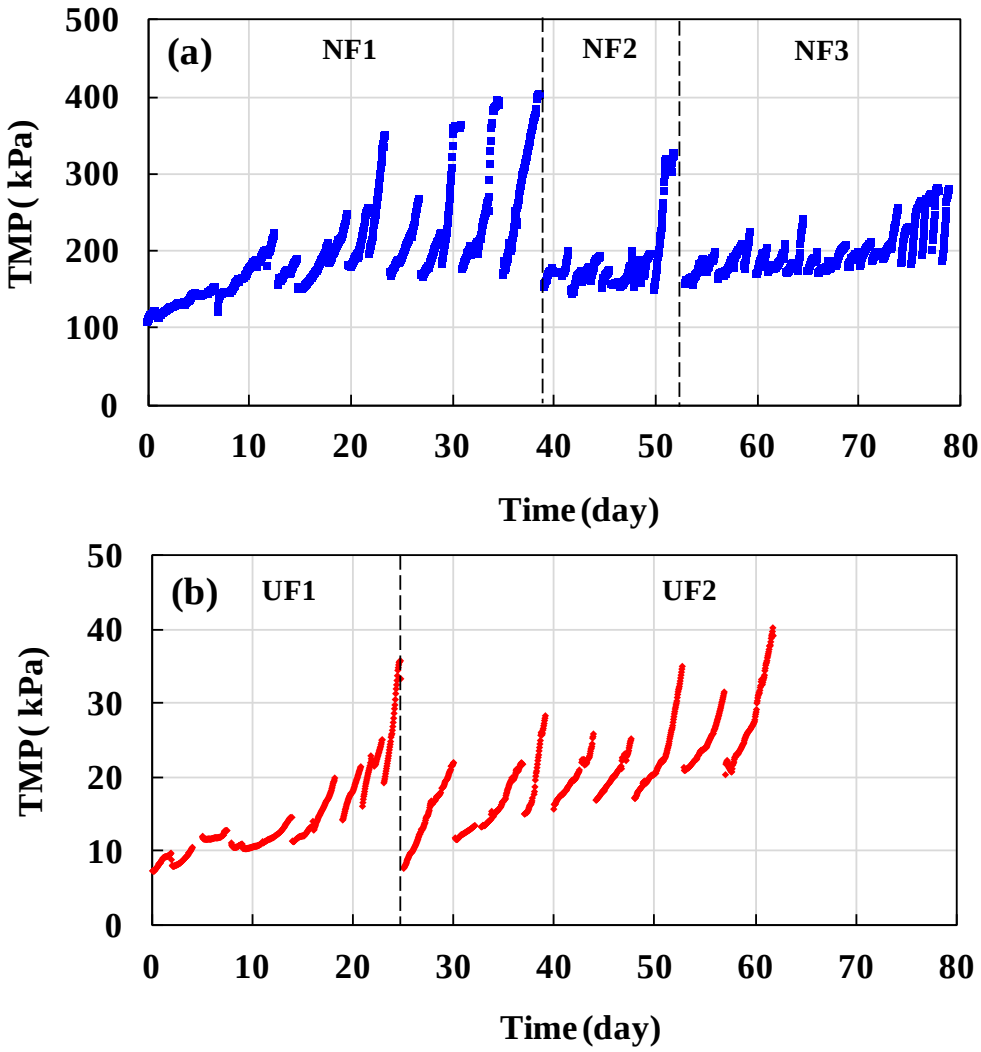

Figure 4-5. TMP profiles in the (a) NF-MBR and (b) UF-MBR.

On the other hand, in the UF-MBR, the TMP increased from an initial value of ~10 kPa to 40 kPa within 25 days during start-up period (for UF1) and ~ 37 days during the stabilization period (For UF2). The TMP profile of UF2 was compared to the TMP profile of NF3 (from 150 kPa to ~250 kPa in 26 days). In general, the UF membrane was cleaned every 3-5 days, which had lower cleaning frequency compared to the NF membrane.

4.3.3 Fouling mechanism

To further clarify the membrane fouling mechanisms in the NF-MBR and UF-MBR, the membrane pure water permeability (PWP) was measured (at a fixed pressure of 100 kPa) after each physical cleaning cycle (Figure 4-6a). A gradual decline of the NF membrane PWP over time was noticed, which means predominance of cake layer fouling and slow build-up of irreversible fouling. On the other hand, the UF membrane experienced (i) a dramatic drop in the PWP in the first cycle, and (Hori et al.) a continuing loss in the PWP where irreversible fouling has caused 90% loss in PWP after 7 cycles. These observations implied that the membrane fouling mechanisms in the NF-MBR and UF-MBR appeared to be dissimilar. The fouling experienced by the NF-MBR was highly reversible by physical cleaning due to the formation of cake layers on the NF membrane (it is noted that the NF membrane with pore size distribution ranging from 200-300 Da). In contrast, irreversible fouling was predominant in the UF-MBR as internal pore blocking and pore plugging were likely to take place in the UF membrane. Despite the difference in the content of mixed liquors where the NF-MBR had greater amount of potential foulants than UF-MBR as well as the difference in fouling mechanisms, both membranes exhibited approximately similar final value of irreversible fouling resistance (i.e., $R_{irr} = R_{total} - R_{membrane}$) as shown in Figure 4-6b. The results suggest that both membranes may have very similar amount of attached foulants that cannot be easily removed by the employed physical cleaning. Upon examining the TMP and resistance data, the additional pressure (i.e. energy), ΔTMP (Figure 4-6c), required for UF-MBR was mainly to overcome the increase in irreversible fouling rather than reversible fouling. Conversely, the main contribution for the additional pressure in the NF-MBR was due to the CEOP effect. The magnitude of total resistance (i.e., reversible and irreversible fouling) of the NF-MBR was similar to that in the UF-MBR as both had the same amount of extracted foulants (refer to Section 4.3.4).

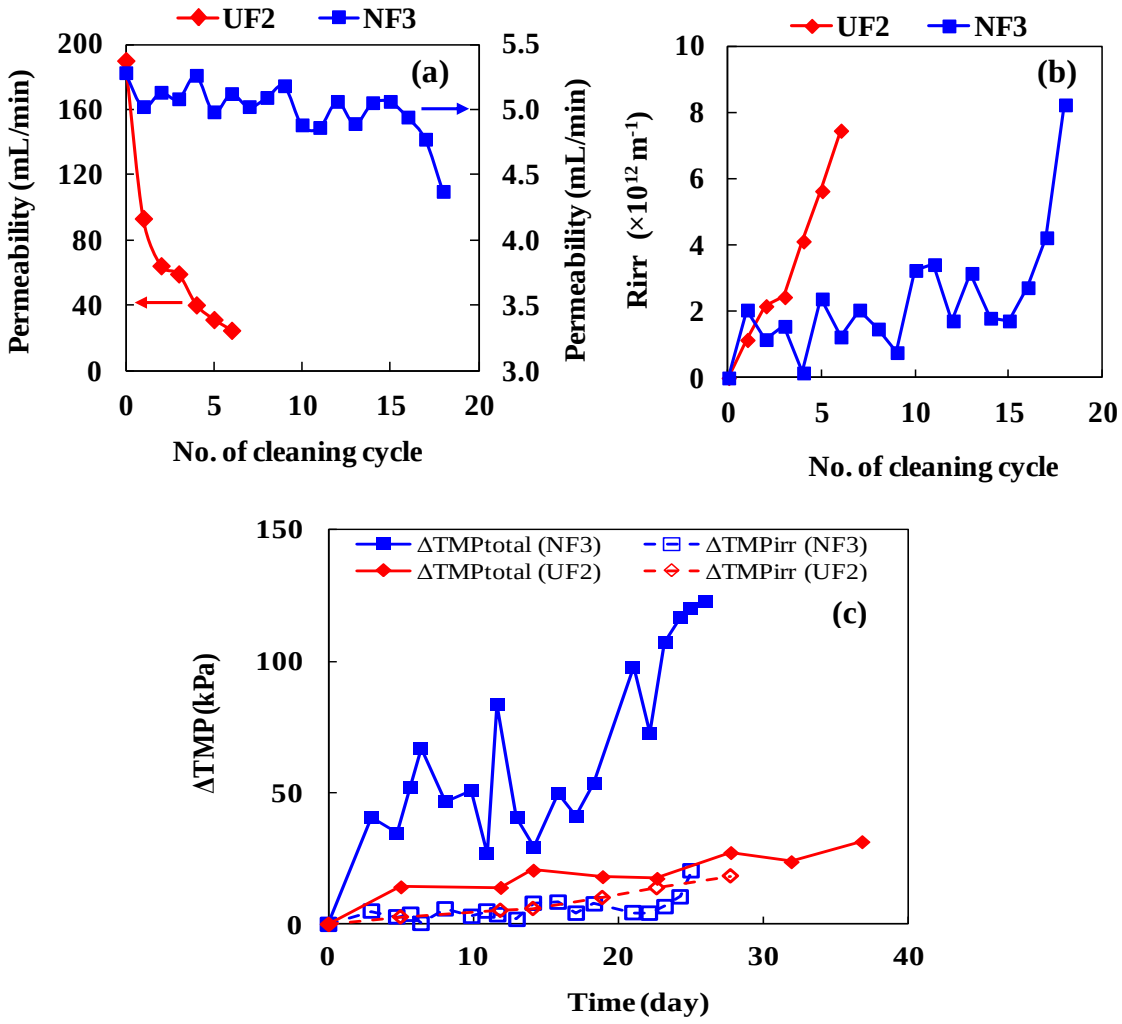

Figure 4-6. (a) Membrane water permeability, (b) irreversible fouling resistance after each cleaning cycle, and (c) ΔTMP increase for UF2 and NF3. Note that the test period is 37 and 26 days for UF2 and NF3, respectively.

Based on the experimental data, to achieve sustainable operation of high retention NF-MBR, it is crucial to maintain the system at low operating pressures (i.e., by frequent membrane cleaning) to prevent the collapse and compression of the cake layer, which could possibly contribute to the irreversible fouling. Nevertheless, effective periodically physical cleaning strategies (backwashing and flushing) could help extend operation lifespan of the membrane. This finding allows us to further optimize physical membrane fouling control methods in the NF-MBR in order to achieve better membrane

performance, for example, employing two-phase flow cleaning protocol (Wibisono et al., 2014).

4.3.4 Organic foulant analysis

From LC-OCD analysis, the organic fractions in the feed, mixed liquor, permeate of both MBRs and the key organic fractions that are responsible for organic fouling in MBRs and ROs were presented in Figure 4-7 and Table 4-4. The contribution ratio of each organic fraction to the DOC was presented in Figure 4-8. In general, the biopolymer fraction (typically MW >10 kDa) accounting for ~24 % of the total DOC in the feed was removed effectively in both MBRs (>98.5%). The UF-MBR removed less humic substances (59%), building blocks (70%), and LMWs (76%) than the NF-MBR (>95%). It was noted that humic substances (MW ~500 Da), building blocks (MW ~300 Da), LMWs (MW ~200-250 Da) had smaller sizes than the UF membrane pore size (~50 kDa). Partial removal of these substances by the UF membrane could be due to retention by the cake layer formed on the membrane or adsorption in the membrane pores (Aslam et al., 2017).

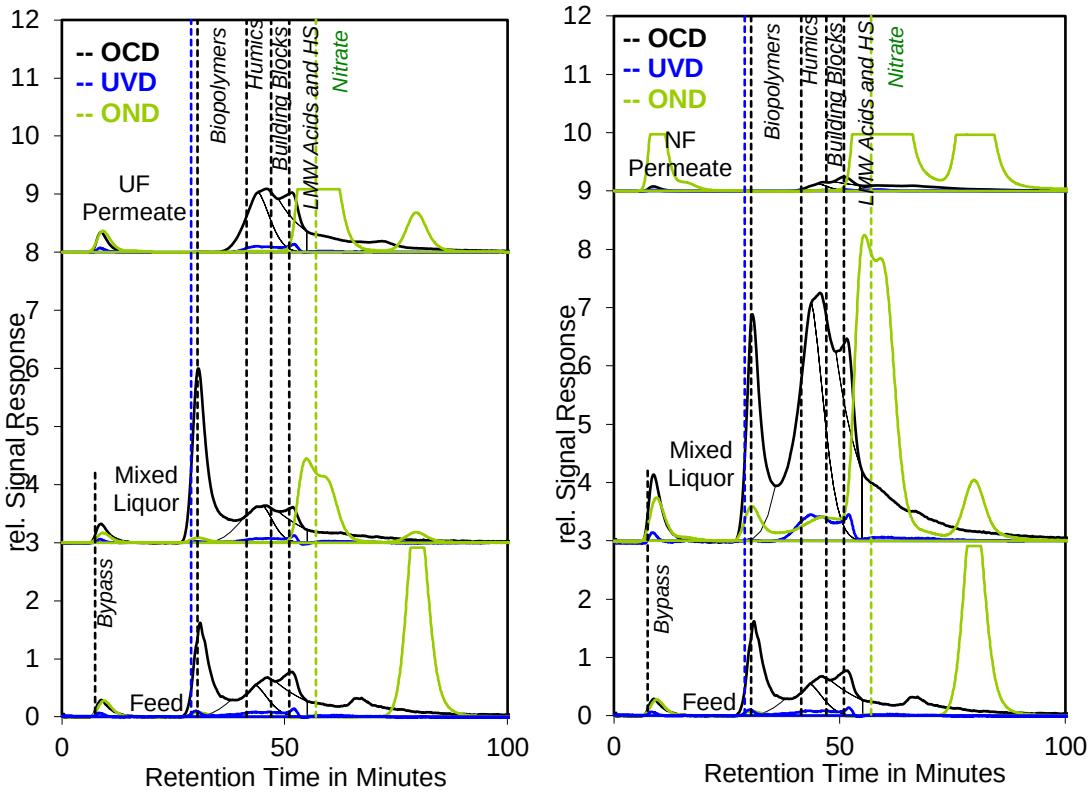

Figure 4-7. LC-OCD chromatograms of feed, mixed liquor and permeate of UF-MBR and NF-MBR.

The high rejection of organic substances by the NF membrane resulted in their accumulations in the NF-MBR with concentration factors of 2.1, 6.0, 4.9, and 2.5 for biopolymers, humic substances, building blocks, and LMWs, respectively. The difference in the concentration factors could be due to the difference in biodegradability of these compounds; for example, biopolymers and LMWs were easily biodegraded than humic substances and building blocks. This finding was similar to the observation in the high retention FO-MBR (Qiu et al., 2016). The nominal retention time of the soluble organic matters in the NF-MBR was reflected by its SRT instead of HRT. Thus, the retention time of trace organic contaminants (TrOCs) in the bioreactor was increased by 33 times from its HRT of 22 hr to SRT of 30 day in the NF-MBR for more effective biodegradation.

Table 4-4. Concentrations of dissolved organic fractions in the feed, mixed liquor, permeate and foulant of the MBRs and ROs.

		DOC	Biopolymers	Humic substances	Building blocks	LMW
	Feed (mg/L)	35.6	8.4	7.8	5.0	8.2
UF-MBR + RO	Mixed Liquor (mg/L)	16.7	7.7	4.1	2.0	2.8
	Permeate (mg/L)	8.0	0.1	3.2	1.5	2.0
	UF foulant[a] (mg/m^2)	201.2	159.2	N.D.[e]	37.6	13.4
	RO foulant[b] (mg/m^2)	104.5	45.3	N.D.	25.4	32.5
NF-MBR + RO	Mixed Liquor (mg/L)	109.5	17.8	46.9	24.3	20.9
	Permeate (mg/L)	0.9	N.D.	0.1	0.1	0.4
	NF foulant[c] (mg/m^2)	198.3	128.1	43.4	17.2	37.8
	RO foulant[d] (mg/m^2)	22.6	7.0	N.D.	4.6	5.6

[a] UF2 membrane was removed for autopsy at the end of cycle.
[b] RO membrane was operated for ~8 days, after which a TMP of 6.5 bar was reached (equivalent to ~ 20% increase in TMP).
[c] NF3 membrane was removed for autopsy at the end of cycle.
[d] RO membrane was operated for ~26 days, after which a TMP of 6.5 bar was reached (equivalent to ~ 20% increase in TMP).
[e]N.D. represents "not detectable".

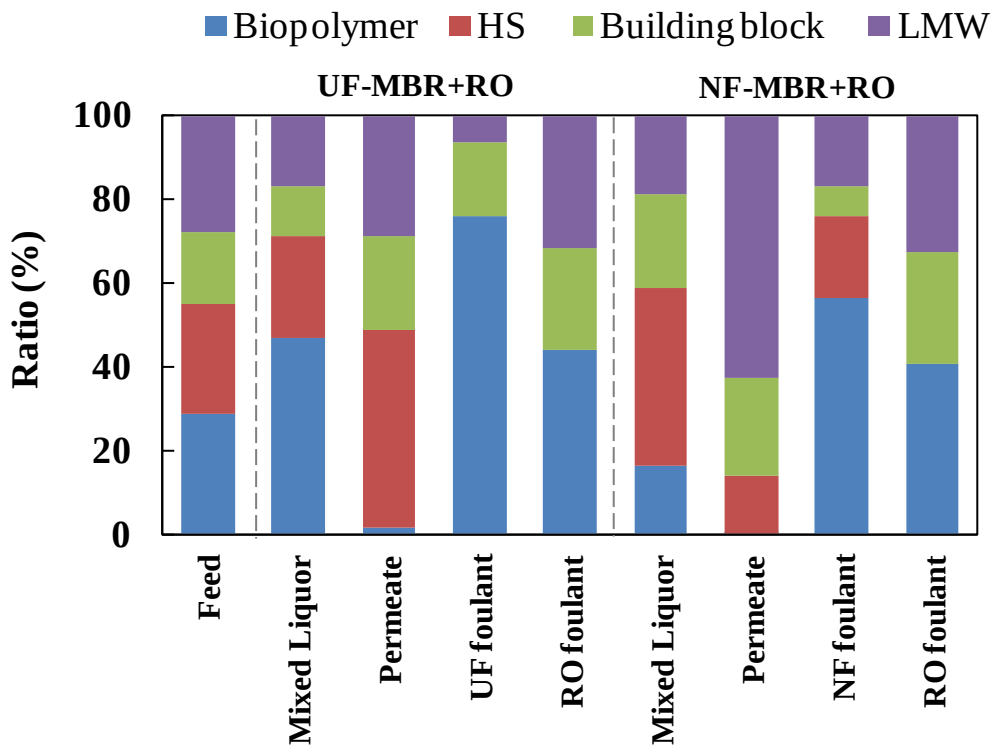

Figure 4-8. Contribution ratios of dissolved organic fractions in feed, mixed liquor, permeate and foulants of UF-MBR+RO and NF-MBR+RO.

The EEM fluorescence spectroscopy analysis was also carried out to characterize the organics and SMP compositions of mixed liquor, permeate and foulant solution. The compositions of five fluorescence organic components were classified according to the regional classification suggested by Chen et al. (2003), namely aromatic protein I (tyrosine) (Region I), aromatic protein II (tryptophan) (Region II), soluble microbial by-product-like substances (Region III), fulvic acid-like substances (Region IV), and humic acid-like substances (Region V) as presented in Figure 4-9. It was observed that the humic acid-like substances (Region V) had a much stronger intensity in the mixed liquor of the NF-MBR compared to the UF-MBR (Figure 4-9a and 9b). This can be explained by the high rejection of humic acid-like substances by the NF membrane and was corroborated by LC-OCD results discussed above. As a result, the permeates from the UF-MBR demonstrated a much higher intensity in Region III (soluble microbial by-product-like substances), Region IV (fluvic-like substances), and Region V (humic-like

substances) compared to the permeates from NF-MBR (Figure 4-9e and 9f). Although no obvious protein-like fluorescence peak was observed in the EEM spectra contour, proteins in MBR permeates were detected by the chemical method as shown in Figure 4-9. Our findings were in agreement with Wu et al. (2012), in which the aromatic protein-like peaks (tyrosine and tryptophan) may be obscured by the other peaks due to their strong signals. It was known that the aromatic proteins present in the mixed liquor were the most difficult to break down in the conventional MBR (Zhang et al., 2016). Due to their persistence to the biodegradation, these aromatic proteins present subsequently in the MBR permeates and become potential foulants to the RO process. However, in the case of HR-MBR, low intensity of aromatic proteins was observed in the NF-MBR permeates, indicating that NF membrane was effective in retaining aromatic proteins within the bioreactor.

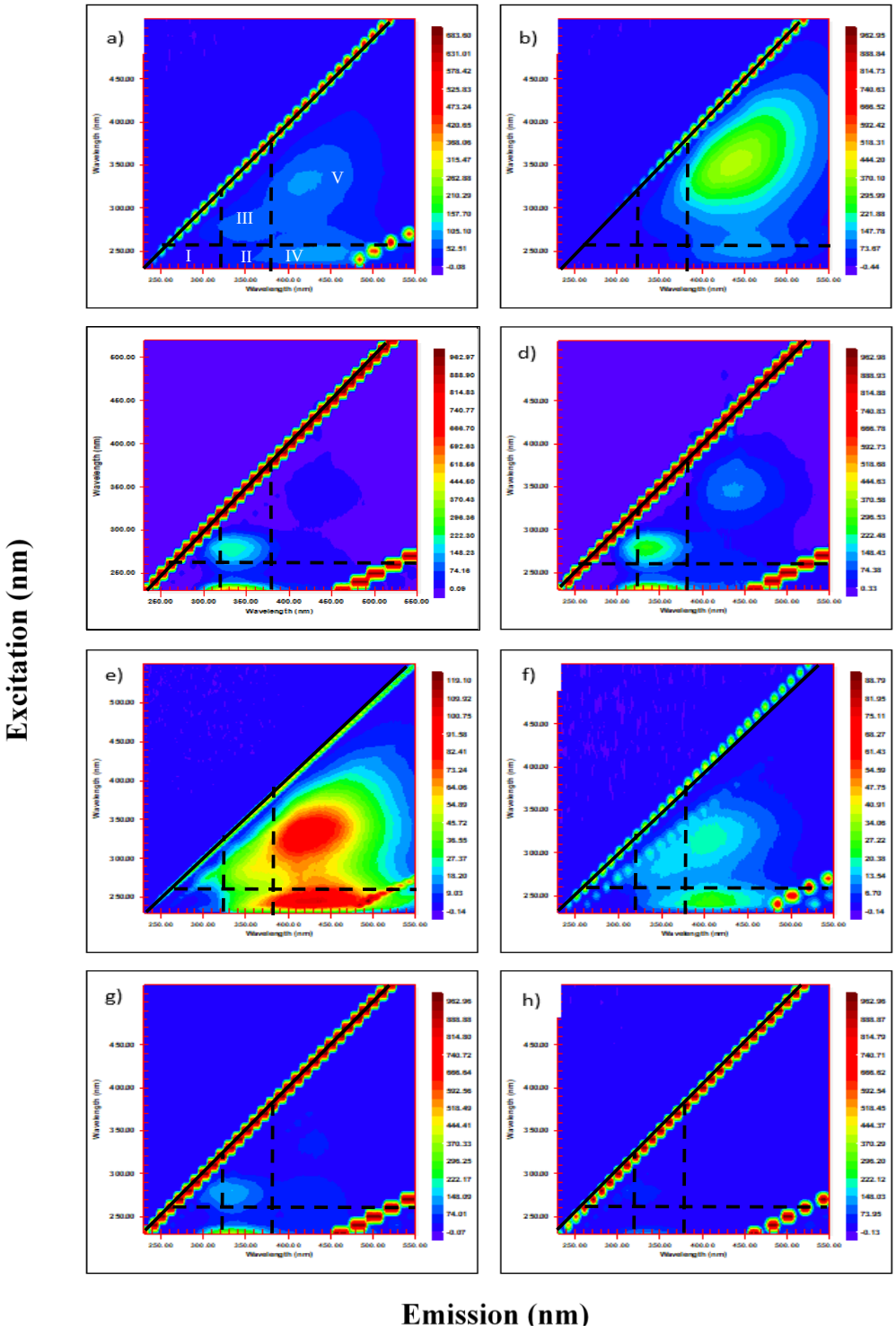

Figure 4-9. Fluorescence EEM spectra of. a) MLS of UF-MBR; b) MLS of NF-MBR; c) soluble foulants from UF membrane; d) soluble foulants from NF membrane; e) UF-MBR permeate; f) NF-MBR permeate; g) soluble foulants from

the RO membrane fed with UF-MBR permeate; h) soluble foulants from the RO membrane fed with NF-MBR permeate.

4.3.5 Correlation between organic fractions in mixed liquor and fouling

In the UF-MBR, majority of the foulants were biopolymers (75.7% or 159.2 mg/m^2) due to the high retention property of the UF membrane towards large MW biopolymers. However, it shall be noted that despite the smaller amount of the low MW fractions, i.e., building blocks and LMW, in the foulant, the impact of these components towards the overall resistance could be more critical than the biopolymer fraction due to the effect of pore plugging that resulted in irreversible fouling (Chen et al., 2016). On the other hand, in the NF-MBR, the foulants were comprised of 56.6% biopolymers (128.1 mg/m^2), 19.2% humic substances (43.4 mg/m^2), 7.6% building blocks (17.2 mg/m^2), and 16.7% LMWs (37.8 mg/m^2). In addition, by comparing the ratio of organic fractions in the mixed liquor and foulant, it was noticed that the NF membrane was more prone to fouling caused by biopolymer than other organic fractions. Furthermore, both extracted foulants from UF2 and NF3 membranes have comparable amount of DOC and organic fractions, which corroborated with the fouling resistance tendency (Figure 4-6).

4.3.6 RO performance

4.3.2.1 TMP Profiles of ROs

After about 20 days of operation of both MBRs, the permeate of UF-MBR and NF-MBR were collected and directly fed to the respective RO systems to assess the fouling propensity of the MBRs permeate. At recovery of ~ 0% (since the permeate was fully returned to the RO feed tank), the permeate of UF-MBR caused more severe fouling on RO membrane (~3.7 times higher) compared to the permeate of NF-MBR (Figure 4-10a). The higher fouling rate observed in the RO system fed with UF-MBR permeate was corroborated by the presence of higher amount of soluble organic compounds (Figure 4-4 and Table 4-4). This could result in organic fouling by adsorption of the organics onto the membrane surface (i.e., formation of conditioning film), which subsequently initiated the bacterial deposition (Suwarno et al., 2016). Further, these

organic compounds could serve as the carbon sources which promote the biofilm formation on the RO membrane.

In another attempt to simulate the membrane fouling at a high recovery of 90%, the collected MBRs permeate were concentrated by discharging the RO permeate until the concentration equivalent to 90% recovery was attained. Subsequently, the test was continued with a full recycle of permeate back to the feed tank to assess the membrane fouling. As shown in Figure 4-10b, the initial TMP increased from 5.3 to 8.5 bar and from 4.5 to 7.0 bar when the recovery ratio was increased from 0 to 90% for UF-MBR and NF-MBR, respectively. The lower initial operating pressure required for the concentration process in the NF-MBR could be attributed to its superior permeate quality with less divalent ions and dissolved organics. At a high recovery rate of 90%, the membrane fouling is more severe compared to that at 0% of recovery ratio, i.e., the dTMP/dt at ~ 0.30 and 0.094 bar/day for the RO system fed with UF-MBR and NF-MBR permeate, respectively. Nevertheless, with the improved quality of the RO feed water, the fouling rate of the RO membrane in the NF-MBR+RO was ~ 3.3 times lower than that in the UF-MBR+RO. The lower fouling tendency could translate into energy saving and operation cost saving (e.g., chemical cleaning) associated with fouling.

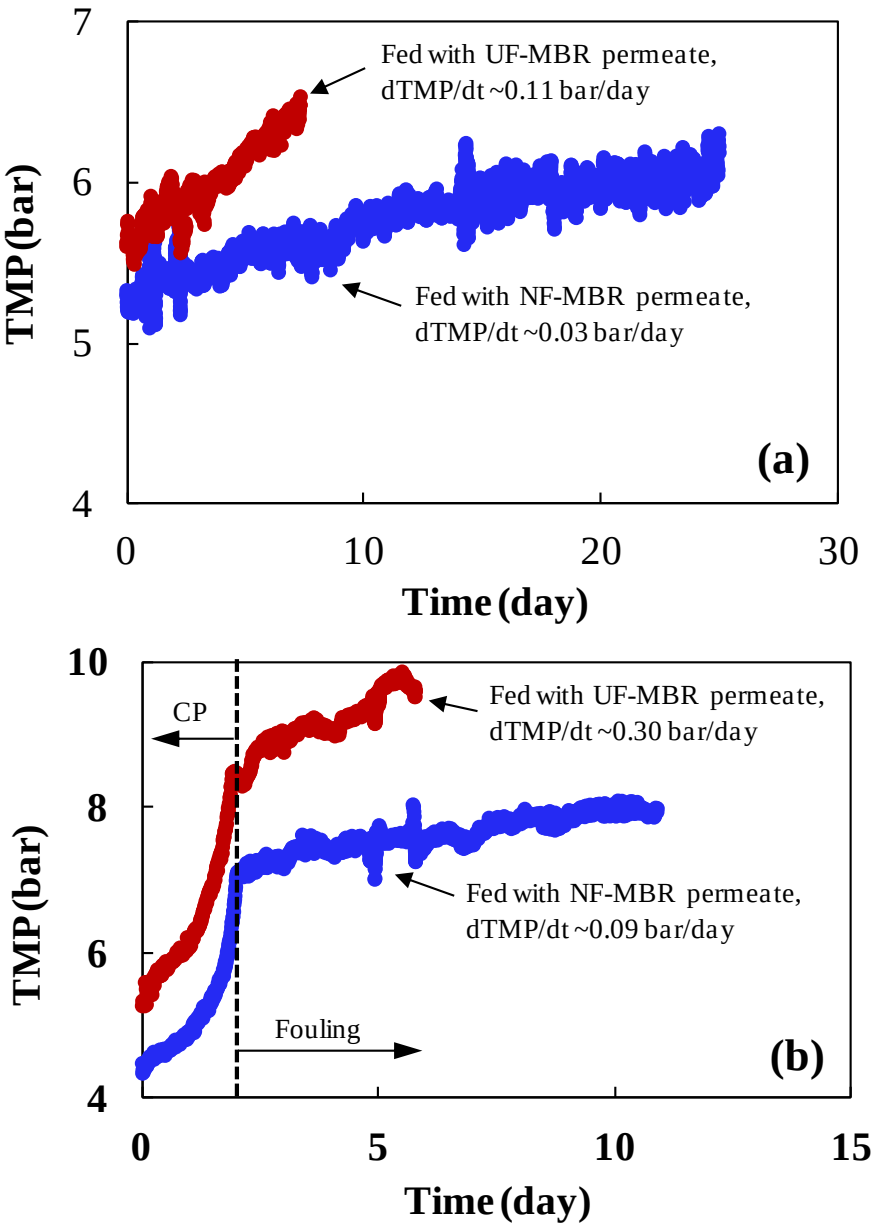

Figure 4-10. TMP profiles of the RO systems fed with permeate from UF-MBR and NF-MBR at a concentration equivalent to (a) 0% recovery (b) 90% recovery. CP represents the concentration process to increase the concentration of the solution from 0 to 90% recovery equivalent.

4.3.2.2. Foulant analysis

Shown in Figure 4-8, in the RO fouling test with UF-MBR permeate, the ratio of biopolymers in the RO foulant was 43.9%, significantly higher than that in the permeate (1.7%), which suggested a greater tendency of their accumulation onto the RO membrane. Meanwhile, the ratios of building blocks (24.6%) and LMWs (31.5%) were comparable to those in the permeate (22.1% and 29.0% respectively). Similarly in the NF-MBR+RO system, a high ratio of biopolymer (40.7%) in the RO foulants was observed. The biopolymer appeared to be the major component of the RO foulants despite both permeates had different compositions, more importantly very low amount of biopolymers. The possible mechanism is the transformation of smaller organic molecules to the larger biopolymers through aggregation or bio-conversion; future studies on this aspect will be performed. In addition, there was no humic substance (i.e., non-detectable) deposited onto the RO membranes.

4.3.2.3. Correlation between organic fractions in MBRs permeate and RO fouling

It was found that the amount of biopolymers, building blocks, and LMWs were ~ 5 to 6 times higher in RO foulant with UF-MBR permeate than with NF-MBR permeate (Table 4-4). The autopsy results agreed well with the TMP profiles in Figure 4-10. Thus, the removal of organic fractions was crucial to the sustainable operation of downstream RO process. In fact, in a recent work (Kimura et al., 2016c), where an NF membrane was used to pretreat the MF/UF-MBR effluent prior the RO process, has shown that (1) severe membrane fouling occurred only in the co-presence of organics and silica; (2) the removal of the organic matter from the RO feed water could significantly reduce the RO membrane fouling. From EEM analysis, it is worth noting that high intensities of aromatic protein I (tyrosine), aromatic protein II (tryptophan) and soluble microbial by-product-like substances were observed especially for the RO system fed with UF-MBR permeates, implying that these aromatic proteins and soluble microbial by-product-like substances show greater tendency to attach onto the RO membranes compared to the humic acid-like and fluvic acid-like substances.

4.3.7 Comparison of energy consumption of NF-MBR+RO and UF-MBR+RO system

Energy consumption is an important aspect in evaluating the feasibility of NF-MBR+RO process for high recovery water reclamation. In MBR+RO processes, aeration energy and pump energy are practically the two major contributors to the total energy demand. The total aeration energy is the sum of power consumption of blowers for membrane (only for submerged membrane configuration) and biological process. Based on the typical values applied in the aerobic MBRs, normalized biological aeration demand of 10 Nm^3 air/m^3 product (Qin et al., 2007) and a specific membrane aeration demand of 0.3 Nm^3/m^2h (Judd and Judd, 2006) were chosen. A power consumption of 0.019 kWh/Nm^3 air for coarse bubble aeration was taken for calculation (Maere et al., 2011). Pump energy usage was evaluated using the pump power requirement equation (Judd and Judd, 2006):

$$P_p = \frac{Q\rho gH}{1000\xi} \qquad \text{(Eq. 4-1)}$$

where P_p is the pump energy demand (kW), Q_R is the volumetric liquid flow rate (m^3/s), ρ is the pumped fluid density (kg/m^3), g is gravitational field strength (9.8 N/kg), H is water head (m, which is equivalent to ~10 times of the feed pressur e (bar)), and ξ is pump efficiency (assuming 80% in this study).

Table 4-5 summarizes the total energy consumption (kWh/m^3 product) of the submerged UF-MBR+RO and side-stream NF-MBR+RO at a recovery rate of 75% or 90%. It is noted that if the RO membrane is operated at recovery of 90% in the submerged UF-MBR+RO systems, additional RO pre-treatment (i.e., MBR post-treatment, such as activated carbon adsorption process (Wang et al., 2014a) or low-pressure NF process (Kimura et al., 2016a)) is generally necessary in order to achieve consistent RO performance. Thus, this scenario is not discussed in this study.

In the NF-MBR+RO system, increasing the RO recovery rate from 75% to 90%, the energy consumption only inclines from 0.732 to 0.739 kWh/m^3, both are slightly lower

than that of the submerged UF-MBR+RO (0.770 kWh/m^3) at 75% of recovery rate. This signifies the feasibility of NF-MBR+RO for high recovery water reclamation process. It is worth noting that the capital cost of NF-MBR+RO may be higher than UF-MBR+RO due to relatively lower NF permeate flux (10 L/m^2h) and larger NF membrane area is required. A decrease in capital cost of NF-MBR+RO could be foreseen with improved permeability by developing novel NF membranes and advanced NF membrane fouling control strategies.

Table 4-5. A comparison of energy consumption (kWh/m^3 product) for NF-MBR+RO and UF-MBR+RO at different recovery ratios.

		Submerged UF-MBR+RO (75% recovery)	**Side-stream NF-MBR+RO (75% recovery)**	**Side-stream NF-MBR+RO (90% recovery)**
MBR	Feed pump	0.005	0.005	0.004
	Waste pump	0.0001	0.0001	0.0001
	UF/NF crossflow pump	-	0.231[a]	0.193
	UF permeate pump	0.012	-	-
	Aeration (biological)	-	0.190	0.190
	Aeration (membrane)	0.447[b]	-	-
RO	High-pressure pump	0.306[c]	0.306	0.352[d]
Total		0.770	0.732	0.739

[a] Feed pressure of NF at 100% of recovery was set at 2.5 bar.
[b] UF flux was set at 17 L/m^2h.
[c] Feed pressure of RO at 75% of recovery was set at 6.62 bar.
[d] Feed pressure of RO at 90% of recovery was set at 9.12 bar.

4.4 Concluding Remarks

In this study, a novel NF-MBR+RO system for high recovery water reclamation was developed and compared with a UF-MBR+RO system. The following conclusions can be drawn:

(1) The NF-MBR achieved higher organic removal than the UF-MBR. The extended retention time could enhance the biodegradation of the retained organics in the bioreactor.

(2) No deterioration in the permeates quality was observed throughout the experimental period. The NF membrane exhibited excellent membrane stability in biologically active environment and is suitable to be incorporated into the NF-MBR system.

(3) The fouling experienced by the NF-MBR in the early stage was highly reversible in which the PWP can be restored by physical cleaning, while irreversible fouling was predominant the throughout the operation of the UF-MBR.

(4) The subsequent RO membrane fed with the NF-MBR permeate displayed better performance than that with the UF-MBR permeate mainly due to lower organic substances present in the NF-MBR permeate.

(5) In both NF-MBR+RO and UF-MBR+RO system, the biopolymers were identified as the predominant organic foulant in the MBR and RO process.

(6) The calculated energy consumption of the NF-MBR+RO system at 90% recovery was comparable to that of the UF-MBR+RO at 75% recovery, which supports the feasibility of NF-MBR+RO for high recovery reclamation.

Chapter 5

Impact of Salt Accumulation in the Bioreactor on the Performance of NF-MBR+RO process

5.1 Introduction

Chapter 4 has demonstrated the successful integration of the low-pressure NF membrane in the NF-MBR setup. However, the major disadvantage is the retention that leads to the accumulation of dissolved ions in the bioreactor by the high rejection membranes (Qiu and Ting, 2013). The concentration factor, CF, defined as the ratio of concentration of mixed liquor in the bioreactor, C_{ml}, to the feed concentration, C_f, is related to the sludge retention time (SRT) and hydraulic retention time (HRT), in which the maximum value, CF_{max} = SRT/HRT (Lay et al. 2010).

In conventional MF/UF-MBR, the SRT has also been identified as a factor relating to biomass physiological state and sludge characteristics, which subsequently influence the organic removal efficiency and membrane fouling potential (Wu et al., 2011). For example, extending the SRT generally promoted lower soluble microbial products (SMP), lower specific bound EPS production, better bio-flocculation, and formation of a more permeable cake layer, therefore, resulting in less membrane fouling (Ng et al., 2006, Wu et al., 2011, Van den Broeck et al., 2012, Massé et al., 2006). It is noted that longer SRT was often adopted to maintain high biomass concentrations (lower F/M ratio), reduce solids production, and minimize reactor volume (Pollice et al., 2004). In addition, longer SRT was preferred for more effective nitrification since the autotrophic nitrifiers are very slow-growing microorganisms among other aerobic bacteria (Rittmann and Mccarty, 2003). It shall be noted that extending the SRT in conventional MF/UF-

MBR does not result in the accumulation of salt because no rejection by the MF/UF membranes.

On the other hand, extending the SRT in HR-MBR essentially means increasing the salt accumulation, which can potentially impact the physical-chemical properties of the feed solution, bioprocess, and membrane operation (Luo et al., 2014, Lay et al., 2010). First, effective distribution of oxygen in the aerobic bioreactor, which is governed by the oxygen transfer rate of mixed liquor, is of fundamental importance to bacteria metabolism and oxidation of contaminants (Metcalf et al., 2003). When salinity increases, solubility of oxygen decreases linearly, which leads to lower oxygen transfer rate (Colt, 2012). This substantially reduces the effectiveness of aeration, which is translated into higher energy requirement to achieve the desired DO level. Regarding the impact of salinity on bioprocess, in both FO-MBR and MD-MBR, it has been found that elevated salinity could lead to a shift in microbial community, lower growth yield and lower microbial kinetics of the activated sludge necessary for the biological treatment and eventually resulted in process deterioration (Luján-Facundo et al., 2018, Nawaz et al., 2013, Wijekoon et al., 2014). Acclimatization and proliferation of halotolerant/halophilic bacteria could be the feasible approach for biological carbon removal, however, acclimatization of nitrifying bacteria is extremely difficult as they are sensitive and vulnerable to the high salinity environment (Lay et al., 2010, Qiu and Ting, 2013). Consider the fact that majority of the microbial community in the activated sludge involved in the conventional wastewater treatment are non-halophilic, it would be a great challenge to retrofit the existing treatment facility into FO-MBR. In term of impact of salinity on membrane operation, in general, higher feed salinity means reduced net driving force and greater transport of solutes across the membrane that lower the permeate flux and quality. In addition, accumulation of dissolved ions such as Ca^{2+}, Mg^{2+}, SO_4^{2-}, PO_4^{3-}, etc. can increase the risk of membrane scaling and aggravate colloidal fouling due to higher supersaturation index. Furthermore, the increase in extracellular polymeric substances (EPS) production under high salinity environment was found to increase the fouling propensity in FO-MBR (Qiu and Ting, 2013).

Although the abovementioned negative effects of salt elevation, i.e., through a longer SRT, could be intimidating for HR-MBR, they often counteract with the positive effects of longer SRT for conventional MF/UF-MBR. In addition, it shall be noted that most of the work reported on impacts of salt accumulation were related to FO-MBR and MD-MBR, the in-depth study to address this issue for NF-MBR application was not available. Indeed, research work on NF-MBR in the literature was rather limited, possibly associated with the poor permeability of NF membranes, typical flux was less than 1 L/m^2h (Choi et al. 2002, Choi et al. 2006), except in our previous work where flux of 10 L/m^2h was attained with the use of a low pressure NF membrane, which possesses positively-charged surface that allows the passage of monovalent ions while rejects the divalent ions via electrostatic repulsion (Tay et al. 2018). Therefore, it is unclear the observations found in FO-MBR and MD-MBR are applicable to NF-MBR. For instance, the driving force and membrane properties such as structure, permeability and rejection of FO, MD, and NF membranes differ from each other, which could have imposed different effects arisen from salt accumulation in the bioreactors on the bioprocess and membrane operation. Thus, in this study, the impacts of salt accumulation, through the manipulation of SRT, on microbial behaviors, bioreactor performance, permeate quality and membrane fouling of NF-MBR as well as the subsequent RO performance for water reclamation are investigated.

5.2 Materials and methods

5.2.1 Experimental protocol

Two parallel lab-scale moving bed biofilm reactors employing side-stream NF membrane modules were set up. The two biofilm reactors were operated at SRT of 30 days and 60 days (hereinafter denoted as NF-MBR_30-LS and NF-MBR_60-HS), respectively. Each bioreactor had a total effective working volume of 7.0 L and filled with 234 pieces of K3 bio-carriers. The filling ratio of this experiment was ~20 %, which was doubled of that in Chapter 4 (~10% of filling ratio) to improve biological activity in the bioreactors. The biofilm reactor was inoculated with the aerobic activated sludge (collected from Ulu Pandan wastewater treatment plant of Singapore) at a mixed liquor suspended solid (MLSS) concentration of 1 g/L. The aeration rate was set at 500 mL/min which was one-sixth of the aeration rate (i.e., 3 L/min) used in Chapter 4. The reduced aeration rate was intended for simultaneous nitrification and denitrification. The hydraulic retention time (HRT), pH, and temperature of the biofilm reactors were kept at 22 h, 6.8±0.5, and 20±1°C, respectively. The permeate flux of both NF-MBR systems was maintained at 10 L/m^{2}h via a mass flow controller installed on the permeate stream. The pressures of feed, retentate and permeate were recorded by digital pressure transducers (Ashcroft, USA) connected to a data logging system (LabVIEW, National Instrument, USA). The municipal wastewater was collected from Ulu Pandan wastewater treatment plant of Singapore (after sieving with a 1 mm opening mesh) periodically and stored in a cool room at 4°C. The operating parameters of the NF-MBRs and the characteristics of the municipal wastewater are summarized in Tables 5-1 and 5-2, respectively.

Table 5-1. Operating parameters of NF-MBRs

Parameter	NF-MBR_30-LS	NF-MBR_60-HS
HRT (h)	22	22
SRT (d)	30	60
Flux (L/m^{2}h)	10	10
Organic loading Rate (g COD/L.day)	0.41	0.41
F/M Ratio (g COD/g MLSS.d)	0.23	0.22
NF membrane crossflow velocity (m/s)	0.10	0.10
pH	6.2 – 6.9	6.2 – 6.9
Aeration (mL/min)	500	500
DO level (mg/L)	4.3-5.0	4.2-4.9
Biocarrier filling ratio (%)	20	20

In this study, SMTC's in-house fabricated glutaraldehyde cross-linked layer-by-layer polyelectrolyte hollow fiber NF membranes with PES UF as substrate were used and their properties can be found in Chapter 3. Each membrane module consisted of 40 pieces of hollow fibers (0.34 m in length; a total effective area of 0.031 m^2) and filtration was performed in an inside (lumen)-out (shell) configuration. During first 30 days of operation, mixed liquor in the bioreactor was directly fed to the NF membrane, denoted as NF1, which caused severe membrane fouling. Then, a sponge column (sponge pore size of ~ 0.5 mm) was installed at the effluent outlet of the bioreactor before the NF module, aiming to retain the larger sized particles of >0.5 mm; a new NF membrane (NF2) was used the subsequent test.

Table 5-2. Characteristics of feed municipal wastewater (n=21)

Parameter	Level
tCOD (mg/L)	378.6 ± 116.5
sCOD(mg/L)	120.5 ± 28.3
DOC (mg/L)	55.3 ± 27.7
Ca^{2+} (mg/L)	26.1 ± 2.6
Mg^{2+} (mg/L)	10.4 ± 2.9
Na^{+} (mg/L)	99.0 ± 17.5
Fe^{3+} (mg/L)	0.45 ± 0.18
TN (mg/L)	39.7 ± 7.5
NH_4-N (mg/L)	39.3 ± 5.2
NO_3^--N (mg/L)	0.4 ± 0.1
NO_2^--N (mg/L)	N.D.
TP (mg/L)	15.8 ± 2.6
TDS (mg/L)	666.4 ± 72.1
Conductivity (μs/cm)	970.7 ± 87.3

Note: tCOD: total chemical oxygen demand; sCOD: soluble chemical oxygen demand;DOC: dissolved organic carbon; TN: total nitrogen; TP: total phosphorus; N.D.: not detectable.

5.2.2 Membrane cleaning protocol

Periodic physical cleaning (every two days) of membrane was performed in order to maintain constant permeate flux at 10 L/m^2h throughout the test. In detail, the fouled NF module was first removed from the NF-MBR and physical cleaning was conducted in a separate batch setup according to the following steps, i) flushing with tap water at 500 or 800 mL/min (equivalent to crossflow velocity of 0.5 or 0.8 m/s) for 30 s to remove clogged particles inside the lumen; ii) backwashing with ultrapure water at pressure of 2 or 3 bar for 15 min to detach the cake layer on the membrane surface; iii) flushing with tap water at 500 or 800 mL/min for 3 min to remove the residual foulants inside the

lumen. After each physical cleaning cycle, the recovery of membrane permeability was checked by pure water flux measurement.

5.2.3 Modelling for salts accumulation

Salts accumulation is an inherent phenomenon in the NF-MBR system due to the high rejection properties of the NF membrane. Salts level in the system increases when the inflowing salt load is higher than the out flowing salts. In the context of NF-MBR, the accumulation of divalent ions is significant than the monovalent ions, i.e., Na and K due to the low monovalent ions of the NF membrane. The effect of SRT cannot be isolated from the effect of salts accumulation as SRT is directly related to the concentration factor (CF) in the system under constant HRT. In view of the significant effect of elevated salts conditions to the biomass and system performance, it is important to predict the steady-state salts concentration for the experimental design.

In this study, a simple mathematical model was developed to model the concentrations of divalent ions in the NF-MBR as presented below. The mass balance developed in this work, which relates the SRT, HRT and NF membrane rejection, η_{NF}. As the inflowing concentration fluctuates over time and the rejection rates of the NF membrane varied with fouling conditions, the average inflowing concentration, C_{in} and the average rejection rate, η_{NF} respectively was used to predict the equilibrium concentration. This model does not consider of the mass that absorbed onto the biomass and colloidal particles.

Mass balance for the NF-MBR:

$$V_{\mathrm{BR}} \cdot \frac{\mathrm{d}C}{\mathrm{d}t} = Q_{\mathrm{in}}C_{\mathrm{in}} + Q_{\mathrm{R}}C_{\mathrm{R}} - Q_{\mathrm{BR,out}}C - Q_{\mathrm{w}}C \quad \text{..... Eq. (1)}$$

Derivation from the above:

$$\therefore \quad \frac{\mathrm{d}C}{\mathrm{d}t} + \frac{\left[Q_{\mathrm{NF,out}}(1-\eta_{\mathrm{NF}})+Q_{\mathrm{w}}\right]}{V_{\mathrm{BR}}}C = \frac{Q_{\mathrm{in}}}{V_{\mathrm{BR}}}C_{\mathrm{in}} \quad \text{..... Eq. (2)}$$

Derived ions concentration in the mixed liquor:

$$C_{ml}(t) = C_{\mathrm{f}}\left[\left(1 - \frac{1}{\alpha}\cdot\frac{1}{\mathrm{HRT}}\right)\cdot e^{-\alpha\cdot t} + \frac{1}{\alpha}\cdot\frac{1}{\mathrm{HRT}}\right]$$

where $\alpha = \left[\left(\frac{1}{\mathrm{HRT}} - \frac{1}{\mathrm{SRT}}\right)(1-\eta_{\mathrm{NF}}) + \frac{1}{\mathrm{SRT}}\right]$

…….…….……. Eq. (3)

Eq. (3) differs from the previous work that assumes the membrane (i.e., FO membrane) has perfect rejection (Lay et al. 2010). Eq. (3) assumes no salt precipitation in the bioreactor and scaling on the membrane surface, as well as no adsorption of inorganic ions onto the biomass or biofilm on the biocarriers. The discrepancies observed between the predicted and measured values could be due to these reasons.

5.3 Results and Discussion

5.3.1 Impact of salt accumulation on NF-MBR performance

During 90-day operation of NF-MBRs, a gradual build-up and accumulation of scale-forming ions such as Ca, Mg, and PO4, as well as TDS, DOC, and sCOD in the bioreactors was observed as expected due to their rejection by the NF membranes (Figure 5-1). The water quality of feed, mixed liquor ad permeate of NF-MBRs at steady state are summarized in Figure 5-2.

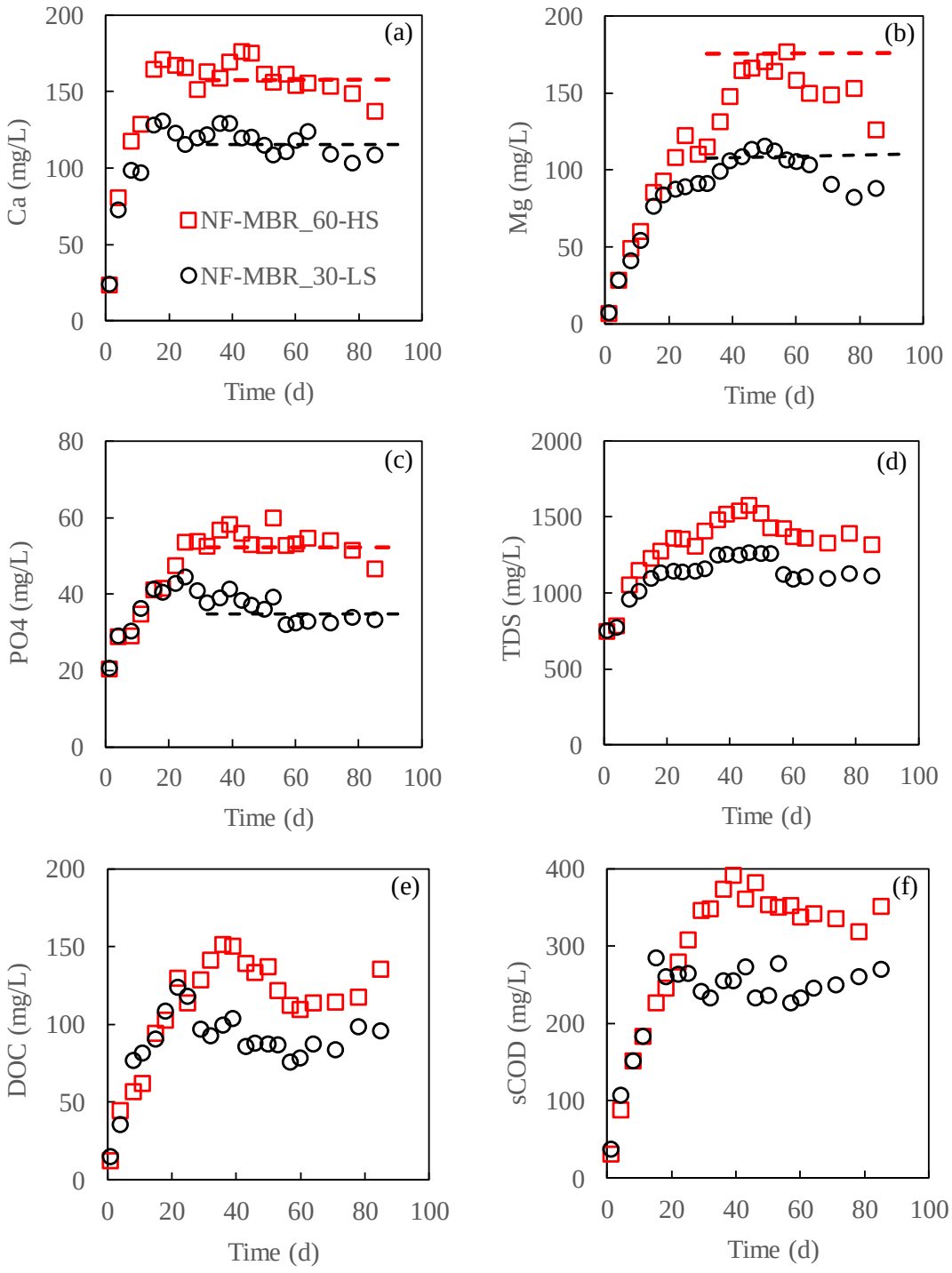

Figure 5-1. (a) Ca, (b) Mg, (c) PO_4, (d) TDS, (e) DOC, and (f) sCOD in the mixed liquor of NF-MBRs. Dotted-lines in the plot for Ca, Mg, PO_4 indicate the concentrations at steady state as predicted by Eq. (3).

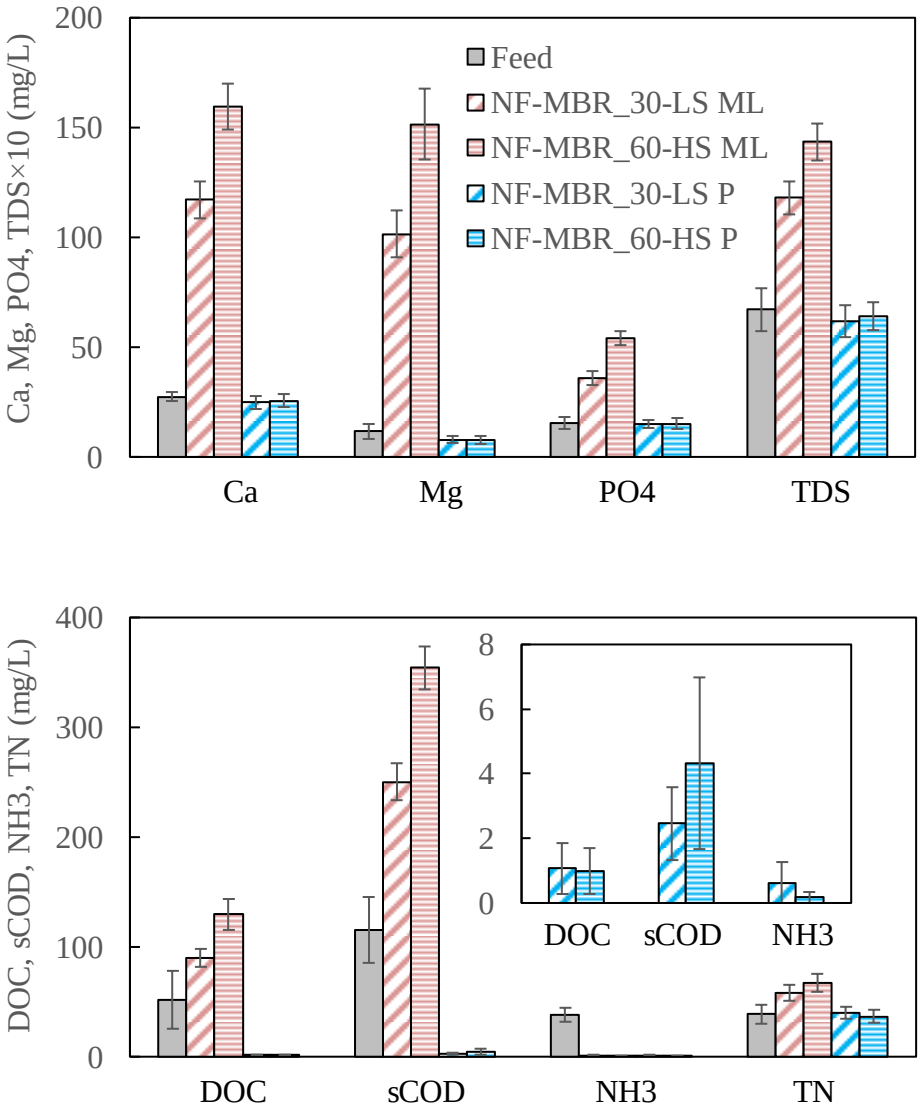

Figure 5-2. Water quality of feed, mixed liquor, and permeate of NF-MBRs at steady state.

Increasing the SRT, the measured concentrations of Ca (159.5±10.6 mg/L), Mg (151.4±16.3 mg/L), PO_4 (53.9±3.3 mg/L), and TDS (1434.2±85.3 mg/L) in the mixed liquor of NF-MBR_60-HS during steady state were approximately 36, 49, 51, and 22% higher than those in the NF-MBR_30-LS (Ca at 116.9±8.3 mg/L, Mg at 101.4±10.7 mg/L, PO_4 at 35.7±3.1 mg/L, and TDS at 1179.0±74.5 mg/L), respectively (Figure 5-1). The results correlated well within 15% error with the predicted concentrations, i.e., Ca =

115.3 and 157.7 mg/L, Mg = 108.6 and 175.6 mg/L, PO_4 = 34.8 and 52.2 mg/L for NF-MBR_30-LS and NF-MBR_60-HS, respectively, based on the mass balance developed in this work.

The accumulation of salts in the bioreactor had an implication on the overall removal efficiency of dissolved ions (Figure 5-2). Despite the good rejection properties of NF membrane, i.e., Ca = 79 - 84%, Mg = 92 - 95%, PO_4 = 58 - 72%, the overall removal attained for Ca, Mg, PO_4 was only <10, <35, and <2%, respectively, thus the NF-MBR permeate has almost similar concentrations of Ca and PO_4 as the incoming feed. Further optimization work such as chemical assisted precipitation is required to increase the removal efficiency. Tuning the NF membrane to get higher rejection, i.e., increase the number of polyelectrolyte layers or make a tighter membrane, is a complicated issue as on one hand excellent removal of divalent ions is desired but on the other hand increase rejection of monovalent ions can cause an increase in osmotic pressure.

The soluble organics in terms of DOC and sCOD in the mixed liquors also increased gradually before reached steady values of DOC = 89.7±7.9 and 129.2±14.3 mg/L, sCOD = 250.1±17.1 and 354.1±19.7 mg/L for NF-MBR_30-LS and NF-MBR_60-HS, respectively (Figure 5-1). The accumulation of soluble organics in the NF-MBRs could be attributed to their rejections by the NF membrane and their slowly-biodegradable or non-biodegradable natures. Similar to inorganic ions, greater accumulation of soluble organics was found in the NF-MBR with longer SRT. The impact of salt accumulation on the biodegradation efficiency of NF-MBR can be assessed by estimating the biodegradation rate at steady state, which was defined as:

$$\text{Biodegradation rate (\%)} = (1 - C_{ml,\ measured}/C_{ml,\ predicted}) \times 100\% \quad \text{Eq. (4)}$$

$C_{ml,\ measured}$ is the measured concentration of organics in the mixed liquor while $C_{ml,\ predicted}$ is the concentration of organics in the bioreactor assuming no biodegradation and negligible adsorption onto the membrane, which can be obtained using Eq. (3). The results showed that the biodegradation rate of DOC attained in NF-MBR_30-LS and NF-

MBR_60-HS were ~92.0% ($C_{ml,\ predicted}$ = 1115.5 mg/L) and ~92.3% ($C_{ml,\ predicted}$ = 1679.8 mg/L), respectively, showing insignificant effect from salt accumulation at different SRT (p>0.05).

Both NF-MBRs produced permeates with comparable DOC contents (1.1±0.8 mg/L in NF-MBR_30-LS *vs.* 1.0±0.7 mg/L in NF-MBR_60-HS; p>0.05), achieving >97% of DOC removal (Figure 5-2). The NF-MBR_60-HS produced a permeate with slightly higher COD level compared to the NF-MBR_30-LS (4.3±2.7 mg/L *vs.* 2.5±1.1 mg/L; p<0.05). Nevertheless, both NF-MBRs could achieve COD removal of >99% (Figure 5-2). Not surprising, the superior permeate quality was owing to the excellent rejection properties of NF membranes toward organic matters, i.e., >98.5%, thus no obvious impact of salt accumulation on permeate quality in terms of DOC and sCOD could be observed, unlike in the case of dissolved ions.

In addition, both NF-MBRs achieved excellent nitrification levels (ammonia removal ratios >98%) and produced permeates with very low NH_3 levels (<1 mg/L) despite the elevated salinity condition in the bioreactors (Figure 5-3). In contrast, the inhibition of nitrification process was commonly observed in FO-MBR and MD-MBR due to the accumulation of NaCl (Wang et al., 2016, Qiu and Ting, 2013, Wijekoon et al., 2014). The nitrifiers responsible for the two-step bioprocess, i.e., ammonia oxidizing bacteria (AOB) and nitrite oxidizing bacteria (NOB), are sensitive to high salt environment (Moussa et al., 2006, Campos et al., 2002). In the NF-MBR system applied in this study, the negative impact arisen from the accumulation of NaCl was alleviated by allowing the passage of monovalent ions. Our findings suggested that the accumulation of Ca, Mg, and PO_4 has no adverse influence on the nitrification process.

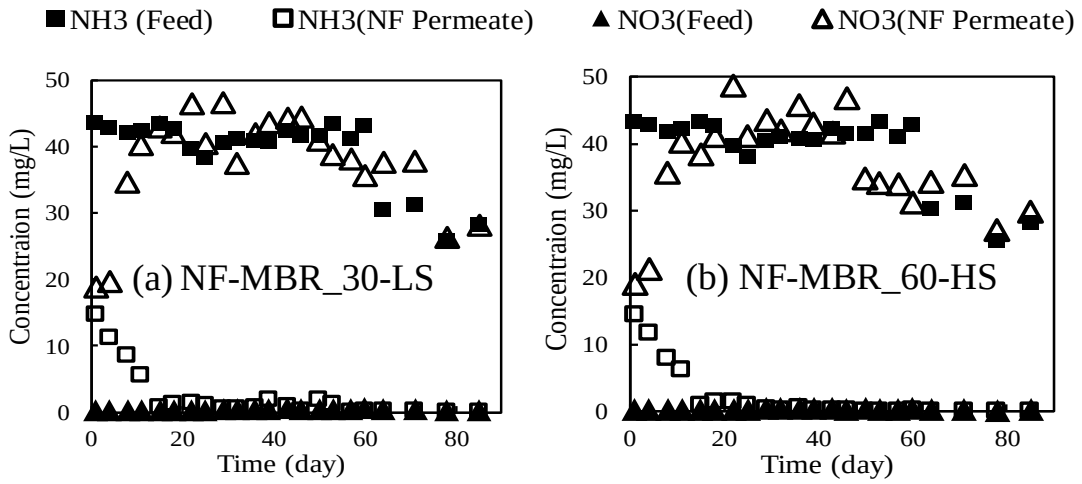

Figure 5-3. NH_3 removal of NF-MBRs.

Despite lowering the aeration rate to 500 mL/min, the desired effect of simultaneous nitrification and denitrification (due to DO level gradient in the attached growth biomass) was not achieved in this experiment. This could be attributed to two factors: i) relatively high DO levels in the NF-MBRs (Table 5-1) as compared to the recommended DO range of 0.5-3.0 mg/L (Wang et al., 2012); ii) the thickness of biofilm on the biocarriers was inadequate to prevent oxygen from penetrating through the biofilm. Real time aeration control or intermittent aeration should be implemented to further explore the possibility of simultaneous nitrification and denitrification in the NF-MBRs (Puznava et al., 2001).

The organic compositions of feed, mixed liquor, and permeate of NF-MBRs were analyzed by LC-OCD (Table 5-3). In both NF-MBRs, it was observed that (1) NF membranes demonstrated complete rejection of biopolymers, >99% rejection of HS&BB, and >95% rejection of LWM; (2) HS&BB accounted for ~75% of total soluble organics in the bioreactors compared to ~31% in the feed, indicating their larger accumulation rates, i.e., highest concentration factor, due to their slowly-biodegradable or non-biodegradable nature; (3) Limited accumulation of biopolymers (~10%) and LMW (~14%) in the bioreactors due to their easily-biodegradable nature. In addition, the biodegradation rate of each fraction was estimated as summarized in Table 3, and no

obvious impact of salt accumulation was observed since both NF-MBRs had similar biodegradation efficiencies for all components.

Table 5-3. Compositions of soluble organics in the feed, mixed liquor, permeate, of NF-MBRs analyzed by LC-OCD (n=5).

		Biopolymers	HS&BB	LMW
	Feed (mg/L)	5.2 ± 0.9 (14.9%)	11.0 ± 4.9 (31.1%)	18.9 ± 2.9 (54.0%)
NF-MBR_30-LS	Mixed Liquor (mg/L)	8.1 ± 0.5 (10.3%)	55.3 ± 5.0 (75.7%)	10.9 ± 1.5 (14.0%)
	CF[b]	1.55	5.02	0.57
	Biodegradation rate (%)	94.37	77.73	95.38
	Permeate (mg/L)	N.D.[a] (0%)	0.1 ± 0.0 (14.3%)	0.5 ± 0.3 (85.7%)
NF-MBR_60-HS	Mixed Liquor (mg/L)	12.4 ± 2.3 (11.0%)	83.5 ± 3.8 (74.4%)	16.5 ± 2.3 (14.6%)
	CF	2.38	7.59	0.87
	Biodegradation rate (%)	94.13	75.81	94.21
	Permeate (mg/L)	N.D. (0%)	0.1 ± 0.0 (20%)	0.4 ± 0.1 (80%)

[a] N.D. represents not detectable;

[b] CF represents concentration factor, $CF = C_{ml}/C_f$.

5.3.2 Impact of salt accumulation on biomass characteristics

In the first test, short-term impact of rapid exposure of high concentration of divalent ions, i.e., relative to the feed concentration, on biomass characteristics was performed by spiking of salts into the bioreactors at different concentrations, namely control (no addition of salts), 200 and 400 mg/L Ca, 100 and 200 mg/L Mg. The physiological responses in terms of cell viability, microbial activity, and EPS production on Day 0, 4 and 7 are summarized in Figure 5-4. Interestingly, the abrupt change in salt concentrations did not show any negative impact on the biomass characteristics. As compared to control, the addition of Ca increased the viability of biomass by 52 and 33% for 200 and 400 mg/L Ca, respectively, whereas no changes for samples spiked with Mg. In addition, the microbial activity as reflected by SOUR analysis showed 29% increase at 200 mg/L Ca while no notable change for 400 mg/L Ca, 100 and 200 mg/L Mg. The improved viability and SOUR could be attributed to the important role of calcium ions in maintaining the cell structure, cell division, and signal transduction that subsequently promote cell growth and increase microbial activity (Yu and Margolin, 1997, Dominguez, 2004). Furthermore, the EPS production was increased by 35 and 34% when spiked with 100 and 200 mg/L Mg, respectively, but comparable EPS production as control when spiked with 200 and 400 mg/L Ca, which indicated that an increase in Ca had negligible impact on EPS production in NF-MBRs.

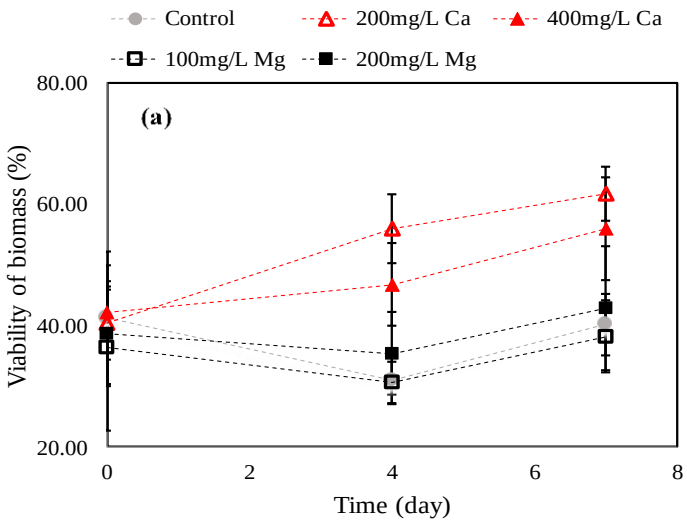

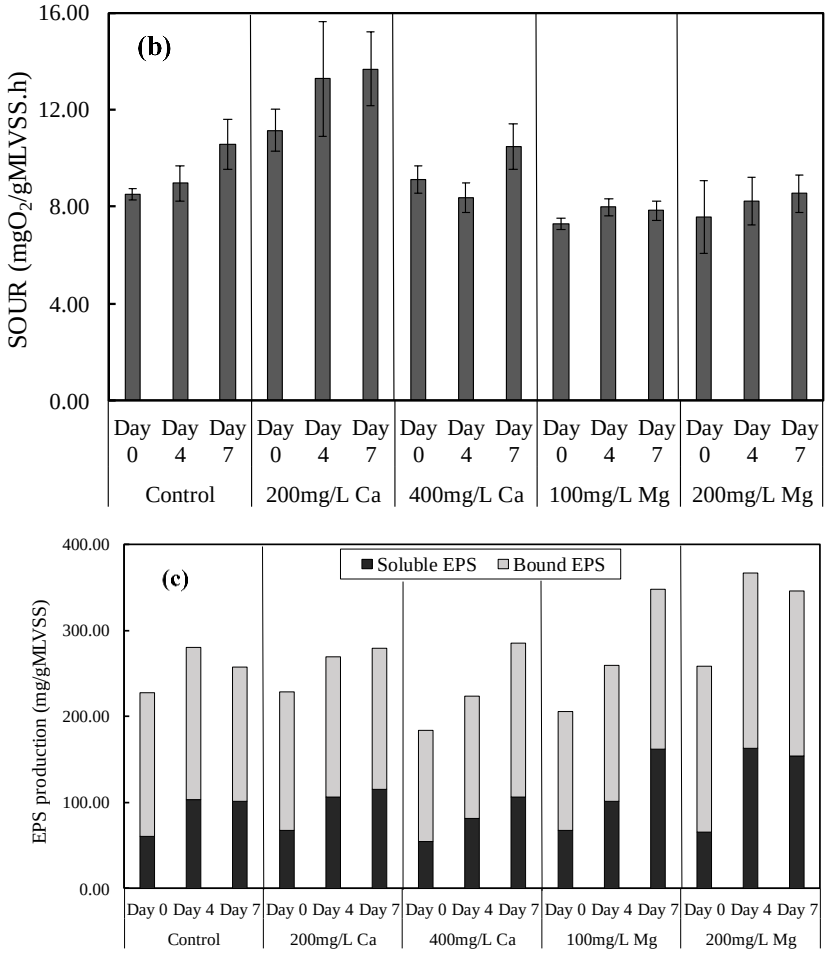

Figure 5-4. Effects of divalent ions spike on biomass characteristics (a) cell viability, (b) SOUR, and (c) EPS.

The characteristics of biomass in mixed liquor (i.e., suspended biomass) and on biocarriers (i.e., attached biomass) during long term operation of NF-MBRs, i.e., gradual accumulation of salts until steady state, are summarized in Table 5-4. The average MLSS (i.e., total suspended solids) concentrations in NF-MBR_30-LS and NF-MBR_60-HS were relatively comparable at 1277±286 mg/L and 1282±240 mg/L (p>0.05), respectively. In contrast, the attached solids on biocarriers of NF-MBR_60-HS (594±132 mg/L) was higher than NF-MBR_30-LS (515±134 mg/L; p<0.05), leading to a higher total solids amount (p<0.05). Both NF-MBRs also had similar MLVSS/MLSS ratio (0.79-0.89; p>0.05). Possibly, such higher concentrations of Ca, Mg, PO_4 in the

bioreactor at higher SRT could interact with the attached biomass, leading to an increase of attached solids in NF-MBR_60-HS. The viability and activity of the suspended biomass were examined by ATP and SOUR analysis (Table 5-4). In both NF-MBRs, the viability increased gradually with time, but SOUR maintained relatively constant (Figure 5-5). Averagely, in NF-MBR_30-LS, the biomass had viable ratio of 59±9% and SOUR of 11.2±1.9 mgO_2/gMLVSS·h, whereas the viability and SOUR in NF-MBR_60-HS were 60±12% and 12.4±2.4 mgO_2/gMLVSS·h, $p>0.05$, respectively. Although the viability and SOUR in NF-MBR_60-HS were slightly higher, the values were not statistically significant, suggested that the impact of Ca accumulation was not remarkable in the long-term operation of NF-MBR. Nevertheless, it was noted that the SOUR levels in both NF-MBRs were comparable to those reported for conventional aerobic MBRs (Han et al., 2005, Huang et al., 2001, Faust et al., 2014, Barreto et al., 2017).

In addition, the soluble and bound EPS productions of suspended biomass in both NF-MBRs experienced increase during initial stage, followed by slow decrease, regardless of SRT (Figure 5-6). The rapid increase of EPS may be attributed to several facts. First, the NF membrane showed high retention of the soluble EPS, part of which had slowly-biodegradable nature, leading to their accumulation in the bioreactor (Wang et al., 2014b). The increasing trend of soluble EPS corresponded well with the DOC and sCOD profiles during initial stage (Figure 5-1). Second, it was believed that microorganisms tended to excrete more EPS as a protection mechanism when they were suddenly exposed to unfavorable conditions, such as increase in divalent ions (Song and Leff, 2006, Ye et al., 2016). The results agreed with the spike test above, which showed Mg had greater impact on EPS production. It was also noted that soluble EPS accounted for almost 50% of the total EPS in our NF-MBRs and such ratio was higher than those reported in conventional MBRs (Wu et al., 2011, Zhang et al., 2010). Table 5-4 further compares the compositions of EPS (i.e., polysaccharides and protein) in both NF-MBRs at steady state. The amount of protein was almost three folds of polysaccharides for both soluble and bound EPS, regardless of the SRT. In addition, higher soluble polysaccharides (i.e., ~35%) were present in NF-MBR_60-HS than NF-MBR_30-LS ($p<0.05$), while

comparable soluble proteins were found in both NF-MBRs (p>0.05). Both NF-MBRs produced comparable amount of bound proteins (p>0.05) and bound polysaccharides (p>0.05). The results suggested that SRT could influence soluble EPS production in NF-MBRs, especially soluble polysaccharides.

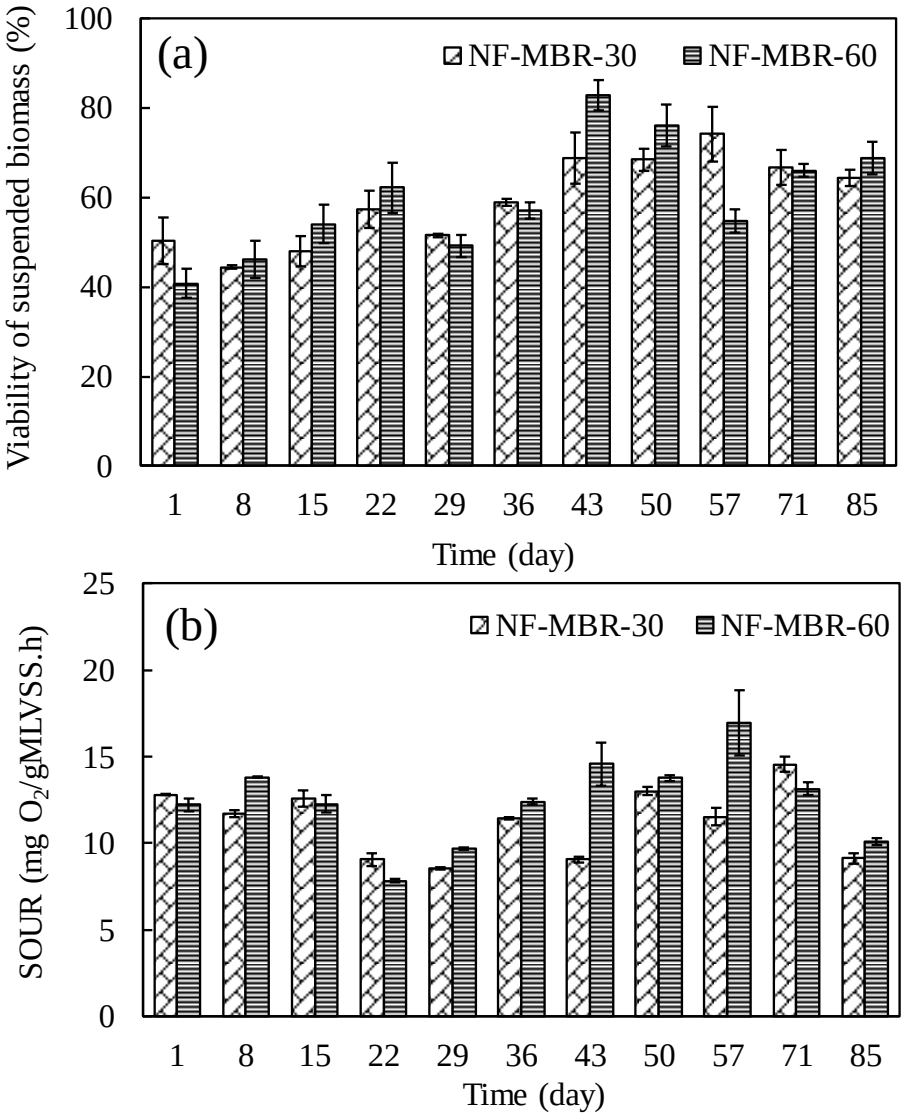

Figure 5-5. Comparison of (a) SOUR and (b) Microbial viability between the NF-MBR-30 and NF-MBR-60.

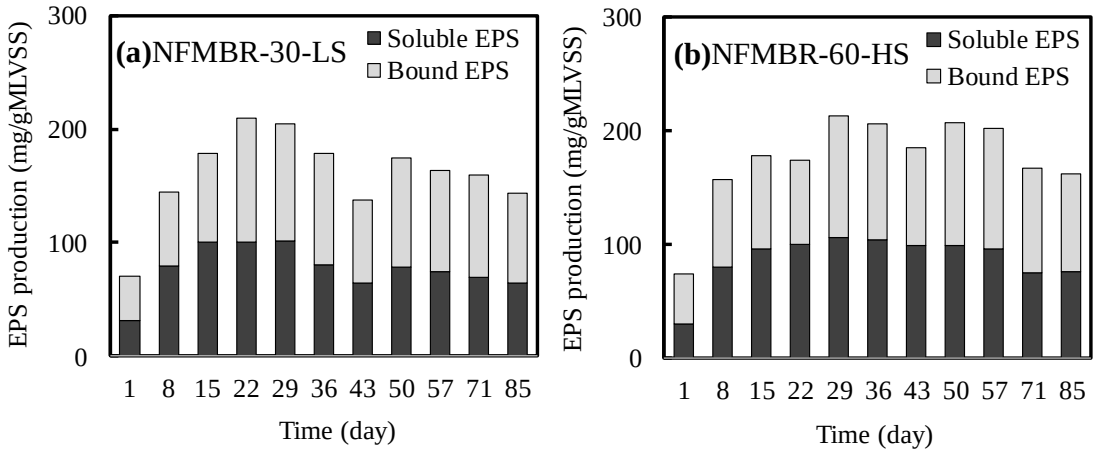

Figure 5-6. Soluble and bound EPS productions of suspended biomass in NF-MBRs.

Furthermore, the suspended biomass in NF-MBR_60-HS had larger floc sizes (p<0.05) and less negative surface charges (p<0.05) compared to those in NF-MBR-30-LS, (Table 5-4). This could be attributed to the presence of higher concentrations of divalent cations under longer SRT, which enhanced the bridging between negatively-charged functional groups of the bioflocs, in particular the charge neutralization effect and decrease in zeta potential to become less negative was more pronounced for Ca (Sobeck and Higgins, 2002). It has been reported that bioflocculation could be beneficial to membrane fouling reduction in conventional MBRs (Van den Broeck et al., 2012), its impact in NF-MBRs will be discussed in Section 5.3.3.

Table 5-4. Characteristics of biomass in the NF-MBRs (n=11).

Biomass characteristics		NF-MBR_30-LS	NF-MBR_60-HS
Attached biomass	Total solids (mg/L)	515±134	594±132
	Total biomass (mg/L)	453±117	515±107
	Total solids (MLSS) (mg/L)	1277±286	1282±240
	Total biomass (MLVSS) (mg/L)	1084±274	1061±223
	Viability (%)	59±9	60±12
	SOUR (mgO_2/gMLVSS·h)	11.2±1.9	12.4±2.4
	Soluble protein (mg/gMLVSS)	56±10	63±9

Suspended biomass	Soluble polysaccharides (mg/gMLVSS)	23±5	31±4
	Bound protein (mg/gMLVSS)	69±7	70±10
	Bound polysaccharides (mg/gMLVSS)	23±6	25±4
	Particle size (μm)	95±4	114±5
	Zeta potential (mV)	-11.7±0.8	-9.9±1.0

In addition, the microbial community compositions and relative abundances of bacterial populations at phylum level of suspended activated sludge in both NF-MBRs are illustrated in Figure 5-7. It was found that at phylum level, Proteobacteria (48.7% in NF-MBR_30-LS *vs.* 51.2% in NF-MBR_60-HS) and Planctomycetes (15.7% in NF-MBR_30-LS *vs.* 14.9% in NF-MBR_60-HS) were the predominant microbial communities. This observation was similar to the reported findings in conventional MBRs (Takimoto et al., 2018, Jo et al., 2016, Xia et al., 2012). Also, the microbial communities in both NF-MBRs had comparable relative abundances (Figure 5-7) with similar observed OTU, Chao1, Shannon and Simpson diversity indexes (Table 5-5). It implied that the microbial communities in NF-MBRs were not significantly affected by the increased organic and salt accumulations with extending SRT. However in previous studies on conventional MBRs, it was observed that the microbial communities of activated sludge were affected by organic loading rate (i.e. F/M ratio; 0.33 and 0.52 gCOD/gVSS day) (Xia et al., 2010) and salinity (10, 20, and 40 g NaCl/L) (Wu et al., 2008). Such dissimilar findings may be associated with the different organics/salt accumulation concentrations in the bioreactors and MBR operation parameters, such as MLSS, aeration rate, etc.

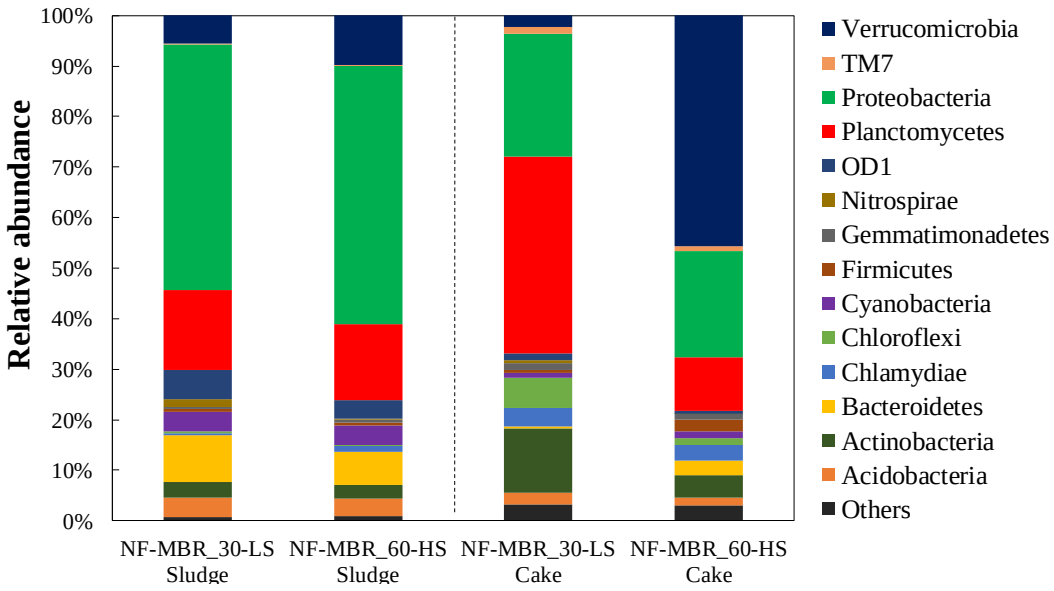

Figure 5-7. Prokaryotic community compositions of activated sludge and cake layers at the phylum level. All classified taxa with relative abundance lower than 1% and unclassified taxa were assigned to "Others".

Table 5-5. The observed OTU, Chao1, Shannon and Simpson diversity indexes of prokaryotic communities in NF-MBRs.

Sample	Observed OTU	Chao1	Shannon	Simpson
NF-MBR_30-LS sludge	555	585.9	4.129	0.943
NF-MBR_60-HS sludge	635	659.5	4.165	0.940
NF-MBR_30-LS cake	791	829.7	5.095	0.983
NF-MBR_60-HS cake	349	361	3.424	0.821

5.3.3 Impact of salt accumulation on NF membrane fouling

5.3.3.1. TMP and permeability of NF-MBRs

Figure 5-8a describes the TMP profile of NF-MBRs. During initial stage of operation before the NF-MBRs reached steady operation and without applying the sponge column

(from Day 0 to 30, NF1), severe fouling accompanied by rapid increase in TMP was observed due to high loading of bioflocs directly to the NF module, i.e., clogging of lumen. Hence, the discussion will be focused on the later stages (II, III and IV) of operation for NF2. In general, the TMP profile displayed a 'sawtooth' pattern, in particular during stage III and IV, which was associated with the interplay between reversible, irreversible fouling and cake-enhanced osmotic pressure effect (CEOP) (Tay et al., 2018). To further examine the NF membrane fouling mechanisms, the irreversible fouling resistance, $R_{irr}(t)$, $\Delta TMP_t = (TMP(t) - TMP(0))$ and $\Delta TMP_{irr} = J\mu R_{irr}(t)$, as shown in Figure 5-8b and c, were calculated from the clean membrane pure water permeability, membrane pure water permeability after each physical cleaning cycle and TMP profile (Figure 5-8a) according to the model developed in our previous publication (refer to Supplementary Data) (Tay et al., 2018). During Stage II operation, at backwashing pressure of 2 bar and flushing crossflow velocity of 0.5 m/s, there was an initial slow build-up (i.e., first 10 days of operation of NF2) followed by an exponential increase of irreversible fouling, where R_{irr} = ~20 and 30 × 10^{12} m^{-1} after 25 days of operation of NF2 for NF-MBR_30-LS and NF-MBR_60-HS, respectively. In Stage III, the flushing crossflow velocity was increased from 0.5 m/s to 0.8 m/s with a fixed backwashing pressure of 2 bar in order to improve the cleaning efficiency, where the R_{irr} dropped to 12 and 27 × 10^{12} m^{-1} for NF-MBR_30-LS and NF-MBR_60-HS, respectively. The cleaning protocol appeared to be effective for the case of NF-MBR_30-LS as it prevented further increase in R_{irr}, but not for the case of NF-MBR_60-HS as there was a linear (average) increase in R_{irr}. In Stage IV, the backwashing pressure was increased from 2 to 3 bar with a fixed flushing crossflow velocity of 0.8 m/s, but it did not further remove the irreversible fouling for NF-MBR_30-LS, only maintained R_{irr} at the same level. Meanwhile, the R_{irr} continued to increase linearly (average) for NF-MBR_60-HS, hence physical cleaning was not effective in this case. These observations implied that the cake layer morphology in NF-MBRs may be different (×3.5 higher in final R_{irr} value), i.e., more compact cake layer in NF-MBR_60-HS compared to NF-MBR_30-LS, as a result of salt accumulation effect (discussed below). In addition, chemical cleaning was

performed using citric acid after 43 and 52 days of operation of NF2 for both NF-MBRs. Apparently, the membrane permeability of NF-MBR_60-HS could be restored by ~12-42%, suggesting partial irreversible fouling was removed by chemical cleaning. However, the effect of chemical cleaning in NF-MBR_30-LS was not remarkable (<5% restoration), indicating the limitations of chemical cleaning using citric acid in the restoration of membrane permeability. Therefore, further optimization of chemical cleaning protocol is crucially important in future studies on NF-MBR. The NF membrane (layer-by-layer polyelectrolytes of PAH and PSS) used in this work cannot tolerate pH>8, one option is to apply chemical-enhanced backwashing with weak acid, EDTA, or SDS (Lateef et al., 2013).

Since the CEOP effect, which can be approximated by $\Delta TMP_{CEOP} \approx (\Delta TMP_t - \Delta TMP_{irr})$, is associated with the cake thickness, porosity and tortuosity (Chong et al., 2008), hence there was no immediate and sharp rise in TMP (i.e., the upward part of the 'sawtooth') during initial stage (first 10 days) of NF2 operation until a substantial cake layer was formed during later stage in Stage II as well as throughout Stage III and IV. As shown in Figure 5-8c, the CEOP effect was the predominant contributor and more severe in TMP increase for NF-MBR_60-HS, which was attributed to the thicker and more compact cake layer as well as higher salt concentration (i.e., osmotic pressure), as compared to NF-MBR_30-LS.

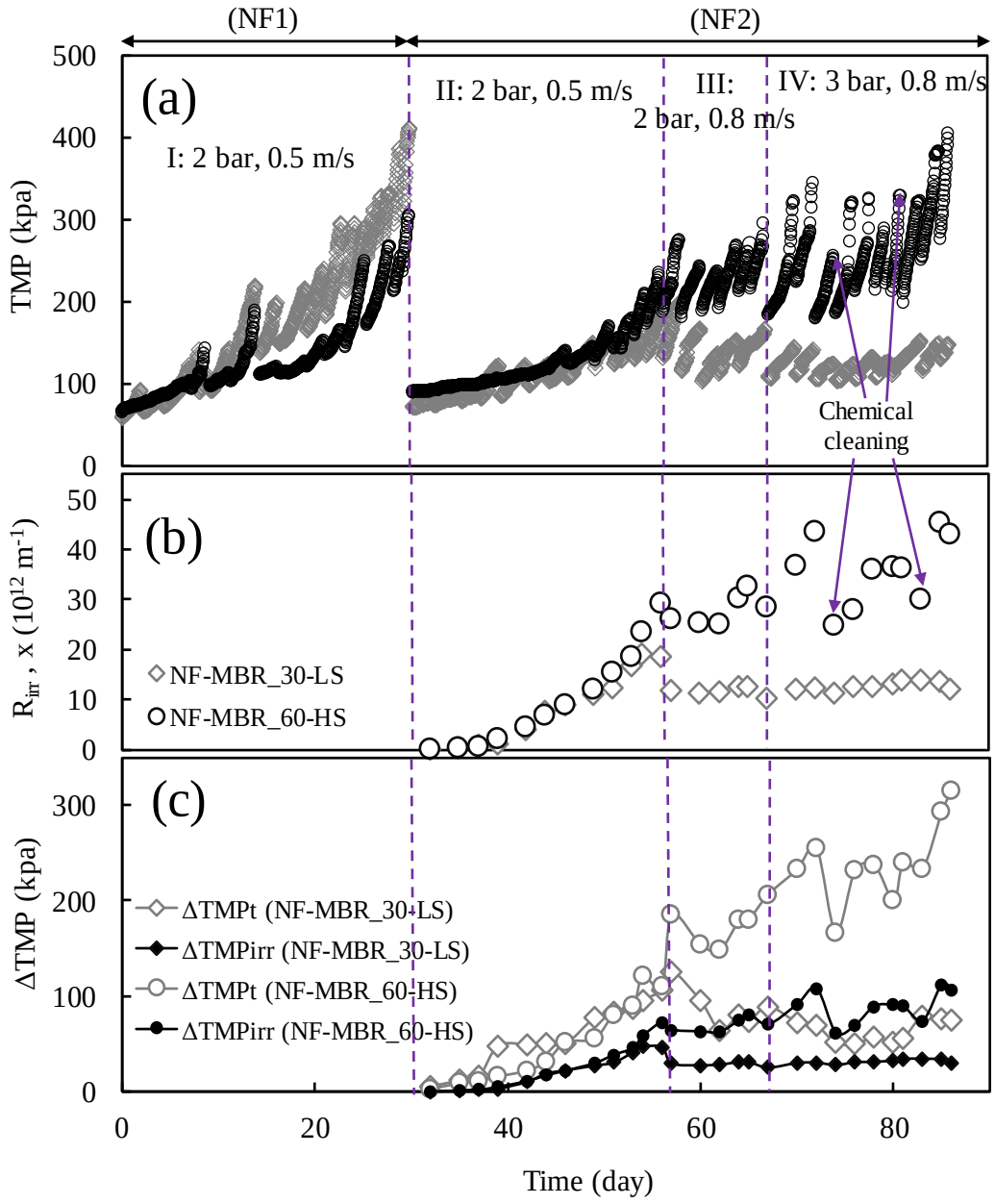

Figure 5-8. (a) TMP profiles, (b) Irreversible fouling resistance, R_{irr}, and (c) ΔTMP_t and ΔTMP_{irr} for NF-MBRs.

5.3.3.2. Effectiveness of physical cleaning and chemical cleaning

The effectiveness of the cleaning methods was further investigated by measuring the membrane filtration resistance of the fouled membrane before and after the physical cleaning and chemical cleaning (Figure 5-9). On day 72, the fouled NF membranes were removed and subjected to various cleaning methods to assess the recovery of pure water permeability (PWP) of the NF membranes. The filtration resistances of the virgin membranes, R_m were measured and denoted as "Virgin membrane" whereas the total membrane resistances, R_t of the fouled membranes were denoted as "Fouled membrane". The total foulant resistances, R_f were represented by the difference between the "Fouled membrane" and "Virgin membrane". The reversible foulant resistances (by physical cleaning) were represented by the difference between the "Fouled membrane" and "3 bar, 0.8 m/s" whereas the reversible foulant resistances (by chemical cleaning) were represented by the difference between the "3 bar, 0.8 m/s" and "Citric acid". The effectiveness of each cleaning method can be estimated by comparing the difference between the filtration resistances before and after the cleaning.

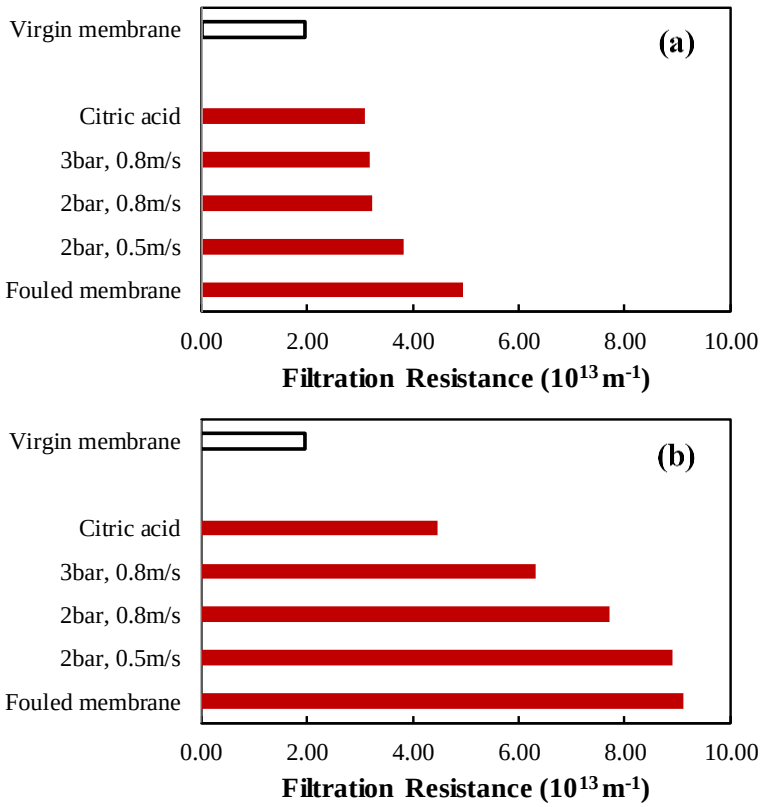

Figure 5-9. Filtration resistances of the fouled NF membrane measured before and after cleaning for (a) NF-MBR_30-LS and (b) NF-MBR_60-HS.

Figure 5-9 shows that the total foulant resistances of the fouled membranes in the NF-MBR_60-HS was significantly higher than that of the NF-MBR_30-LS, confirming the more serious fouling experienced by the NF-MBR_60-HS. The effect of physical cleaning with backwashing pressure of 2 bar and flushing crossflow velocity of 0.5 m/s, denoted as "2 bar, 0.5 m/s" was marginal with very little recovery of permeability for the NF-MBR_60-HS whereas the cleaning effect was significantly better for the NF-MBR_30-LS in which the filtration resistance was reduced by ~ 37%.

With the flushing at higher crossflow velocity of 0.8 m/s, notable decrease in filtration resistance (~17-20%) can be seen for both NF-MBRs, indicating the significance of the higher crossflow velocity that provides sufficient shear force in removing the residual cake foulants in the hollow fibers. The cleaning was followed by the increase in

backwashing pressure to 3 bar. The effect of increasing backwashing pressure was more significant in the NF-MBR_60-HS, suggesting that there could be further detachment of foulants with higher backwashing pressure. Lastly, chemical cleaning with citric acid was applied to both NF membranes. The chemical cleaning was effective in recovering membrane permeability especially for the NF-MBR_60-HS in which the filtration resistance was further reduced by ~26%.

The inorganic matter in the extracted foulants removed by backwashing, crossflow flushing, and chemical cleaning were measured and shown in Figure 5-10. The amounts of extracted elements presented were normalized to the membrane area. As mentioned above, the chemical cleaning was effective for the restoration of permeability of the fouled membranes. Therefore, the extracted elements could be the important inorganic foulants that responsible for the increase in filtration resistance. Large amounts of Ca and P were extracted during the chemical cleaning with citric acids, suggesting the important role of calcium phosphate scaling in NF fouling. In addition, notable amounts Ca and S were removed by crossflow flushing whereas negligible amount of P was extracted during crossflow flushing. The present of S in the extracted foulants reflects the possibility of the involvement of sulfates in membrane fouling. The results also suggested that physical cleaning could remove part of the calcium compounds in the foulants, however, it was not effective in controlling calcium phosphate scaling that occurred to the NF membrane. Interestingly, very little silica was extracted by both physical and chemical cleaning, suggesting that silica may not be the critical foulant in NF fouling.

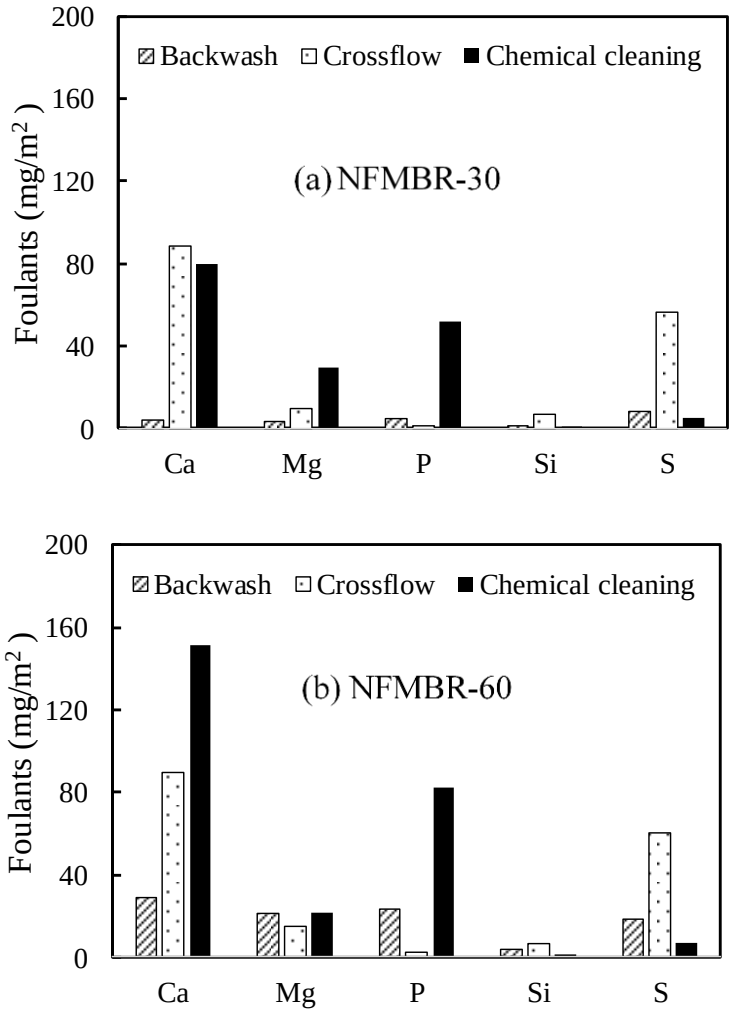

Figure 5-10. Amounts of inorganic matter extracted by physical cleaning and chemical cleaning.

However, even after a series of physical and chemical cleaning, the filtration resistance remained high for the NF-MBR_60-HS, indicating that there were more resistant foulants on the NF membranes that are persistent to the cleaning protocol and eventually resulted in irreversible fouling. Therefore, further study on chemical cleaning is needed to deal with the irreversible fouling, i.e., chemically enhanced backwashing (CEB) using EDTA and SDS (Lateef et al., 2013). The relationship of cake layer morphology and compositions with NF membrane fouling potential will be discussed in the following section.

5.3.3.2. NF membrane foulants

(1) Morphology of cake layer foulants

To examine the morphology cake layer foulants, the CLSM images of cells (live cells and dead cells) and EPS (proteins, α-d-glucopyranose-D polysaccharides, β-polysaccharides and intracellular lipids) were taken. Figure 5-11 summarizes the CLSM images and Table 5-6 presents the calculated biovolumes of the examined components. In both NF-MBRs, the dead cells abundantly distributed in both inner and outer regions of the cake layers, whereas the live cells were majorly present on the cake layer surface. First, the higher amount of live cells and EPS production were due to greater availability of DOC and no inhibition of salt accumulation to support the biofilm formation. Second, the higher amount of EPS, especially polysaccharides, was associated with the greater amount of Ca that formed polysaccharides-Ca complex with strong gelation properties (Meng et al., 2011), which could not be easily removed by physical cleaning. Third, the higher amount of dead cells could be due to the greater operating pressure, which led to the formation of a compact cake layer that hindered the oxygen and nutrient transfer to the inner region of cake layer.

The biovolumes of α-d-glucopyranose-D polysaccharides and β-polysaccharides in the NF foulants of the NF-MBR_60-HS were ~9 times and ~ 4 times more than those in the NF-MBR_30-LS, respectively. Among the examined foulant EPS components, α-d-glucopyranose-D polysaccharides were dominant, accounting for more than half of the total foulant EPS in both NF-MBRs. The total polysaccharides (α-d-glucopyranose-D polysaccharides and β-polysaccharides) were ~81% and 96% of the total foulant EPS for the NF-MBR_30-LS and NF-MBR_60-HS respectively. In addition, the biovolume of proteins in the NF-MBR_30-LS was 5% more than that of the NF-MBR_60-HS. Almost no intracellular lipids were detected in the foulants for both NF-MBRs.

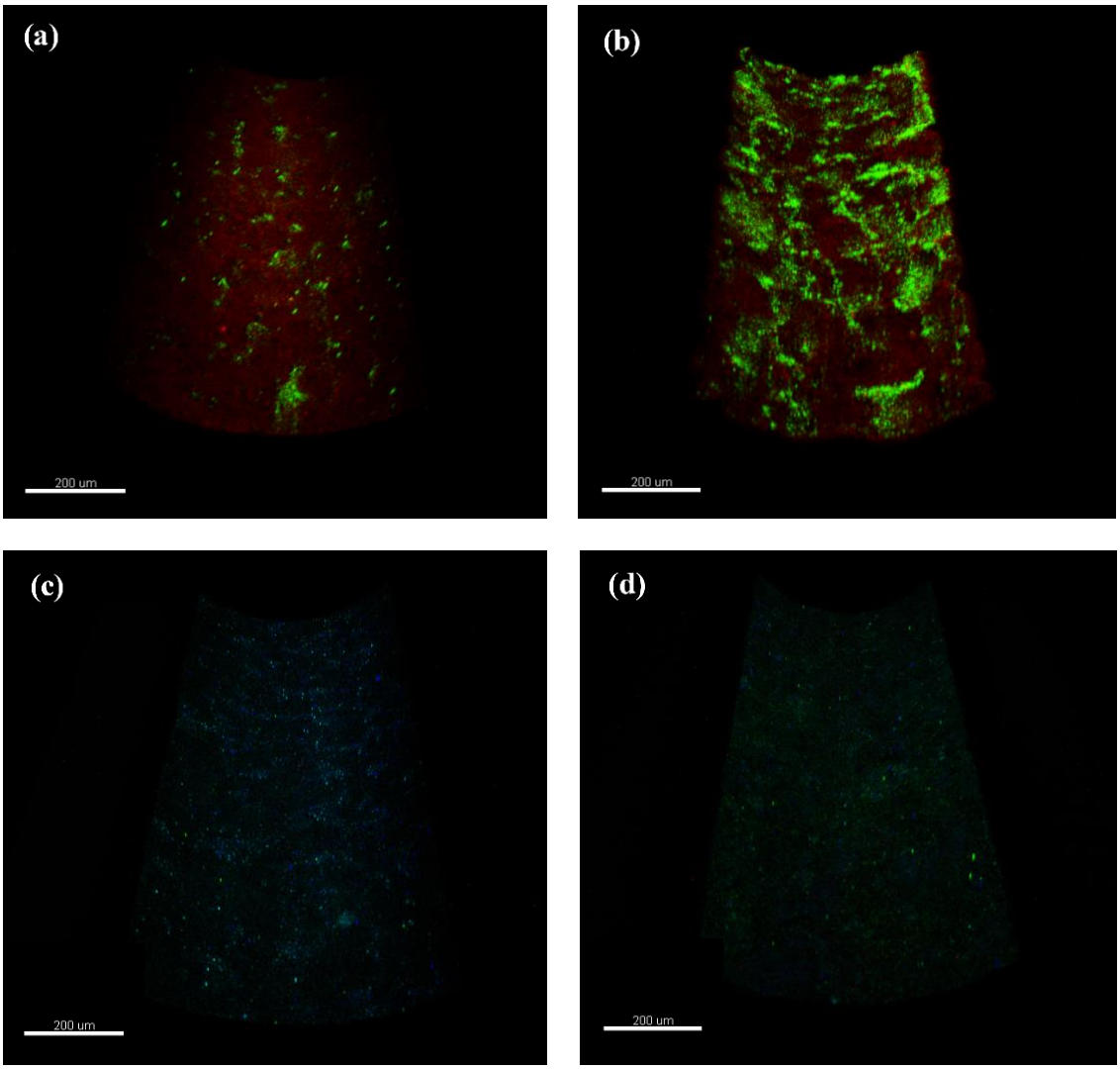

Figure 5-11. CLSM images of cake layer foulants on the NF membranes. Images of live/dead cells in (a) NF-MBR_30-LS and (b) NF-MBR_60-HS; Images of proteins (FITC), α-d-glucopyranose polysaccharides (Con A), β-polysaccharides (calcofluor white), and intracellular lipids (Nile red) in (c) NF-MBR_30-LS and (d) NF-MBR_60-HS.

Table 5-6. Characteristics of cake layer foulants in the NF-MBRs (n=2).

Foulants characteristics		NF-MBR_30-LS	NF-MBR_60-HS
CLSM image analysis	Live cells ($\mu m^3/\mu m^2$)	0.23 ± 0.02	1.75 ± 0.07
	Dead cells ($\mu m^3/\mu m^2$)	0.93 ± 0.43	1.69 ± 0.11
	Protein (10^5 $\mu m^3/cm^2$)	2.86 ± 0.18	2.72 ± 0.22
	α-d-glucopyranose polysaccharides (10^5 $\mu m^3/cm^2$)	3.36 ± 2.10	29.23 ± 11.34
	β-polysaccharides (10^5 $\mu m^3/cm^2$)	8.77 ± 3.33	34.27 ± 7.70
	Intracellular lipids (10^5 $\mu m^3/cm^2$)	N.D.[a]	N.D.
LC-OCD analysis	Biopolymers (mg/m^2)	200.6 ± 10.3	305.5 ± 21.5
	HS & BB (mg/m^2)	93.1 ± 11.4	235.36 ± 22.4
	LMW (mg/m^2)	31.8 ± 1.1	57.1 ± 3.0
ICP-OES analysis	Ca (mg/m^2)	160.6 ± 21.6	226.1 ± 14.1
	Mg (mg/m^2)	49.2 ± 2.7	97.6 ± 7.1
	P (mg/m^2)	103.0 ± 13.2	142.2 ± 31.5
	S (mg/m^2)	30.0 ± 20.6	48.8 ± 37.8
	Si (mg/m^2)	21.0 ± 12.4	19.1 ± 5.4

[a] N.D. represents "not detectable".

(2) Organic compositions

The dissolved organic foulants in the cake layer were analyzed by LC-OCD and shown in Table 5-6. In both NF-MBRs, the biopolymers were the predominant species, accounting to 51-61%. The results agreed well with our previous study on NF-MBRs operated at different conditions (Tay et al., 2018). The organic fractions (i.e., biopolymers, HS&BB, and LMW) in the cake layer foulants of NF-MBR_60-HS were greater than NF-MBR_30-LS. Possibly, this was due to more adsorption from the higher concentration in the bulk solution as well as more dead cell lysis in the cake layer biofilm.

(3) Inorganic compositions

The inorganic compositions of the fouling layers were analyzed by ICP-OES and described in Table 5-6. Obviously, the accumulation amounts of Ca (226.1 mg/m^2), Mg (97.6 mg/m^2), P (173.6 mg/m^2), S (48.8 mg/m^2), and Si (19.1 mg/m^2) on the NF membrane in the NF-MBR_60-HS were significantly higher than those in the NF-MBR_30-LS (Ca of 160.8 mg/m^2, Mg of 49.2 mg/m^2, P of 103.0 mg/m^2, S of 30.0 mg/m^2, and Si of 21.0 mg/m^2), respectively. In paticular, Ca and P accounted for more than 60% of total inorganic foulants on the NF membranes in both NF-MBRs. This suggested that extending SRT from 30 to 60 days could accelerate inorganic fouling, which may be majorly attributed by the calcium phosphate scaling. Note that the solubility limit of $Ca_3(PO_4)_2$, i.e. 2.07×10^{-33}, has been far exceeded in the bioreactors.

(4) Microbial community compositions

Figure 5-7 summarized the dominant microbial community compositions of the cake layer foulants in both NF-MBRs. It was found that in the cake layer foulants of NF-MBR_30-LS, Planctomycetes and Proteobacteria were the dominant phyla, accounting for 38.9% and 24.4% respectively. These microbial communities were also well observed in the cake layer foulants of conventional aerobic MBRs (Chen et al., 2016). In contrast, the dominant microbial community in the cake layer foulants of NF-MBR_60-HS was Verrucomicrobia (45.7%), which however had a low relative abundance in the suspended activated sludge (Figure 5-7). It has been reported that Verrucomicrobia, the obligate anaerobic bacteria that form propionate and acetate as a major fermentation product could survive and grow well within the cake layer (Chin et al., 2001). In addition, these obligate heterotrophs were associated with the ability to hydrolyze high-molecular-weight substrates such as polysaccharides (Cardman et al., 2014). Nevertheless, it suggested that extending SRT could significantly affect the composition of microbial communities in the cake layer foulants of NF-MBRs.

Shown in Table 5-5, the observed OTU and Chao1, Shannon, and Simpson diversity indexes of microbial communities in the cake layers of NF-MBR_60-HS were 55.9%, 56.5%, 32.8%, and 16.5% lower than those of NF-MBR_30-LS, respectively. Such significant differences in microbial community structure may be attributed to several facts. (1) The cake layer samples were collected from both NF-MBRs after 56 days of NF membrane filtration, but at different TMP levels (~1.5 bar *vs.* 2.5 bar; Figure 5-8). Gao et al. (2013) has pointed out that the microbial community of cake layers could change with the TMP increase although the stable microbial community of activated sludge remained in the conventional MBRs. (2) Different compositions and contents of EPS on the membrane surface (Table 5-6) could lead to different bacterial attachment behaviors (Tsuneda et al., 2003), resulting in dissimilar microbial community. (3) Chemical cleaning frequency (Figure 5-8) may cause dissimilar microbial resistance responses to cleaning chemicals, in turn leading to the changes in the microbial community (Lim et al., 2005).

(5) The factors influencing NF membrane fouling

The analysis of NF membrane foulants revealed that greater amounts of soluble organics (especially polysaccharides) and divalent ions (i.e., Ca^{2+} and Mg^{2+}) accumulated on the cake layer foulants of NF-MBR_60-HS (Table 5-6), corresponding to its higher membrane fouling potential. It is well known that polysaccharides generally have larger size, stronger gelation and lower biodegradation properties, leading to higher fouling propensity than proteins and humic substances (Meng et al., 2011). It was noted that the concentrations of Ca^{2+} and Mg^{2+} in the mixed liquor were greater than that of PO_4^{3-} (Figure 5-2). Therefore, the presence of free Ca^{2+} and Mg^{2+} ions could enhance the gelation behavior of polysaccharides on the NF membranes by forming the crosslinked network between the carboxyl groups in polysaccharides and the divalent ions, particularly Ca^{2+} (Jermann et al., 2007, Xin et al., 2016). In addition, the SEM-EDX results (Figure 5-12 and Table 5-7) also revealed that greater amounts of calcium and phosphorus were accumulated on the NF membrane of NF-MBR_60-HS, attributed by

higher concentrations of calcium and phosphate in the mixed liquor of NF-MBR_60-HS (Figure 5-2). Such polysaccharides-Ca^{2+} complex and $Ca_3(PO_4)_2$ inorganic scales could lead to cake enhanced concentration polarization (CECP) near the NF membrane due to their dense nature (Xu et al., 2010), as a result, accelerating membrane fouling in the NF-MBR_60-HS.

It was recalled that in the NF-MBR_60-HS, greater sizes of microbial flocs were formed due to the more accumulation of divalent cations under longer SRT (Table 5-4). Dissimilar to the observations in the conventional MBRs (Van den Broeck et al., 2012), in this study, such greater-sized flocs did not display any benefit to the membrane performance. Possibly, greater-sized flocs tended to form loose-attached cake layers on the NF membranes, which could be readily removed by periodically backwash and therefore did not perform a role in influencing cake layer resistance.

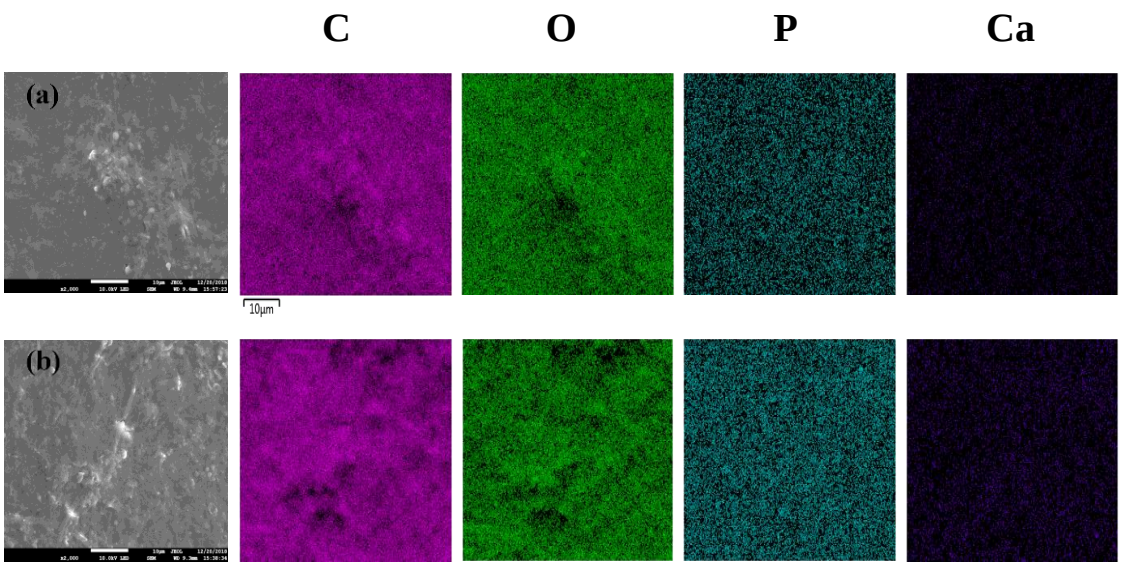

Figure 5-12. SEM-EDX element mapping images of carbon, oxygen, phosphorus and calcium of the membrane surface of the NF membrane in (a) NF-MBR-30 and (b) NF-MBR-60.

Table 5-7. Elemental composition of virgin and fouled NF membrane surface by SEM-EDX.

Element	Virgin Membrane (%)	Fouled membrane (%)	
		NF-MBR-30	NF-MBR-60
C	69.2	62.3	69.1
O	23.8	32.1	24.2
S	7.0	1.8	1.4
Ca	n.d.	1.6	1.9
Mg	n.d.	0.3	0.6
P	n.d.	1.6	2.3
Si	n.d.	0.3	0.6

5.3.4 Impact of salt accumulation in NF-MBRs on downstream performance of RO

After 60 days of NF-MBR operation, the NF-MBR permeates were collected and concentrated by not discharging the RO permeate until the concentration equivalent to 90% recovery was attained. As shown in Figure 5-13, when the recovery ratio was increased from 0 to 90%, the TMP increased from ~5.3 to 7.5 bar and 8.5 bar in NF-MBR_30-LS and NF-MBR_60-HS respectively. Subsequently, the RO membrane filtration was continued with a full recycle of permeate back to the feed tank to assess the RO membrane performance. At a high recovery rate of 90%, TMP increase rate (dTMP/dt) for the RO system fed with the NF-MBR_30-LS and NF-MBR_60-HS permeate was at ~ 0.25 and ~0.38 bar/day, respectively, showing better RO membrane performance in the NF-MBR_30-LS+RO system.

In conventional MF/UF MBR+RO systems, it has been demonstrated that the higher organic levels (in terms of TOC, COD, EPS) in MBR permeate could lead to more serious RO membrane fouling (Wu et al., 2013). However, in this study, the permeates

of both NF-MBRs had comparable quality (except higher sCOD for permeate of NF-MBR_60-HS), but resulted in relatively higher fouling rate for permeate of NF-MBR_60-HS. It is noted that the superior rejection capability of NF membranes ensured greatly less contents of smaller-sized organics in the NF-MBR permeate (~ 1 mg/L of DOC; almost no biopolymers and humic substances) compared to that in conventional MF/UF MBRs (~8 mg/L of DOC; biopolymers and humic substances accounted for 50% of total organics) (Tay et al., 2018) in treating municipal wastewater. Indeed, the treated wastewater permeate by NF-MBRs had comparable organic levels as those in seawater and surface water. In addition, previous studies had emphasized that assimilable organic carbon (AOC) was an important parameter in determining the biofouling potential of RO feed water in seawater desalination (Wu et al., 2017, Lee et al., 2019), which had very low DOC concentration (< 2 mg/L) similar to the permeate of NF-MBR. Therefore, it was unclear the difference in fouling rate was due the difference in sCOD level or rather the compositions of organics. Further study will be focused on the effect of AOC in NF-MBR permeate on RO membrane performance in order to further advance the NF-MBR+RO for water reclamation.

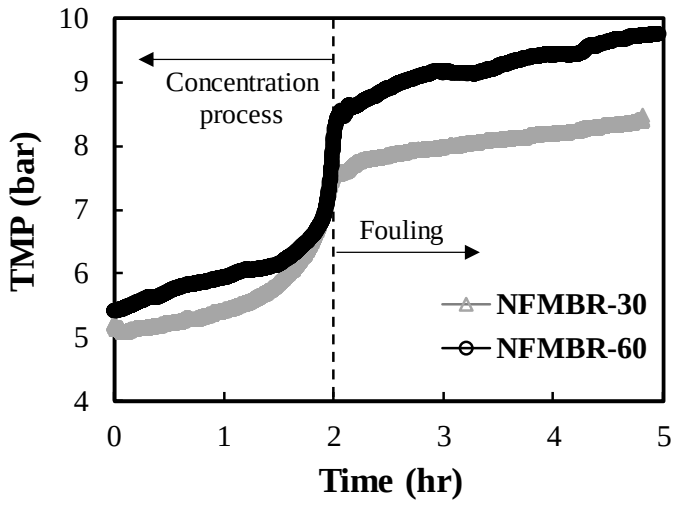

Figure 5-13. TMP profiles of RO membranes in NF-MBR+RO systems.

5.4 Concluding Remarks

This study compared the bioreactor and membrane performances in parallel NF-MBR+RO systems for water reclamation application under different salt accumulation conditions in NF-MBRs, which were operated under SRT of 30 and 60 days, respectively. The following conclusions can be drawn:

(1) The concentration factor is a function of SRT, HRT and membrane rejection. Increasing the SRT resulted in greater accumulation of scale-forming inorganic salts (i.e., Ca, Mg, PO_4) and organic compounds (i.e., DOC, sCOD, and especially HS&BB due to its poor or non-biodegradable nature). The accumulation of divalent ions did not pose adverse impact to the biodegradation efficiency and both NF-MBRs achieved superior organic removal (>97%) and ammonia removal (>98%).

(2) The elevated divalent ions level promoted bioflocculation, however, the effects on microbial activity and viability were not statistically significant in the long-term experiment. Salt accumulation did not influence the microbial community structure of activated sludge in NF-MBRs, but led to different predominant microbial communities in the cake layer foulants of NF membranes.

(3) More severe membrane fouling in the NF-MBR at longer SRT (i.e., higher salt accumulation) due to combined organic and inorganic fouling by calcium phosphate scaling and Ca-polysaccharides complex that was not easily removed by physical cleaning. The thicker and more compact irreversible fouling layer as well as higher salt concentration caused more severe cake-enhanced osmotic pressure (CEOP) effect in the NF-MBR with longer SRT. Physical cleaning (i.e., backwash and flushing) can be applied to maintain sustainable operation of the NF-MBR at low SRT of 30 d.

(4) Physical cleaning was ineffective in controlling membrane fouling associated with inorganic fouling, i.e., calcium phosphate scaling in the NF-MBR with higher salt accumulation. Optimization of chemical cleaning chemical i.e., enhanced backwashing

with weak acid, EDTA, or SDS could be more promising for sustainable NF-MBRs operation.

(5) Higher RO membrane fouling rate was observed when fed with permeate of NF-MBR with longer SRT, despite having similar water quality, i.e., DOC of <2 mg/L. One possible explanation was the role of AOC towards RO fouling at low DOC level, which required further investigation in future studies

Chapter 6

RO fouling for high recovery water reclamation

6.1 Introduction

RO fouling at high recovery rate is a complex problem associated with many factors. In Chapter 1, it is pointed out that the two significant problems for RO membrane fouling were resulted from organics fouling by dissolved organics and scaling due to saturation of marginally soluble salts i.e., calcium phosphate in the RO feed. The dissolved organics that are not removed by conventional MBR will be present in the secondary effluents, therefore, directly contribute to the colloidal and organic fouling in the RO process. In addition, the availability of carbon source in the RO feed could lead to biofilm development on the membrane surface and result in biofouling which significantly deteriorates the performance of the RO process. On the other hand, calcium phosphate being one of the key scalants in the wastewater desalination process limits the current RO recovery rate to 75 to 85% (Bartels et al., 2005b).

The findings from Chapter 4 showed that the NF-MBR as a pretreatment was effective in reducing membrane fouling in the downstream RO process mainly due to the improved removal of dissolved organics in the RO feed. However, it was unclear whether the improved NF-MBR permeates can be used as the RO feed for sustainable high recovery RO process, i.e., 90% recovery rate. In addition, the composition of inorganic foulants, organic foulants, and their combined effects on the RO membrane and the fouling mechanisms have not been thoroughly elucidated. Therefore, this chapter focuses on investigating the foulant compositions, fouling characteristics and the behavior of the RO membrane associated with different permeate qualities, i.e., UF-MBR permeates and NF-MBR permeates at different RO recovery rates i.e., 75% and 90%.

The following presents the research questions that this chapter seeks to address:

1. How different recovery rates could affect the fouling in the RO process?
2. How important the water quality of the MBR permeates is to the RO fouling?
3. How significant is silica fouling and the synergetic effect of co-presence of silica and organic matter to the RO fouling?
4. The importance of calcium phosphate scaling to the RO fouling?
5. The synergetic effects of the organic foulants and inorganic foulants on RO fouling?
6. Overall energy consumption of the NF-MBR+RO and the UF-MBR+RO process.

6.2 Materials and methods

6.2.1 Experimental protocol

The fouling experiment was conducted by using UF-MBR and NF-MBR permeates as RO feed to study their fouling potential in the RO process. The UF-MBR permeates were collected from IVP demo plant, Ulu Pandan water reclamation plant, Singapore whereas the NF-MBR permeates were collected from a lab-scale NF-MBR setup described in Chapter 5. Water qualities such as TOC, COD, cations concentrations (i.e., Na^{+}, Ca^{2+}, Mg^{2+}, Fe^{3+} and Si), TDS, and conductivity were measured. To simulate the membrane fouling at high recovery rates of 75% and 90%, the collected MBR permeates were concentrated by discharging the RO permeate until concentrations equivalent to 75% and 90% recovery were attained. Subsequently, the test was continued with a full recycle of permeate back to the feed tank to assess the membrane fouling. The pH in the feed tank was maintained at pH 6.3 throughout the experiment by acid dosing. The pH adjustment was to control the scaling during the concentration phase. The operating parameters of the fouling experiment were summarized in Table 6-1.

Table 6-1. Operating parameters of the RO setup

Parameter	
Effective RO membrane area (m^2)	0.0186
Crossflow rate (L/h)	18
Crossflow velocity (m/s)	0.1
Flux (L/m^2h)	20
Permeates flow rate (L/h)	0.372

The details of the RO setup used for the fouling experiment were described in Chapter 3. The RO flat sheet membranes (BW-30, DOW FilmTec, USA) were cut and soaked in ultrapure water for at least 24 h and subsequently sterilized in 70% ethanol solution (Merck, USA) for 1.5 h before they were used for the fouling experiment. To ensure stable condition in the RO cell, the RO membrane was compacted at 50 L/m^2h for 1h with ultrapure water prior to the fouling experiment.

6.2.2 Membrane autopsy

Upon completion of each experiment, the fouled membranes were removed from the system for autopsy study. Three 4cm x 4cm membrane coupons covering the inlet, middle and outlet of the RO cell were cut as shown in Figure 6-1. The foulants were detached by soaking the membrane coupons in 30 mL of ultrapure water before placing them in the ultrasonicator (Fisher Scientific) for 30 minutes and vortex for 1 min. The inorganics were extracted by 2% nitric acid digestion prior to ICP-OES analysis. The autopsy study including LC-OCD, EEM fluorescence spectroscopy, flow cytometry, polysaccharides and protein assay were conducted for each membrane coupon and the averaged value of the three membrane coupons are presented. In addition, image analysis of the fouled membranes using scanning electron microscope equipped with energy dispersive X-ray (SEM-EDX) and CLSM observation were also carried out in this study.

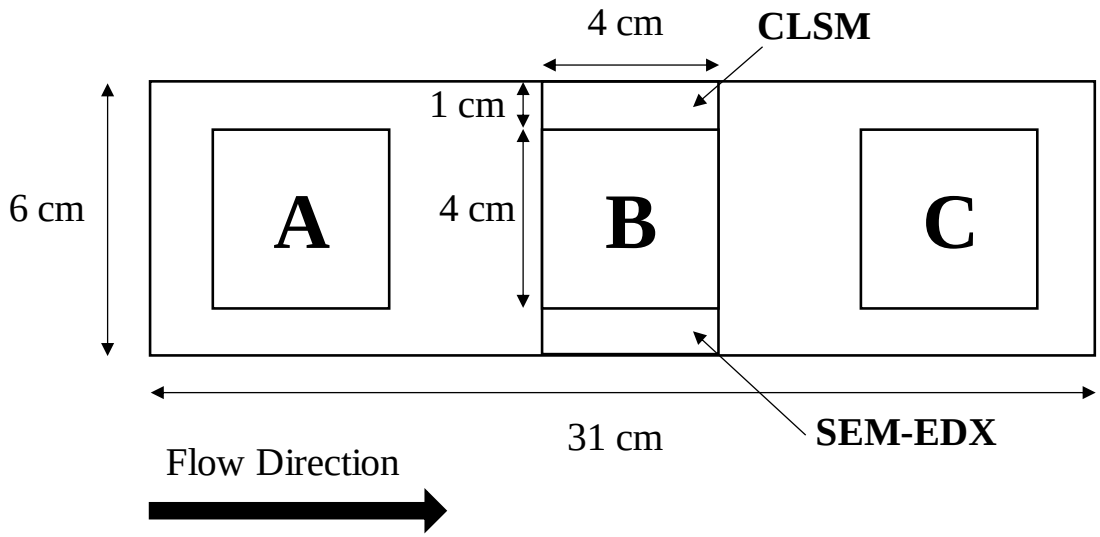

Figure 6- 1. Location of membrane coupons for autopsy study

6.3 Results and discussion

6.3.1 Water quality of the NF-MBR and UF-MBR permeates

6.3.1.1 Dissolved organic matter (DOM) fractions and EPS

The water qualities of the NF-MBR and UF-MBR permeates were presented in Figure 6-2. The DOM fractions present in the permeates were analyzed by LC-OCD. As shown in Figure 6-2, the DOM in NF-MBR permeate was significantly lower the than that of the UF-MBR due to the superior treatment efficiency of the NF-MBR. For example, the concentrations of total dissolved organic carbon (tDOC) (~ 6.26 mg/L), hydrophobic organic carbon (HOC) (~ 1.26 mg/L), and hydrophilic organic carbon (DOC) (~ 5.01 mg/L) in the UF-MBR permeate were approximately 7.5, 3.9, and 9.7 times higher than those in the NF-MBR permeate (tDOC at 0.84 mg/L, HOC at 0.33 mg/L, and DOC at 0.51 mg/L), respectively. The hydrophilic organic fractions were further classified into biopolymers, humic substances, building blocks, LMW acids, and LMW neutrals based on their molecular weight. It is noted that the biopolymers and humic substances were

not present in the NF-MBR permeates while 0.034 mg/L of biopolymers and 2.423 mg/L of humic substances were present in the UF-MBR permeates. Organic fractions with smaller molecular weights such as building blocks LMW acids, and LMW neutrals were found in both NF-MBR and UF-MBR permeates, however, the concentrations in the NF-MBR were considerably lower than that of the UF-MBR permeates.

In addition, SMP which comprised of proteins and polysaccharides were analyzed and compared as shown in Figure 6-2. The concentrations of polysaccharides found in the NF-MBR permeates and UF-MBR permeates were relatively comparable at 1.89 mg/L and 2.03 mg/L respectively. However, the proteins concentration in the UF-MBR permeates (6.23 mg/L) were approximately 21 times higher than those in the NF-MBR permeate (0.30 mg/L). The SMP detected in the permeates was mainly originated from the biological activity in the MBR system since SMP with molecular weight lower than 10 kDa was able to pass through the UF membranes. In this case, proteins in the MBRs were able to pass through the UF membrane but not the NF membrane (Zhao et al., 2010). On the other hand, the polysaccharides with molecular weight < 10 kDa could pass through the UF membrane whereas only monosaccharides and disaccharides with molecular weight < 300 kDa, such as glucose, fructose and sucrose could pass through the NF membrane (Aydoğan et al., 1998). The results obtained from this study showed that the NF-MBR could significantly improve the permeates qualities in terms of organic removal, therefore, it is expected to reduce organic fouling in the RO process.

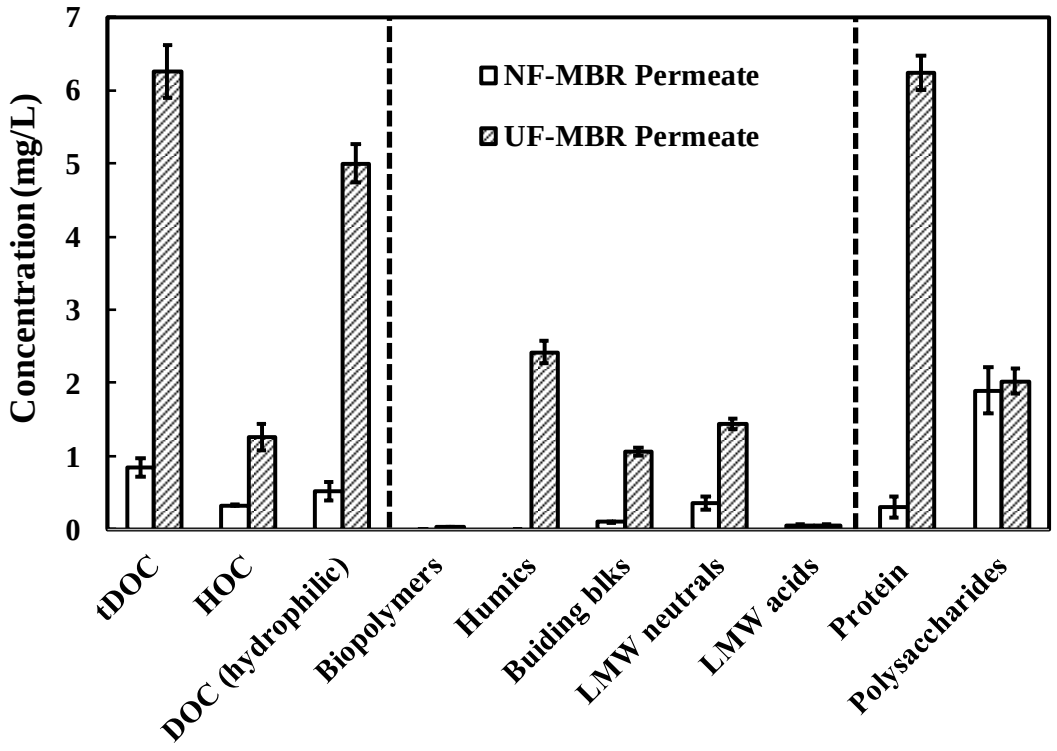

Figure 6-2. Comparison of DOM fractions, proteins and polysaccharides of the NF-MBR and UF-MBR permeates.

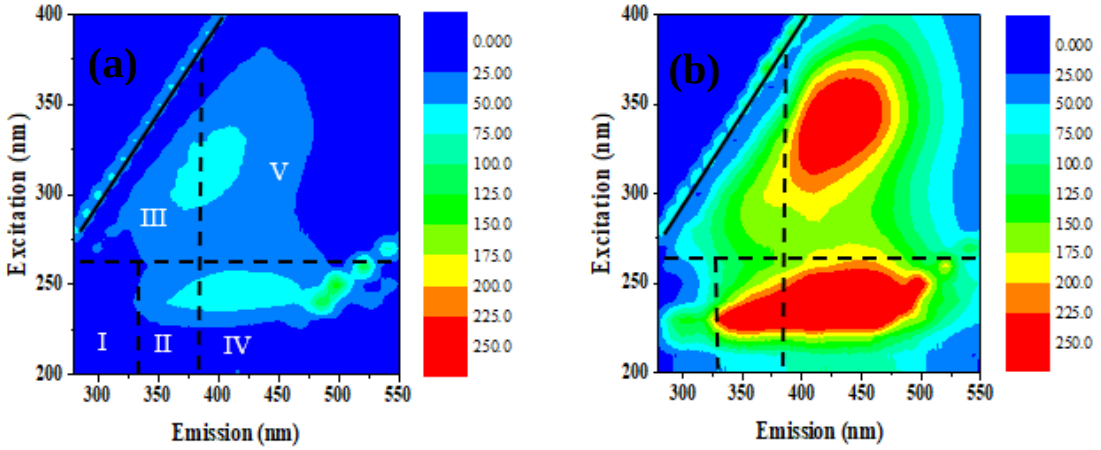

Figure 6-3. Fluorescence excitation emission matrix (F-EEM) of the (a) NF-MBR and (b) UF-MBR permeates.

The LC-OCD size-exclusion based technique could only separate the hydrophilic organic fractions but not the hydrophobic portion. In view of the above, the EEM fluorescence spectroscopy analysis was also carried out to characterize the organics and SMP compositions of MBR permeates. In addition, the EEM analysis could further divide the humic substances into humic and fulvic acids based on their solubility. Figure 6-3 shows that both NF-MBR and UF-MBR permeates contained two dominant peaks, i.e., fulvic acid-like (peak IV) and humic acid-like substances (peak V). The fulvic and humic acids were the products of degradation of organic matter in the wastewater, therefore, they are persistent to the biodegradation in the MBR system (Theng, 2012b). Interestingly, although biopolymers, i.e., proteins in the UF-MBR permeates were not detected by the LC-OCD analysis mainly due to its hydrophobic nature, they were reflected abundantly in the EEM fluorescence spectroscopy analysis as evidenced by the strong signals in region I (aromatic protein I) and II (aromatic protein II) at excitation/emission wavelengths (Ex/Em) of 230-260/280-380 nm. Similarly, both humic and fulvic acids in the NF-MBR permeates were detected by the EEM analysis, indicating that some hydrophobic humic substances could pass through the NF membrane. Nevertheless, the peak intensities of humic and fulvic acids in the NF-MBR permeates (59.45 and 66.88 respectively) were considerably lower than those of the UF-MBR permeates (296.87 and 324.67 respectively).

6.3.1.2 Inorganic components

The concentrations of Ca^{2+}, Mg^{2+}, Fe^{3+}, Si, phosphate, TDS, conductivity, and turbidity of the NF-MBR and UF-MBR permeates were summarized in Figure 6-4. The ICP-OES analysis revealed that both NF-MBR and UF-MBR permeates have comparable concentration of Ca^{2+}, Fe^{3+} and Si. The turbidities of both MBR permeates were well below 0.1 NTU, indicating that there were negligible particulate matters in the permeates. The concentration of Mg^{2+} in the UF-MBR permeates at 8.84 mg/L were 17% higher than that of the NF-MBR (7.55 mg/L). In contrast, the concentration of phosphate, TDS, conductivity in the NF-MBR permeates at 12.90 mg/L, 522.4 mg/L, and 832.9 μS/cm were 57%, 23%, and 29% higher than that of the UF-MBR (8.20 mg/L, 425.7 mg/L,

645.1 μS/cm). The higher phosphate concentration in the NF-MBR permeates was mainly attributed to the accumulation of total phosphate in the NF-MBR system.

During the early stage of the project, one of the motivations to incorporate NF membrane into the MBR system was to improve the removal of the multivalent ions i.e., Ca^{2+}, Mg^{2+}, Fe^{3+}, and phosphate. However, the long-term experiment described in Chapter 4 and 5 revealed that the concentrations of these multivalent ions in the NF-MBR permeates increased gradually over time and eventually reached an equilibrium concentration that is similar to the feed. This phenomenon was further explained and verified by the mass balance calculation described in Chapter 5.

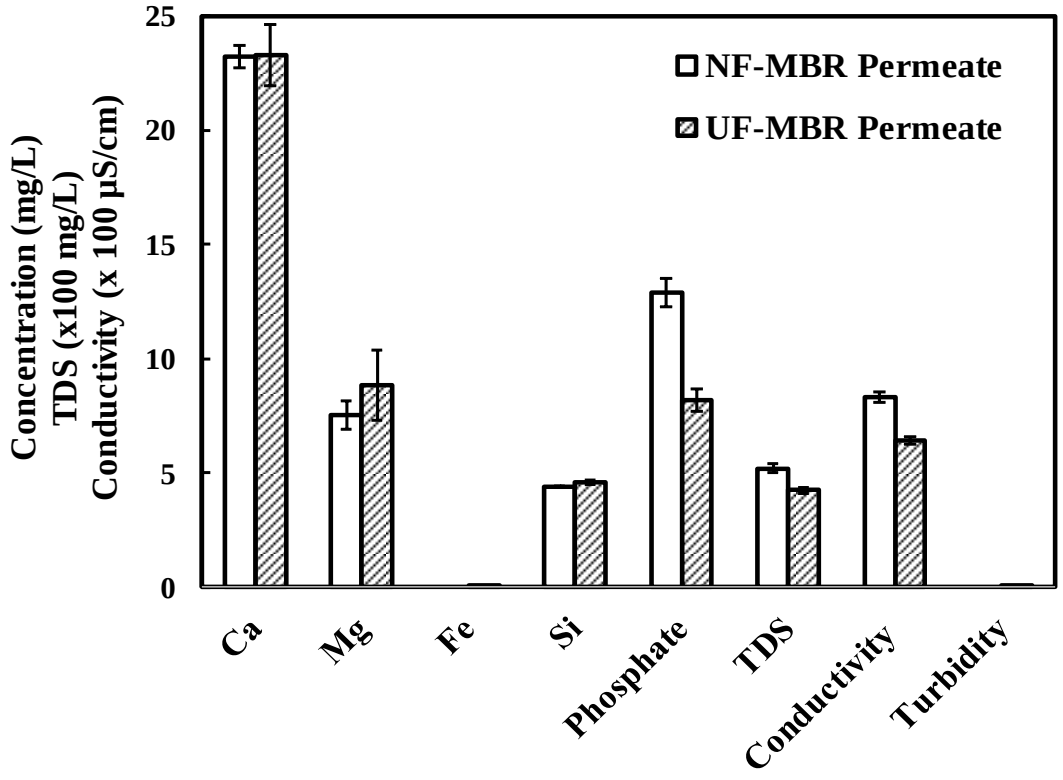

Figure 6-4. Concentrations of Ca^{2+}, Mg^{2+}, Fe^{3+} and Si, phosphate, TDS, conductivity, and turbidity of the NF-MBR and UF-MBR permeates.

6.3.2 RO fouling behavior

(1) RO fouling with the increasing recovery rates

To simulate the membrane fouling at a high recovery of 90%, the NF-MBR and UF-MBR permeates were concentrated by discharging the RO permeate until the concentration equivalent to 90% recovery was attained. The increase in TMP was monitored throughout the concentration stage and the normalized TMP profiles, TMP/TMP_0 were plotted against recovery rate as shown in Figure 6-5. The results show that the 90% recovery rate was attained for the NF-MBR permeates in which a gradual rise in TMP can be observed during the concentration stage. The increase in TMP was mainly attributed to the increase in osmotic pressure, ~2.2 bar as a result of increasing salt concentrations in the RO feed.

In contrast, the maximum recovery rate attained for the UF-MBR permeates was ~81%. A surge in the TMP was observed when the recovery rate exceeded 75% for the UF-MBR permeates in which the RO fouling rate increased dramatically from 4.2 kpa/h to 127.2 kpa/h. Before 75 % recovery rate was attained, it was noted that the increase in TMP at the same recovery rate was slightly greater for RO fed with UF-MBR permeate compared to NF-MBR permeates, suggesting that minor fouling could have occurred during the concentration stage owing to the higher organic contents in UF-MBR permeates (Figure 6-3). Thereafter, the TMP skyrocketed within a very short period, i.e., 3 hr and eventually the permeate flux could not be maintained at 20 LMH. The rapid increase in TMP observed when recovery > 75% was mainly due to membrane fouling since the increase in osmotic pressure only accounted for ~30 % of the increase in TMP, i.e., ~ 2 bar.

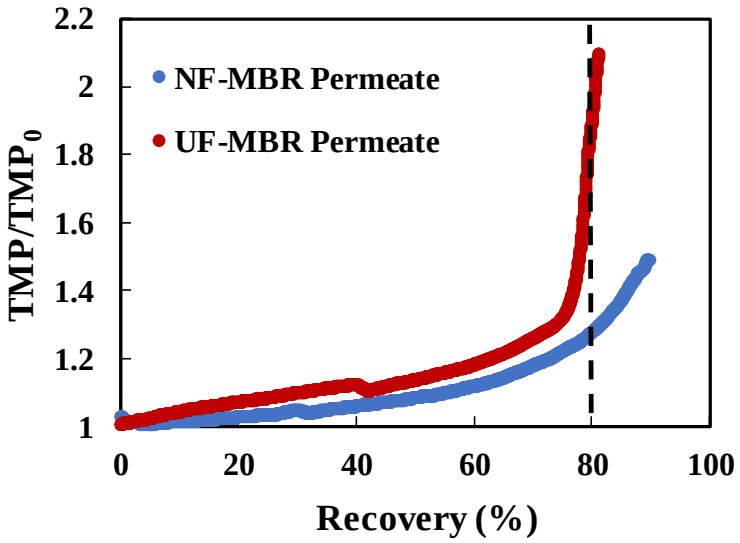

Figure 6-5. TMP profiles for the NF-MBR and UF-MBR permeates during the concentration stage.

(2) RO fouling at 75% and 90% recovery

To investigate the fouling propensity of the NF-MBR and UF-MBR permeates at the desired recovery level, i.e., fixed at 75% or 90%, the concentrated NF-MBR permeates equivalent to 75% and 90% recovery and the UF-MBR permeates equivalent to 75% recovery (denoted as 75-NFP, 90-NFP and 75-UFP respectively hereinafter) were subsequently used for the RO fouling experiment. The TMP increase rate presented as normalized TMP/TMP_0 was monitored over the duration of 3 to 5 days as illustrated in Figure 6-6. The results show that the much steeper gradient could be observed for the 90-NFP curve compared to that of the 75-UFP and 75-NFP, i.e., the fouling rate of 90-NFP was 0.0334 d^{-1}, which means 90-NFP had the most serious fouling among the 3 conditions. On the other hand, at 75% RO recovery, the process fed with NF-MBR permeates has a slower fouling rate than the one fed with UF-MBR permeates as indicated by the gradient values of 0.0115 d^{-1} and 0.0168 d^{-1} for the 75-NFP and 75-UFP slope respectively. Overall, the rate of fouling can be summarized in order as: 75-NFP < 75-UFP < 90-NFP.

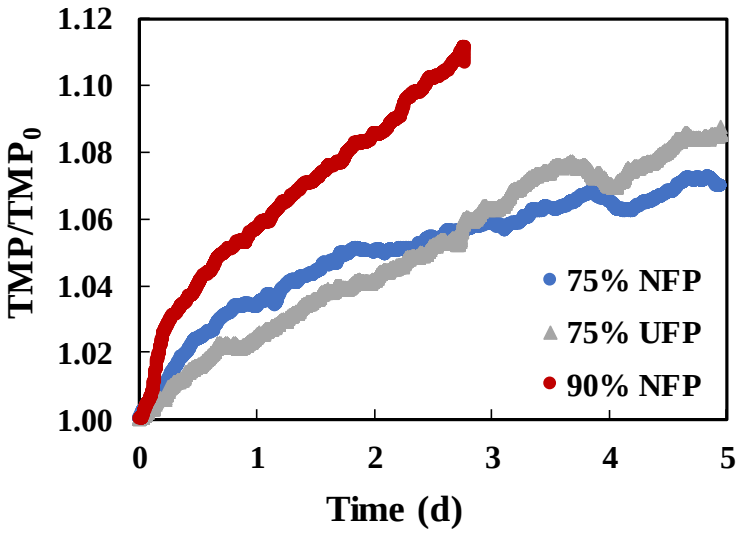

Figure 6-6. TMP profiles of fouling experiments with the NF-MBR and UF-MBR permeates at 75% and 90% recovery level.

6.3.3 Membrane autopsy

At the end of the fouling experiment, the fouled RO membranes for 75-UFP, 75-NFP, and 90-NFP were removed for autopsy study. In view of the maximum attainable recovery rate of the UF-MBR permeates at 81%, fouling experiment simulating 90% recovery for the UF-MBR permeates was not conducted. For comparison purpose, the fouled membrane used for the concentration process for the UF-MBR permeates as shown in Figure 6-5 was characterized (denoted as 81-UFP hereinafter).

(1) Inorganic compositions of the fouling layers

The inorganic compositions of the fouling layers were analyzed by ICP-OES as shown in Figure 6-7. The results showed that the large amounts of Ca and P were detected in the fouling layer of 81-UFP, suggesting that calcium phosphate was the major contributor to the serious fouling occurred at high recovery rate, i.e., >75% recovery. Calcium phosphates have been reported to be an important scaling agent of RO membranes for water reuse application operated at high recovery rate, which usually results in more drastic membrane fouling than organic or colloidal fouling as shown in Figure 6-5

(Bartels et al., 2005b, Zhao et al., 2010). Although Ca was abundantly found in the foulants layer of 90-NFP, very little phosphate was found. In comparison, there was little inorganic matter found in the foulants of 75-UFP and 75-NFP, indicating no severe inorganic fouling. The synergistic effect due to the co-presence of silica and organic matter was reported to cause severe membrane fouling to the RO process (Kimura et al., 2016b). In this study, only small quantities of Si were detected in all the foulants, suggesting that silica was not greatly involved in the fouling despite the presence of organic matter in the RO feed.

In addition, the results were supported by SEM-EDX analysis that compares the elemental compositions of the virgin membrane to the fouled membranes as shown in Table 6-2. The virgin membrane only showed the presence of three major elements (i.e., C, O, and S) of the polymeric materials. It was noted that the weight percentage of C for the fouled membrane of 81-UFP was lower than that of the virgin membrane (35.5% vs. 79.2%) while other membranes i.e., 75-UFP, 75-NFP, and 90-NFP showed a higher percentage than the virgin membrane (80.5%, 81.0%, and 81.3% respectively). This could possibly due to the substantial coverage of membrane surface by the dense inorganic fouling layer. According to Table 6-2, the weight percentage of Ca, P, and O increased significantly to 15.3%, 7.1%, and 33.7% respectively in the fouled membrane of 81-UFP, confirming the severe fouling caused by calcium phosphate scaling. Generally, these results correlated well with the fouling behavior observed from the TMP profiles (Figure 6-5).

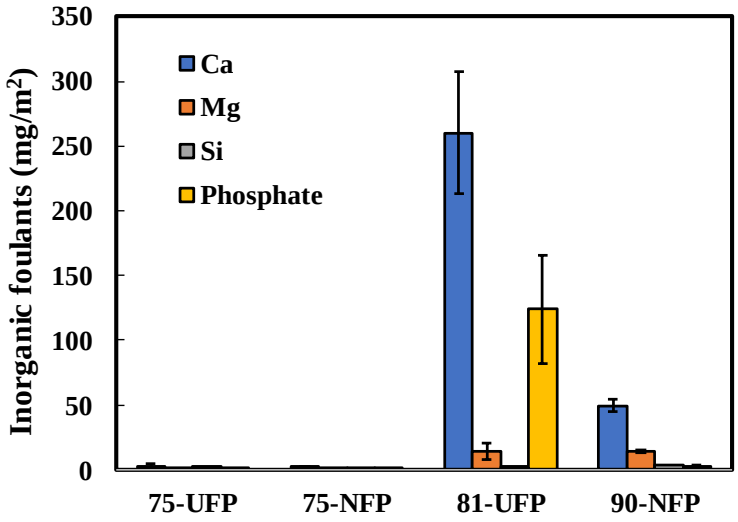

Figure 6-7. Comparison of inorganic compositions of the fouling layers.

(2) Organic compositions of the fouling layer

To determine the nature of the fouling layer, the organic contents of the fouling layer were quantified by LC-OCD analysis as shown in Table 6-3. It was clearly shown that higher organic contents were detected in the RO systems fed with the UF-MBR permeates than NF-MBR permeates. For example, the tDOC of 75-UFP and 81-UFP (20.19 ± 4.97 mg/m^2 and 26.33 ± 3.78 mg/m^2 respectively) was 2 times higher than that of the 75% NFP and 90-NFP (9.49 ± 0.25 mg/m^2 and 12.82 ± 1.17 mg/m^2 respectively), indicating the more important role of organic fouling in the overall fouling process. It was noted that humic substances were abundantly found in the fouling layer of 75-UFP and 81-UFP (3.59 ± 1.40 mg/L and 13.18 ± 1.82 mg/L) accounted for 27% and 79% respectively of the total hydrophilic DOC. Interestingly, at low recovery rate (i.e. 0% recovery), neither UF-MBR or NF-MBR permeates has resulted in the deposition of humic substances on the RO membranes as demonstrated in Chapter 4. The findings suggested that the deposition of humic substances could be promoted at high RO recovery rate. Nevertheless, no humic substance was detected in the RO system fed with NF-MBR permeates even at high recovery rate, i.e., 90% recovery mainly due to the absence of humic substances in the NF-MBRs.

Table 6-2. Elemental composition of virgin and fouled RO membrane surfaces by SEM-EDX.

		Recovery = 90 %	Recovery = 81 %	Recovery = 75 %	
Element (%)	Virgin BW-30	Fouled membrane (NF-MBR permeates)	Fouled membrane (UF-MBR permeates)	Fouled membrane (NF-MBR permeates)	Fouled membrane (UF-MBR permeates)
C	79.2	81.3	40.2	81.0	80.5
O	13.8	13.2	33.7	13.6	13.9
S	7	5.1	2.7	4.8	5.3
Ca	N.D.[a]	0.2	15.3	0.1	0.2
Mg	N.D.	0.1	0.7	N.D.	N.D.
P	N.D.	N.D.	7.1	N.D.	N.D.
Si	N.D.	0.1	0.2	0.1	0.1

[a] N.D. represents "not detectable

In addition, the EPS content in the fouling layer was quantified as shown in Table 6-3. It was noted that the mass of proteins and polysaccharides deposited increased significantly when the recovery rate was further increased from 75% to 90%, as evidenced by the higher mass of proteins and polysaccharides (127.44 ± 50.87 mg/m^2 and 50.87 ± 32.42 mg/m^2 respectively) found in the fouling layer of 90-NFP as compared to 75-NFP (33.54 ± 28.85mg/m^2 and 19.87 ± 6.91 mg/m^2 respectively). The observation supported that the deposition rate of organic matter was enhanced at high RO recovery rate (Zhao et al., 2010). The proteins and polysaccharides deposited in the 75-UFP (187.80 ± 56.18 mg/m^2 and 41.60 ± 4.60 mg/m^2 respectively) and 81-UFP (183.33 ± 30.77 mg/m^2 and 36.56 ± 22.46 mg/m^2 respectively) were relatively comparable possibly due to the shorter experimental duration, i.e., 2 d. Nevertheless, the amount of EPS in 75-UFP and 81-UFP were considerably higher than that of 75-NFP and 90-NFP mainly due to the presence of high SMP content in the UF-MBR permeates.

The fluorescence EEM analysis revealed that all the RO foulants contained one dominant peak (peak II) at excitation/emission wavelengths (Ex/Em) of 230/338 nm, known as the aromatic protein II which is associated with the aromatic protein tryptophan. The intensity signals extend to region I (aromatic protein I) and region III (SMP-like substances) for the 75-UFP and 81-UFP, indicating the presence of these EPS compounds in the foulants. Although the biopolymers content of 81-UFP was among the lowest from the LC-OCD analysis, SMP and EPS which are usually hydrophobic in nature and not detected by LC-OCD were captured by the EEM analysis, proteins and polysaccharides assays. In addition, wide spread signals in region IV (fulvic acid-like substances) and V (humic-acid like substances) were only observed in the foulants of 81-UFP, indicating the abundant presence of humic substances in the foulants as evidenced by the LC-OCD analysis.

Table 6-3. The organic compositions of the RO fouling layers (n=3).

Foulants characteristics		75-UFP	75-NFP	81-UFP	90-NFP
LC-OCD analysis	Total DOC (mg/m^2)	20.19 ± 4.97	9.49 ± 0.25	26.33 ± 3.78	12.82 ± 1.17
	Hydrophobic DOC (mg/m^2)	7.07 ± 1.18	4.14 ± 0.49	9.73 ± 1.05	3.90 ± 0.93
	Hydrophilic DOC (mg/m^2)	13.13 ± 3.58	5.36 ± 0.49	16.60 ± 3.44	8.92 ± 2.02
	Biopolymers (mg/m^2)	2.93 ± 1.49	1.89 ± 0.14	0.79 ± 0.19	2.58 ± 1.31
	Humic substances (mg/m^2)	3.59 ± 1.40	N.D.	13.18 ± 1.82	N.D.
	Building blocks (mg/m^2)	1.36 ± 0.33	0.95 ± 0.10	0.99 ± 0.29	1.76 ± 0.54
	LMW neutrals (mg/m^2)	5.24 ± 0.35	2.44 ± 0.35	1.63 ± 1.44	4.39 ± 0.25
	LMW acids (mg/m^2)	N.D.[a]	0.09 ± 0.02	N.D.	0.19 ± 0.05
EPS analysis	Proteins (mg/m^2)	187.80 ± 56.18	33.54 ± 28.85	183.33 ± 30.77	127.44 ± 50.87
	Polysaccharides (mg/m^2)	41.60 ± 4.60	19.87 ± 6.91	36.56 ± 22.46	50.87 ± 32.42

[a] N.D. represents "not detectable".

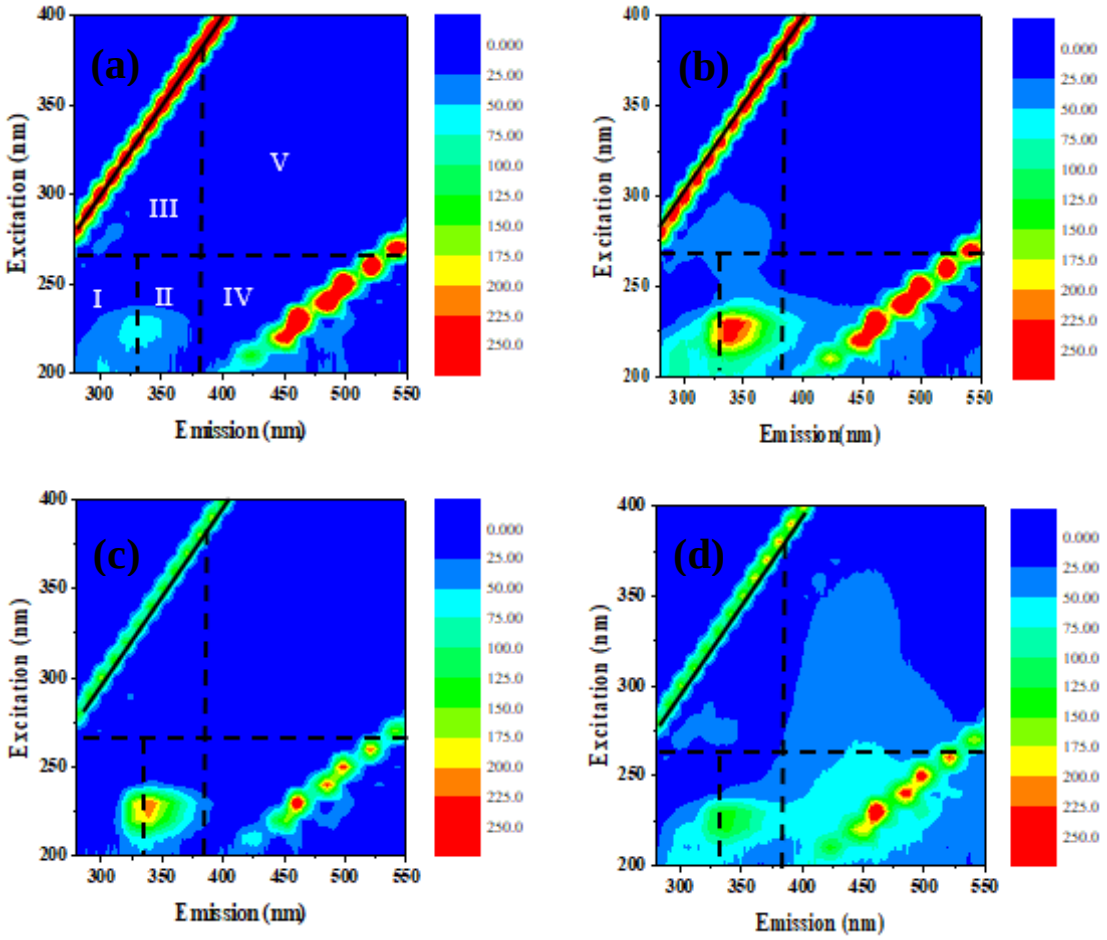

Figure 6-8. Fluorescence excitation-emission matrix (F-EEM) of the RO foulants a) 75-NFP, b) 75-UFP, c) 90-NFP and d) 81-UFP.

(3) Morphology of the RO membrane surface

SEM images of the virgin membranes and fouled membranes are illustrated as shown in Figure 6-9. Noticeable difference in the surface morphology was clearly observed between the virgin membrane and the fouled membranes. At 75% recovery, the morphologies of the cake layer were relatively comparable between the 75-NFP and 75-UFP. It can be observed that the organic macromolecules were sparsely and unevenly distributed across the membrane surface.

In contrast, the morphology of the cake layer for 81-UFP was distinctly different from that of the 75-NFP and 75-UFP. As shown in Figure 6-9(c), the formation of a compact

cake layer with the polymer microstructures of the original RO membrane surfaces totally covered up by the fouling layer was observed. In view of the shorter fouling experimental duration (< 2d) for the 81-UFP, it was expected to have less organic deposition, however, the results by the LC-OCD revealed that the 81-UFP has the highest concentrations of tDOC. Although significant amounts of calcium phosphate precipitates were detected by the SEM-EDX, regular-shaped plate or needle crystals typically observed with inorganic scaling were not found, suggesting that the calcium phosphate scales were not in the form of crystallization but rather amorphous in nature, i.e., dicalcium phosphate, tricalcium phosphate (Greenberg et al., 2005). Alternately, co-deposition and/or co-precipitation of calcium phosphates along with other organic matter could occur due to the high concentration of DOC in the UF-MBR permeates (Zhao et al., 2010). Interestingly, at 90% recovery, the cake layer of 90-NFP was comparable to that of the 75-NFP with some organic foulants deposition can be seen on the surface, suggesting that the cake layer fouling was insignificant.

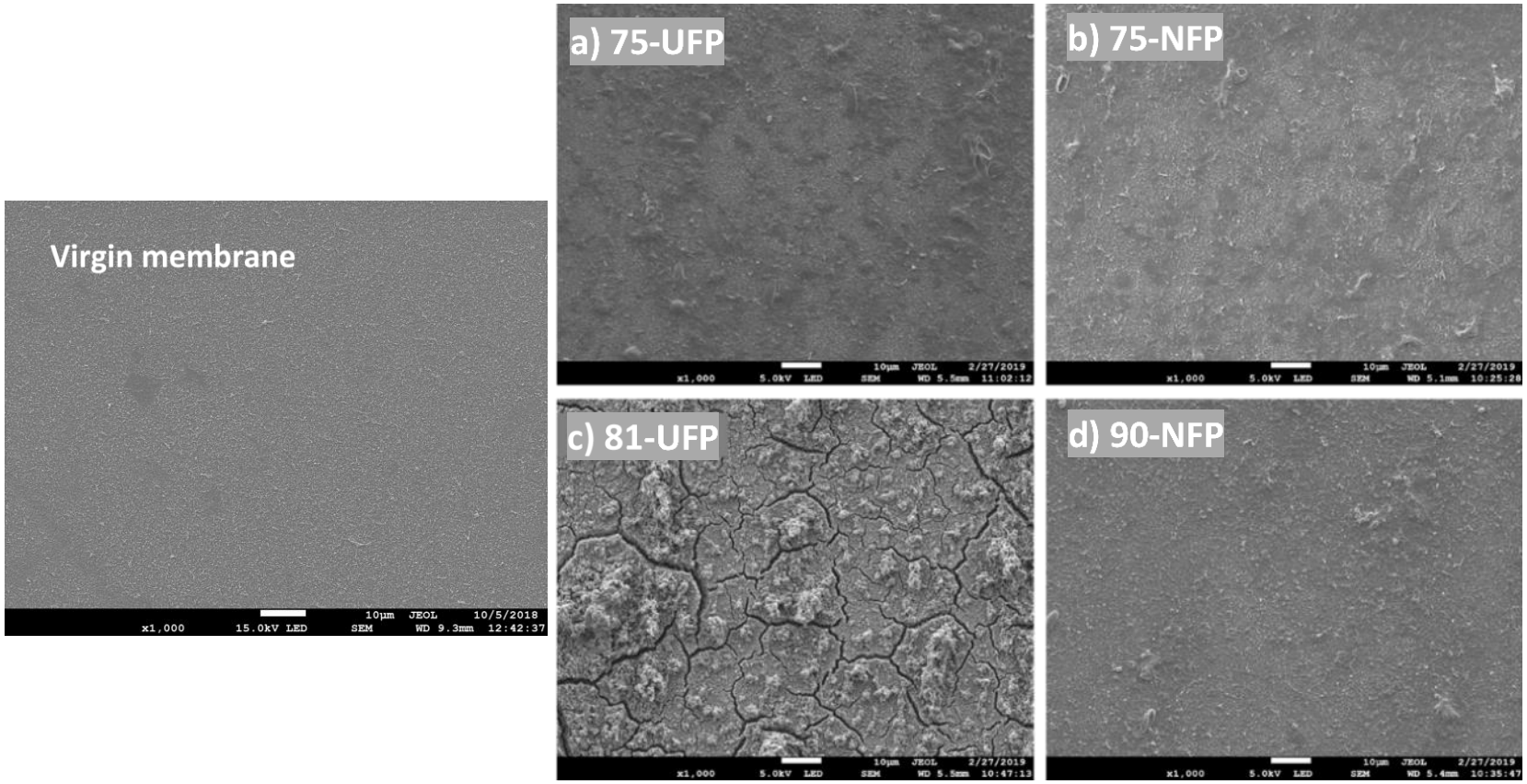

Figure 6-9. Scanning Electron Microscopy (SEM) images of virgin membrane and fouled membranes: (a) 75-UFP, (b) 75-NFP, (c) 81-UFP and (d) 90-NFP (x 1000 magnification).

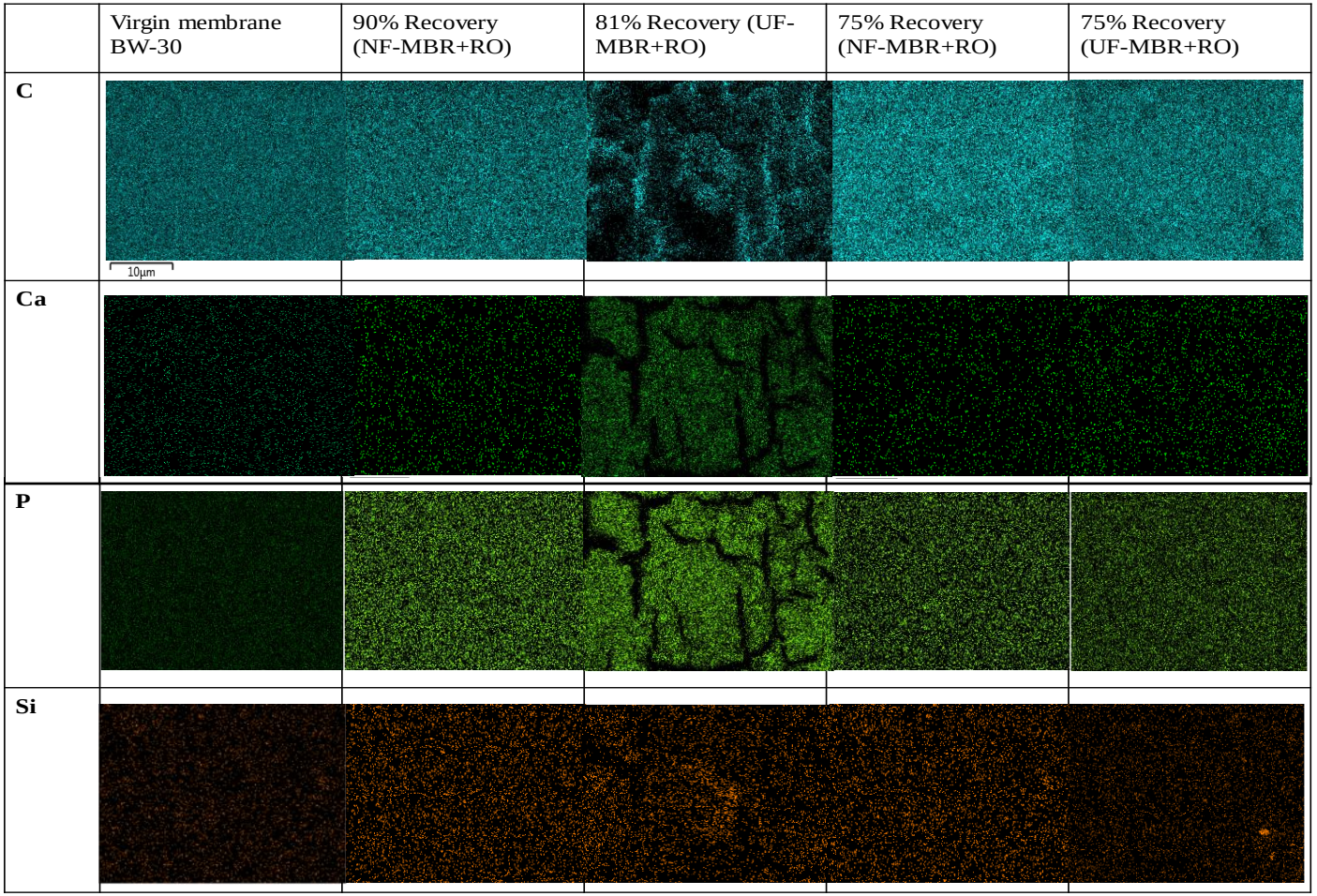

Figure 6-10. **The elemental mappings of Ca, P, C, and Si by SEM-EDX of virgin membrane and fouled membranes: 75-UFP, 75-NFP, 81-UFP and 90-NFP.**

6.3.4 Synergetic effects of organic and inorganic fouling

Based on the water quality analyses, foulant analyses, and TMP profiles, the relationship among permeate quality, recovery level and RO fouling can be established. The results show that the membrane performance in water reuse application especially at high recovery level, i.e., >75% was strongly influenced by the combined effects of organic and inorganic fouling. The NF-MBR permeates which contained relatively higher amount of phosphate, in principle shall have more severe inorganic fouling than the UF-MBR permeates when the solubility limit was exceeded. However, calcium phosphate scaling is a rather complex system that governed by many factors other than the levels of calcium and phosphate present in the RO feed, i.e., pH, temperature, organic functional groups etc. that influence the kinetics and phase of crystals. In addition, the solubility product constants, i.e., -log (Ksp) of the calcium phosphate compounds (i.e., dicalcium phosphate, tricalcium phosphate, tetracalcium phosphate, hydroxyapatite, and fluorapatite) could vary significantly ranging from 6.5 to 60.5 depending on the crystal phase (Chow, 2001).

The serious scaling experienced in the 81-UFP fouling test could be attributed to the presence of large amounts of biopolymers (i.e., proteins and polysaccharides) and humic substances in the UF-MBR permeates. The results from SEM-EDX analysis suggested that the precipitating phosphate species were likely to be dicalcium phosphate, tricalcium phosphate, and hydroxyapatite which are amorphous in nature. The co-deposition and/or co-precipitation of these calcium phosphates along with other organic matter, i.e., biopolymers as evidenced by the membrane autopsy results suggested that the biopolymers that contain a high ratio of anionic amino-acids could induce calcium phosphate scaling by providing the nucleation sites for the biomineralization to take place (Dahdal et al., 2016). The findings are supported by the studies that use Langmuir (π-A) isotherm system to prove that the biopolymers originated from EPS i.e., bovine serum albumin (BSA), fibrinogen, lysozyme and alginic acid, could induce calcium phosphate scaling at the RO membrane surface (Steiner et al., 2010, Dahdal et al., 2016,

Pipich et al., 2013, Dahdal et al., 2014). The scaling accompanied by the deposition of other organic matter, i.e., humic substances, building blocks, etc. makes the fouling scenario a more complex one. Due to the effect of concentration polarization and cake enhanced concentration polarization (CECP), the fouling quickly accelerated and eventually led to the serious fouling that we observed. Therefore, the results suggested the benefit of lowering the DOC content in RO feed water to minimize the negative impact of the combined organic-inorganic fouling.

Interestingly, it was noted that although the amount of organic foulants on 90-NFP was lesser than 75-UFP, the TMP increase appeared to be higher for the former. This could be due to two reasons: (i) the fouling layer formed on 90-NFP membrane was denser (i.e., had lower porosity) than on 75-UFP due to the presence of higher ratio of low molecular weight organics in the NF-MBR permeates that filled up the pores of the cake layer. According to Kozeny-carman equation, specific cake resistance for fouling layer was a strong function of ε, thus dense layer resulted in higher hydraulic resistance; (ii) the cake-enhanced osmotic pressure (CEOP) effect where the back diffusion of rejected solute such as Ca^{2+}, Mg^{2+} etc. were hindered in the un-stirred fouling layer which greatly increased the concentration of solutes at the membrane surface, thus higher osmotic pressure need to be overcome and greater TMP was required (Sim et al., 2011).

6.4 Concluding remarks

In conclusion, this chapter studied the foulant compositions, fouling mechanisms and the impact of pre-treatment with NF-MBR and UF-MBR (i.e., RO feed water quality) on membrane fouling in a lab-scale RO system operated at 75% to 90% recoveries for water reclamation application. Overall, the RO feed water of UF-MBR permeates were found to contain higher DOC but lower Ca and P, which affected the subsequent RO operation. Beyond recovery of 75%, there was a drastic increase in TMP due to the combined effects of organic-inorganic fouling. Therefore, it is necessary to limit the recovery level for this type of RO feed water quality. In contrast, the RO system fed with NF-MBR

permeates with lower DOC but higher Ca and P concentrations, showed less impact from the combined effects of organic-inorganic fouling despite at higher recovery of 90%. This study revealed that when a suitable pre-treatment step was put in place to improve the RO feed water quality, high recovery RO process without excessive fouling is possible for water reclamation application.

Chapter 7

Conclusions and recommendations

7.1 Conclusions

The nanofiltration membrane bioreactor (NF-MBR) is a novel integration of a biological process and a high rejection nanofiltration membrane separation process into a single step. The interest in the NF-MBR lies in the high rejection NF membrane that could retain persistent and low molecular weight organic micro-pollutants, and thereby facilitates a better biodegradation in the bioreactor and offers potential benefits for water reclamation. With the improved MBR permeates as the RO feed, the subsequent RO process could be potentially operated at higher recovery rates with less membrane fouling. This thesis explored and investigated the possibility to integrate the NF-MBR into the current MBR-RO process for a more sustainable water reclamation process for potable water reuse.

The literature review in Chapter 2 summarized the technological challenges of the NF-MBR system and the advantages of NF-MBR over the other HR-MBRs (i.e., FO-MBR and MD-MBR) in the context of water reclamation. Issues of relevance such as membrane stability, salt accumulation and membrane fouling were critically reviewed.

In Chapter 4, a side-stream NF-MBR system was developed and systematically studied with an ultrafiltration membrane bioreactor (UF-MBR) and RO process as a baseline for comparison. The study demonstrated a successful incorporation of the low-pressure hollow fiber NF membrane developed by the Singapore Membrane Technology Centre (SMTC) into the NF-MBR system that allows the system to be operated at a constant flux of 10 L/m^2h (significant improvement compared to previous studies with flux < 5 L/m^2h). The NF-MBR achieved superior permeate quality due to enhanced biodegradation and high rejection capacity of the NF membrane, leading to lower RO

fouling rates (~3.3 times as compared to the UF-MBR). No deterioration in the permeates quality was observed throughout the experimental period. The NF membrane exhibited excellent membrane stability in a biologically active environment and is suitable to be incorporated into the NF-MBR system. In addition, the NF-MBR achieved higher organic removal than the UF-MBR mainly due to extended retention time that enhances the biodegradation of the retained organics in the bioreactor. Apart from that, the study also indicated that the cake layer fouling that caused the cake-enhanced osmotic pressure (CEOP) effect contributed predominantly to the transmembrane pressure (TMP) increase in the NF-MBR, while irreversible pore fouling was the major reason for UF membrane fouling. Lastly, biopolymers were the main organic foulants of NF/UF membranes and RO membranes.

In Chapter 5, the impacts of salt accumulation on the bioprocess as well as membrane performance of a high retention NF-MBR and subsequent RO process for water reclamation were systematically studied. Two lab-scale NF-MBRs were operated in parallel at the solid retention times (SRTs) of 30 and 60 days. The concentration factor is a function of SRT, HRT and membrane rejection. Increasing the SRT resulted in greater accumulation of scale-forming inorganic salts (i.e., Ca, Mg, PO_4) and organic compounds (i.e., DOC, sCOD, and especially humic substances and building blocks due to its poor or non-biodegradable nature). A short-term salt spike test showed that the abrupt change in salt concentrations did not have any negative impact on the biomass and the addition of Ca had positive impacts on cell viability and microbial activity at optimum dosage.

The accumulation of divalent ions did not pose adverse impacts to the biodegradation efficiency and both NF-MBRs achieved excellent organic (> 97%) and ammonia (> 98%) removal ratios. The elevated divalent ions level promoted bioflocculation, however, the effects on microbial activity and viability were not statistically significant in the long-term experiment. Salt accumulation did not influence the microbial community structure of activated sludge in NF-MBRs, but led to different predominant microbial communities

in the cake layer foulants of NF membranes. More severe membrane fouling was observed in the NF-MBR with elevated salinity, due to the formation of a compact cake layer with more accumulation of polysaccharides-Ca^{2+} complex and calcium phosphate on the NF membrane. The thicker and more compact irreversible fouling layer as well as higher salt concentration caused more severe cake-enhanced osmotic pressure (CEOP) effect in the NF-MBR with longer SRT. Combining periodical backwash (pressure of 3 bar) and flushing (velocity of 0.8 m/s) could effectively remove cake layers from the NF membranes, particularly in the NF-MBR at low SRT of 30 d. The study also revealed that physical cleaning was ineffective in controlling membrane fouling associated with inorganic fouling, i.e., calcium phosphate scaling. The effectiveness of chemical cleaning with citric acid is not remarkable (<42% membrane permeability restoration). Optimization of chemical cleaning chemical i.e., enhanced backwashing with weak acid, EDTA, or SDS could be more promising for sustainable NF-MBRs operation.

In Chapter 6, the foulant compositions, fouling characteristics and the behavior of the RO membrane associated with different permeate qualities, i.e., UF-MBR permeates and NF-MBR permeates at different RO recovery rates i.e., 75% and 90% were thoroughly elucidated. The RO feed water of UF-MBR permeates were found to contain higher DOC but lower Ca and P, which affected the subsequent RO operation. Beyond recovery of 75%, severe fouling was observed due to the combined effects of organic-inorganic fouling. Therefore, it is necessary to limit the recovery level for this type of RO feed water quality. In contrast, the RO system fed with NF-MBR permeates with lower DOC but higher Ca and P concentrations, showed less impact from the combined effects of organic-inorganic fouling despite at higher recovery of 90%. In this study, silica fouling was not critical despite the presence of organic matter in the RO feed.

It was demonstrated that when a suitable pre-treatment step, i.e., NF-MBR was put in place to improve the RO feed water quality, high recovery RO process without excessive fouling is possible for water reclamation application. The calculated energy consumption of the NF-MBR+RO system at 90% recovery was comparable to that of the UF-

MBR+RO at 75% recovery. The thesis substantiated the feasibility of NF-MBR+RO for high recovery water reclamation.

7.2 Recommendations

The NF-MBR is a fledgling technology that demands further research and development. The areas of potential and future research are proposed as follows:

i. *Membrane cleaning methods in the NF-MBR*

According to the work presented earlier, membrane fouling remained to be the most pressing issue in the operation of NF-MBR. Although the reversible fouling in the early stage can be controlled by physical backwashing and flushing, the irreversible fouling gradually developed with NF filtration time, which led to an exponential increase of TMP and eventually shorten the membrane lifespan. Calcium phosphates and polysaccharides were found to be the important foulant that caused the irreversible fouling on the NF membrane. The presence of free Ca^{2+} ions in the mixed liquor could enhance the gelation behavior of polysaccharides on the NF membranes by forming the crosslinked network between the carboxyl groups in polysaccharides and the divalent ions. This type of complex fouling was persistent to physical cleaning and the effectiveness of chemical cleaning using citric acids was found to be very limited. Therefore, further study on optimization of chemical cleaning of NF-MBR is required for sustainable operation. As the LBL type NF membranes cannot tolerate chemical cleaning agents with pH>8, chemical enhanced backwashing with enzyme-based cleaning agents, EDTA, or SDS could be more promising for NF-MBRs.

ii. *NF membrane development and module configuration*

The hollow fiber NF membranes used in this work was in an inside-out configuration. The inherent problem with the inside-out configuration was that larger particles, i.e. bioflocs in the mixed liquor could easily clog the

lumen of the entire hollow fiber when the mixed liquor was delivered to the NF membrane and inevitably cause a decrease of effective membrane area. This could lead to an increase of local fluxes (i.e., higher than the operation flux) and subsequently accelerates membrane fouling. In addition, the inside-out configuration also eliminates the possibility of employing the scouring agents (i.e., bubbles and actived carbon) and manual cleaning. Therefore, outside-in configuration is preffered for the ease of fouling control. The mechanical strength of the hollow fiber and the LBL coating technics will be the challenges to producing robust NF membrane with optimal flux and rejection. In addition, process modeling that include the bioprocess, precipitation and membrane properties (i.e., permeability and rejection) can assist in optimizing the NF-MBR as well as designing the ideal NF membrane (i.e. rejection).

iii. Nutrient recovery

Previous attempt of recovering phosphorus in the form of calcium phosphate has been demonstrated in the MF/UF-FO-MBR system. In this hybrid system, the FO membrane can effectively retain phosphate and divalent ions in the bioreactor, while the MF/UF membrane allows these accumulated compounds to be bled out for phosphorus recovery by pH adjustment. Similar to the FO-MBR, the high concentration of phosphorus in the NF-MBR system offers a great potential for nutrient recovery. Based on this rationale, the concentrations of calcium and phosphate could be reduced and maintained below the solubility limit to prevent scaling on the NF membrane. In addition, the concentrations of calcium and phosphates in the NF-MBR permeates were expected to be lower due to the periodic bleeding by the MF/UF membrane, therefore, could be beneficial to the downstream high recovery RO operation.

iv. Removal and fate of TrOCs in the NF-MBR

The presented work has demonstrated the effective retention and enhanced biodegradation of dissolved organics in different range of molecular weight, i.e., biopolymers (MW > 10 kDa), humic substances (MW ~ 1000 Da), building blocks (MW 300-500 Da), low molecular weight organics acids (MW < 350 Da) and neutrals (MW < 350 Da) in an NF-MBR system. However, the biodegradability and the fate of specific TrOCs including pesticides, pharmaceuticals, antibiotics, personal care products, hormones and endocrine disrupters were largely unknown. Future study should aim at quantitatively understanding the removal mechanism of these TrOCs that encompasses both sorption and biodegradation. It is recommended to develop a mathematical model that is able to predict the fate of TrOCs in an NF-MBR system. The effect of accumulation of these recalcitrant TrOCs to the NF-MBR system warrant further investigation.

References

ADAV, S. S., LEE, D. J. & TAY, J. H. 2008. Extracellular polymeric substances and structural stability of aerobic granule. *Water Research,* 42**,** 1644-1650.

ADHAM, S., KUMAR, M. & PEARCE, W. H. 2005. Model developed for brackish and reclaimed water. *International desalination & water reuse quarterly.,* 15.

AL-AMOUDI, A. S. 2010. Factors affecting natural organic matter (NOM) and scaling fouling in NF membranes: A review. *Desalination,* 259**,** 1-10.

AL-JUBOORI, R. A. & YUSAF, T. 2012. Biofouling in RO system: Mechanisms, monitoring and controlling. *Desalination,* 302**,** 1-23.

AMERICAN PUBLIC HEALTH, A., EATON, A. D., AMERICAN WATER WORKS, A. & WATER ENVIRONMENT, F. 2005. *Standard methods for the examination of water and wastewater,* Washington, D.C., APHA-AWWA-WEF.

ANDRADE, L. H., MENDES, F. D. S., ESPINDOLA, J. C. & AMARAL, M. C. S. 2014. Nanofiltration as tertiary treatment for the reuse of dairy wastewater treated by membrane bioreactor. *Separation and Purification Technology,* 126**,** 21-29.

ASATEKIN, A., OLIVETTI, E. A. & MAYES, A. M. 2009. Fouling resistant, high flux nanofiltration membranes from polyacrylonitrile-graft-poly(ethylene oxide). *Journal of Membrane Science,* 332**,** 6-12.

ASLAM, M., CHARFI, A., LESAGE, G., HERAN, M. & KIM, J. 2017. Membrane bioreactors for wastewater treatment: A review of mechanical cleaning by scouring agents to control membrane fouling. *Chemical Engineering Journal,* 307**,** 897-913.

AYDOĞAN, N., GÜRKAN, T. & YILMAZ, L. 1998. Effect of Operating Parameters on the Separation of Sugars by Nanofiltration. *Separation Science and Technology,* 33**,** 1767-1785.

BACCHIN, P., AIMAR, P. & FIELD, R. W. 2006. Critical and sustainable fluxes: Theory, experiments and applications. *Journal of Membrane Science,* 281**,** 42-69.

BAE, T.-H. & TAK, T.-M. 2005. Interpretation of fouling characteristics of ultrafiltration membranes during the filtration of membrane bioreactor mixed liquor. *Journal of Membrane Science,* 264**,** 151-160.

BARNES, R. J., BANDI, R. R., CHUA, F., LOW, J. H., AUNG, T., BARRAUD, N., FANE, A. G., KJELLEBERG, S. & RICE, S. A. 2014. The roles of Pseudomonas aeruginosa extracellular polysaccharides in biofouling of reverse osmosis membranes and nitric oxide induced dispersal. *Journal of Membrane Science,* 466**,** 161-172.

BARRETO, C. M., GARCIA, H. A., HOOIJMANS, C. M., HERRERA, A. & BRDJANOVIC, D. 2017. Assessing the performance of an MBR operated at high biomass concentrations. *International Biodeterioration & Biodegradation,* 119**,** 528-537.

BARTELS, C. R., WILF, M., ANDES, K. & IONG, J. 2005a. Design considerations for wastewater treatment by reverse osmosis. *Water Science and Technology.*

BARTELS, C. R., WILF, M., ANDES, K. & IONG, J. 2005b. Design considerations for wastewater treatment by reverse osmosis. *Water Sci Technol,* 51**,** 473-82.

BRADFORD, M. M. 1976. A rapid and sensitive method for the quantitation of microgram quantities of protein utilizing the principle of protein-dye binding. *Analytical Biochemistry,* 72**,** 248-254.

BRANT, J. A. & CHILDRESS, A. E. 2002. Assessing short-range membrane–colloid interactions using surface energetics. *Journal of Membrane Science,* 203**,** 257-273.

CAMPOS, J. L., MOSQUERA-CORRAL, A., SÁNCHEZ, M., MÉNDEZ, R. & LEMA, J. M. 2002. Nitrification in saline wastewater with high ammonia concentration in an activated sludge unit. *Water Research,* 36**,** 2555-2560.

CARDMAN, Z., ARNOSTI, C., DURBIN, A., ZIERVOGEL, K., COX, C., STEEN, A. D. & TESKE, A. 2014. Verrucomicrobia Are Candidates for Polysaccharide-Degrading Bacterioplankton in an Arctic Fjord of Svalbard. *Applied and Environmental Microbiology,* 80**,** 3749-3756.

CHEN, F., BI, X. & NG, H. Y. 2016. Effects of bio-carriers on membrane fouling mitigation in moving bed membrane bioreactor. *Journal of Membrane Science,* 499**,** 134-142.

CHEN, W., WESTERHOFF, P., LEENHEER, J. A. & BOOKSH, K. 2003. Fluorescence Excitation−Emission Matrix Regional Integration to Quantify Spectra for Dissolved Organic Matter. *Environmental Science & Technology,* 37**,** 5701-5710.

CHENG, X. Q., SHAO, L. & LAU, C. H. 2015. High flux polyethylene glycol based nanofiltration membranes for water environmental remediation. *Journal of Membrane Science,* 476**,** 95-104.

CHEW, M. Y. C., WATANABE, C. & TOU, Y. 2011. The challenges in Singapore NEWater development: Co-evolutionary development for innovation and industry evolution. *Technology in Society,* 33**,** 200-211.

CHIN, K. J., LIESACK, W. & JANSSEN, P. H. 2001. Opitutus terrae gen. nov., sp. nov., to accommodate novel strains of the division 'Verrucomicrobia' isolated from rice paddy soil. *International Journal of Systematic and Evolutionary Microbiology,* 51**,** 1965-1968.

CHO, B. D. & FANE, A. G. 2002. Fouling transients in nominally sub-critical flux operation of a membrane bioreactor. *Journal of Membrane Science,* 209**,** 391-403.

CHOI, J.-H., DOCKKO, S., FUKUSHI, K. & YAMAMOTO, K. 2002. A novel application of a submerged nanofiltration membrane bioreactor (NF MBR) for wastewater treatment. *Desalination,* 146**,** 413-420.

CHOI, J.-H., FUKUSHI, K., NG, H. Y. & YAMAMOTO, K. 2006. Evaluation of a long-term operation of a submerged nanofiltration membrane bioreactor (NF MBR) for advanced wastewater treatment. *Water Science and Technology,* 53**,** 131-136.

CHOI, J.-H., FUKUSHI, K. & YAMAMOTO, K. 2007a. A submerged nanofiltration membrane bioreactor for domestic wastewater treatment: the performance of

cellulose acetate nanofiltration membranes for long-term operation. *Separation and Purification Technology,* 52**,** 470-477.

CHOI, J.-H., LEE, S. H., FUKUSHI, K. & YAMAMOTO, K. 2007b. Comparison of sludge characteristics and PCR–DGGE based microbial diversity of nanofiltration and microfiltration membrane bioreactors. *Chemosphere,* 67**,** 1543-1550.

CHONG, T. H., WONG, F. S. & FANE, A. G. 2008. Implications of critical flux and cake enhanced osmotic pressure (CEOP) on colloidal fouling in reverse osmosis: Experimental observations. *Journal of Membrane Science,* 314**,** 101-111.

CHOW, L. C. 2001. Solubility of calcium phosphates. *Monogr Oral Sci,* 18**,** 94-111.

COLT, J. 2012. 2 - Solubility of Atmospheric Gases in Brackish and Marine Waters. *In:* COLT, J. (ed.) *Computation of Dissolved Gas Concentration in Water as Functions of Temperature, Salinity and Pressure (Second Edition).* London: Elsevier.

DAHDAL, Y. N., OREN, Y., SCHWAHN, D., PIPICH, V., HERZBERG, M., YING, W., KASHER, R. & RAPAPORT, H. 2016. Biopolymer-induced calcium phosphate scaling in membrane-based water treatment systems: Langmuir model films studies. *Colloids and Surfaces B: Biointerfaces,* 143**,** 233-242.

DAHDAL, Y. N., PIPICH, V., RAPAPORT, H., OREN, Y., KASHER, R. & SCHWAHN, D. 2014. Small-Angle Neutron Scattering Studies of Mineralization on BSA Coated Citrate Capped Gold Nanoparticles Used as a Model Surface for Membrane Scaling in RO Wastewater Desalination. *Langmuir,* 30**,** 15072-15082.

DOMINGUEZ, D. C. 2004. Calcium signalling in bacteria. *Molecular Microbiology,* 54**,** 291-297.

DONNAN, F. G. 1995. Theory of membrane equilibria and membrane potentials in the presence of non-dialysing electrolytes. A contribution to physical-chemical physiology. *Journal of Membrane Science,* 100**,** 45-55.

ELIMELECH, M., XIAOHUA, Z., CHILDRESS, A. E. & SEUNGKWAN, H. 1997. Role of membrane surface morphology in colloidal fouling of cellulose acetate and composite aromatic polyamide reverse osmosis membranes. *Journal of Membrane Science,* 127**,** 101-109.

FANG, W., SHI, L. & WANG, R. 2013. Interfacially polymerized composite nanofiltration hollow fiber membranes for low-pressure water softening. *Journal of Membrane Science,* 430**,** 129-139.

FAUST, L., TEMMINK, H., ZWIJNENBURG, A., KEMPERMAN, A. J. B. & RIJNAARTS, H. H. M. 2014. Effect of dissolved oxygen concentration on the bioflocculation process in high loaded MBRs. *Water Research,* 66**,** 199-207.

FLEMMING, H.-C. 1997. Reverse osmosis membrane biofouling. *Experimental Thermal and Fluid Science,* 14**,** 382-391.

GANDER, M., JEFFERSON, B. & JUDD, S. 2000. Aerobic MBRs for domestic wastewater treatment: a review with cost considerations. *Separation and Purification Technology,* 18**,** 119-130.

GAO, D., FU, Y. & REN, N. 2013. Tracing biofouling to the structure of the microbial community and its metabolic products: A study of the three-stage MBR process. *Water Research,* 47**,** 6680-6690.

GEKAS, V., PERSSON, K. M., WAHLGREN, M. & SIVIK, B. 1992. Contact angles of ultrafiltration membranes and their possible correlation to membrane performance. *Journal of Membrane Science,* 72**,** 293-302.

GOH, S., ZHANG, J., LIU, Y. & FANE, A. G. 2013. Fouling and wetting in membrane distillation (MD) and MD-bioreactor (MDBR) for wastewater reclamation. *Desalination,* 323**,** 39-47.

GOH, S., ZHANG, J., LIU, Y. & FANE, A. G. 2015. Membrane Distillation Bioreactor (MDBR) – A lower Green-House-Gas (GHG) option for industrial wastewater reclamation. *Chemosphere,* 140**,** 129-142.

GOLBABAEI KOOTENAEI, F., RAMEZANI, M., AMINIRAD, H., AHMADI, S., POURSHAMSIAN, K. & FALLAHNEJAD, M. 2014. Comparison in reduction of solids, turbidity and EC between nanofiltration membrane bioreactor and activated sludge. *International Journal of Nano Dimension,* 5**,** 21-26.

GONG, M., NANDA, S., ROMERO, M. J., ZHU, W. & KOZINSKI, J. A. 2017. Subcritical and supercritical water gasification of humic acid as a model compound of humic substances in sewage sludge. *The Journal of Supercritical Fluids,* 119**,** 130-138.

GREENBERG, G., HASSON, D. & SEMIAT, R. 2005. Limits of RO recovery imposed by calcium phosphate precipitation. *Desalination,* 183**,** 273-288.

HAN, S.-S., BAE, T.-H., JANG, G.-G. & TAK, T.-M. 2005. Influence of sludge retention time on membrane fouling and bioactivities in membrane bioreactor system. *Process Biochemistry,* 40**,** 2393-2400.

HORI, K. & MATSUMOTO, S. 2010. Bacterial adhesion: From mechanism to control. *Biochemical Engineering Journal,* 48**,** 424-434.

HORI, K., YAMASHITA, S., ISHII, S., KITAGAWA, M., TANJI, Y. & UNNO, H. 2001. Isolation, characterization and application to off-gas treatment of toluene-degrading bacteria. *Journal of Chemical Engineering of Japan,* 34**,** 1120-1126.

HUANG, X., GUI, P. & QIAN, Y. 2001. Effect of sludge retention time on microbial behaviour in a submerged membrane bioreactor. *Process Biochemistry,* 36**,** 1001-1006.

HUBER, S. A., BALZ, A., ABERT, M. & PRONK, W. 2011. Characterisation of aquatic humic and non-humic matter with size-exclusion chromatography – organic carbon detection – organic nitrogen detection (LC-OCD-OND). *Water Research,* 45**,** 879-885.

HWANG, B. K., LEE, W. N., YEON, K. M., PARK, P. K., LEE, C. H., CHANG, I. S., DREWS, A. & KRAUME, M. 2008. Correlating TMP increases with microbial characteristics in the bio-cake on the membrane surface in a membrane bioreactor. *Environmental Science and Technology,* 42**,** 3963-3968.

JAMAL KHAN, S., ILYAS, S., JAVID, S., VISVANATHAN, C. & JEGATHEESAN, V. 2011. Performance of suspended and attached growth MBR systems in treating high strength synthetic wastewater. *Bioresource Technology,* 102**,** 5331-5336.

JANG, D., HWANG, Y., SHIN, H. & LEE, W. 2013. Effects of salinity on the characteristics of biomass and membrane fouling in membrane bioreactors. *Bioresource Technology,* 141**,** 50-56.

JARUSUTTHIRAK, C., MATTARAJ, S. & JIRARATANANON, R. 2007. Influence of inorganic scalants and natural organic matter on nanofiltration membrane fouling. *Journal of Membrane Science,* 287**,** 138-145.

JERMANN, D., PRONK, W., MEYLAN, S. & BOLLER, M. 2007. Interplay of different NOM fouling mechanisms during ultrafiltration for drinking water production. *Water Research,* 41**,** 1713-1722.

JIN, L., ONG, S. L. & NG, H. Y. 2013. Fouling control mechanism by suspended biofilm carriers addition in submerged ceramic membrane bioreactors. *Journal of Membrane Science,* 427**,** 250-258.

JO, S. J., KWON, H., JEONG, S.-Y., LEE, C.-H. & KIM, T. G. 2016. Comparison of microbial communities of activated sludge and membrane biofilm in 10 full-scale membrane bioreactors. *Water Research,* 101**,** 214-225.

JUDD, S. & JUDD, C. (eds.) 2006. *The MBR book : principles and applications of membrane bioreactors in water and wastewater treatment,* Amsterdam ; Boston ; London: Elsevier.

KAPPEL, C., KEMPERMAN, A. J. B., TEMMINK, H., ZWIJNENBURG, A., RIJNAARTS, H. H. M. & NIJMEIJER, K. 2014. Impacts of NF concentrate recirculation on membrane performance in an integrated MBR and NF membrane process for wastewater treatment. *Journal of Membrane Science,* 453**,** 359-368.

KATSIKOGIANNI, M. & MISSIRLIS, Y. F. 2004. Concise review of mechanisms of bacterial adhesion to biomaterials and of techniques used in estimating bacteria-material interactions. *European Cells and Materials,* 8**,** 37-57.

KENT, F. C., FARAHBAKHSH, K., MAHENDRAN, B., JAKLEWICZ, M., LISS, S. N. & ZHOU, H. 2011. Water reclamation using reverse osmosis: Analysis of fouling propagation given tertiary membrane filtration and MBR pretreatments. *Journal of Membrane Science,* 382**,** 328-338.

KHANZADA, N. K., KHAN, S. J. & DAVIES, P. A. 2017. Performance evaluation of reverse osmosis (RO) pre-treatment technologies for in-land brackish water treatment. *Desalination,* 406**,** 44-50.

KIMURA, K., OKAZAKI, S., OHASHI, T. & WATANABE, Y. 2016a. Importance of the co-presence of silica and organic matter in membrane fouling for RO filtering MBR effluent. *J. Membrane Sci.,* 501**,** 60-67.

KIMURA, K., OKAZAKI, S., OHASHI, T. & WATANABE, Y. 2016b. Importance of the co-presence of silica and organic matter in membrane fouling for RO filtering MBR effluent. *Journal of Membrane Science,* 501**,** 60-67.

KIMURA, K., OKAZAKI, S., OHASHI, T. & WATANABE, Y. 2016c. Importance of the co-presence of silica and organic matter in membrane fouling for RO filtering MBR effluent. *Journal of Membrane Science,* 501**,** 60-67.

KOYUNCU, I., TOPACIK, D. & WIESNER, M. R. 2004. Factors influencing flux decline during nanofiltration of solutions containing dyes and salts. *Water Research,* 38**,** 432-440.

KRZEMINSKI, P., LEVERETTE, L., MALAMIS, S. & KATSOU, E. 2016. Membrane bioreactors – a review on recent developments in energy reduction, fouling control, novel configurations, LCA and market prospects. *Journal of Membrane Science*.

LATEEF, S. K., SOH, B. Z. & KIMURA, K. 2013. Direct membrane filtration of municipal wastewater with chemically enhanced backwash for recovery of organic matter. *Bioresource Technology,* 150**,** 149-155.

LAY, W. C. L., LIU, Y. & FANE, A. G. 2010. Impacts of salinity on the performance of high retention membrane bioreactors for water reclamation: A review. *Water Research,* 44**,** 21-40.

LEE, S., CHO, J. & ELIMELECH, M. 2005. Combined influence of natural organic matter (NOM) and colloidal particles on nanofiltration membrane fouling. *Journal of Membrane Science,* 262**,** 27-41.

LEE, S., KIM, J. & LEE, C.-H. 1999. Analysis of CaSO4 scale formation mechanism in various nanofiltration modules. *Journal of Membrane Science,* 163**,** 63-74.

LEE, S., SUWARNO, S. R., QUEK, B. W. H., KIM, L., WU, B. & CHONG, T. H. 2019. A comparison of gravity-driven membrane (GDM) reactor and biofiltration plus GDM reactor for seawater reverse osmosis desalination pretreatment. *Water Research,* 154**,** 72-83.

LI, X., LIU, C., YIN, W., CHONG, T. H. & WANG, R. 2019. Design and development of layer-by-layer based low-pressure antifouling nanofiltration membrane used for water reclamation. *Journal of Membrane Science,* 584**,** 309-323.

LI, X., SHANG, X., LUO, T., DU, X., WANG, Y., XIE, Q., MATSUURA, N., CHEN, J. & KADOKAMI, K. 2016. Screening and health risk of organic micropollutants in rural groundwater of Liaodong Peninsula, China. *Environmental Pollution,* 218**,** 739-748.

LI, X., ZHANG, H., HOU, Y., GAO, Y., LI, J., GUO, W. & NGO, H. H. 2015. In situ investigation of combined organic and colloidal fouling for nanofiltration membrane using ultrasonic time domain reflectometry. *Desalination,* 362**,** 43-51.

LIM, B.-R., AHN, K.-H., SONG, K.-G. & CHO, J. 2005. Microbial community in biofilm on membrane surface of submerged MBR: effect of in-line cleaning chemical agent. *Water Science and Technology,* 51**,** 201-207.

LIN, H., PENG, W., ZHANG, M., CHEN, J., HONG, H. & ZHANG, Y. 2013. A review on anaerobic membrane bioreactors: Applications, membrane fouling and future perspectives. *Desalination,* 314**,** 169-188.

LIN, Y.-L., CHIOU, J.-H. & LEE, C.-H. 2014. Effect of silica fouling on the removal of pharmaceuticals and personal care products by nanofiltration and reverse osmosis membranes. *Journal of Hazardous Materials,* 277**,** 102-109.

LIU, C., SHI, L. & WANG, R. 2015. Crosslinked layer-by-layer polyelectrolyte nanofiltration hollow fiber membrane for low-pressure water softening with the presence of SO42− in feed water. *Journal of Membrane Science,* 486**,** 169-176.

LIU, H. & FANG, H. H. P. 2002. Extraction of extracellular polymeric substances (EPS) of sludges. *Journal of Biotechnology,* 95**,** 249-256.

LUJÁN-FACUNDO, M. J., FERNÁNDEZ-NAVARRO, J., ALONSO-MOLINA, J. L., AMORÓS-MUÑOZ, I., MORENO, Y., MENDOZA-ROCA, J. A. & PASTOR-ALCAÑIZ, L. 2018. The role of salinity on the changes of the biomass characteristics and on the performance of an OMBR treating tannery wastewater. *Water Research,* 142**,** 129-137.

LUO, W., HAI, F. I., PRICE, W. E., GUO, W., NGO, H. H., YAMAMOTO, K. & NGHIEM, L. D. 2014. High retention membrane bioreactors: Challenges and opportunities. *Bioresource Technology,* 167**,** 539-546.

LUO, W., PHAN, H. V., XIE, M., HAI, F. I., PRICE, W. E., ELIMELECH, M. & NGHIEM, L. D. 2017. Osmotic versus conventional membrane bioreactors integrated with reverse osmosis for water reuse: Biological stability, membrane fouling, and contaminant removal. *Water Research,* 109**,** 122-134.

LUO, W., XIE, M., HAI, F. I., PRICE, W. E. & NGHIEM, L. D. 2016. Biodegradation of cellulose triacetate and polyamide forward osmosis membranes in an activated sludge bioreactor: Observations and implications. *Journal of Membrane Science,* 510**,** 284-292.

MAERE, T., VERRECHT, B., MOERENHOUT, S., JUDD, S. & NOPENS, I. 2011. BSM-MBR: A benchmark simulation model to compare control and operational strategies for membrane bioreactors. *Water Res.,* 45**,** 2181-2190.

MAHLANGU, T. O., THWALA, J. M., MAMBA, B. B., D'HAESE, A. & VERLIEFDE, A. R. D. 2015. Factors governing combined fouling by organic and colloidal foulants in cross-flow nanofiltration. *Journal of Membrane Science,* 491**,** 53-62.

MASSÉ, A., SPÉRANDIO, M. & CABASSUD, C. 2006. Comparison of sludge characteristics and performance of a submerged membrane bioreactor and an activated sludge process at high solids retention time. *Water Research,* 40**,** 2405-2415.

MENG, F., CHAE, S.-R., DREWS, A., KRAUME, M., SHIN, H.-S. & YANG, F. 2009. Recent advances in membrane bioreactors (MBRs): Membrane fouling and membrane material. *Water Research,* 43**,** 1489-1512.

MENG, F., ZHOU, Z., NI, B.-J., ZHENG, X., HUANG, G., JIA, X., LI, S., XIONG, Y. & KRAUME, M. 2011. Characterization of the size-fractionated biomacromolecules: Tracking their role and fate in a membrane bioreactor. *Water Research,* 45**,** 4661-4671.

MENG, S., RZECHOWICZ, M., WINTERS, H., FANE, A. G. & LIU, Y. 2013. Transparent exopolymer particles (TEP) and their potential effect on membrane biofouling. *Applied Microbiology and Biotechnology,* 97**,** 5705-5710.

METCALF, AMP & EDDY, I. 2003. *Wastewater engineering : treatment and reuse*, Fourth edition / revised by George Tchobanoglous, Franklin L. Burton, H. David Stensel. Boston : McGraw-Hill, [2003] ©2003.

MOHAMMAD, A. W., TEOW, Y. H., ANG, W. L., CHUNG, Y. T., OATLEY-RADCLIFFE, D. L. & HILAL, N. 2015. Nanofiltration membranes review: Recent advances and future prospects. *Desalination,* 356**,** 226-254.

MOUSSA, M. S., SUMANASEKERA, D. U., IBRAHIM, S. H., LUBBERDING, H. J., HOOIJMANS, C. M., GIJZEN, H. J. & VAN LOOSDRECHT, M. C. M. 2006. Long term effects of salt on activity, population structure and floc characteristics in enriched bacterial cultures of nitrifiers. *Water Research,* 40**,** 1377-1388.

MUSTAFA, G., WYNS, K., BUEKENHOUDT, A. & MEYNEN, V. 2016. New insights into the fouling mechanism of dissolved organic matter applying nanofiltration membranes with a variety of surface chemistries. *Water Research,* 93**,** 195-204.

NAWAZ, M. S., GADELHA, G., KHAN, S. J. & HANKINS, N. 2013. Microbial toxicity effects of reverse transported draw solute in the forward osmosis membrane bioreactor (FO-MBR). *Journal of Membrane Science,* 429**,** 323-329.

NG, H. Y., ONG, S. L. & NG, W. J. 2005. Effects of sodium chloride on the performance of a sequencing batch reactor. *Journal of Environmental Engineering (ASCE)* 131.

NG, H. Y., TAN, T. W. & ONG, S. L. 2006. Membrane Fouling of Submerged Membrane Bioreactors: Impact of Mean Cell Residence Time and the Contributing Factors. *Environmental Science & Technology,* 40**,** 2706-2713.

PALMARIN, M. J. & YOUNG, S. 2019. The effects of biocarriers on the mixed liquor characteristics, extracellular polymeric substances, and fouling rates of a hybrid membrane bioreactor. *Biochemical Engineering Journal,* 141**,** 278-284.

PEARCE, G. 2008. Introduction to membranes–MBRs: Manufacturers' comparison: part 1. *Filtration & Separation,* 45**,** 28-31.

PHAN, H. V., MCDONALD, J. A., HAI, F. I., PRICE, W. E., KHAN, S. J., FUJIOKA, T. & NGHIEM, L. D. 2016. Biological performance and trace organic contaminant removal by a side-stream ceramic nanofiltration membrane bioreactor. *International Biodeterioration & Biodegradation,* 113**,** 49-56.

PHATTARANAWIK, J., FANE, A. G., PASQUIER, A. C. S. & BING, W. 2008a. A novel membrane bioreactor based on membrane distillation. *Desalination,* 223**,** 386-395.

PHATTARANAWIK, J., FANE, A. G., PASQUIER, A. C. S. & BING, W. 2008b. A novel membrane bioreactor based on membrane distillation. *Desalination,* 223**,** 386-395.

PIPICH, V., DAHDAL, Y., RAPAPORT, H., KASHER, R., OREN, Y. & SCHWAHN, D. 2013. Effects of Biological Molecules on Calcium Mineral Formation Associated with Wastewater Desalination as Assessed using Small-Angle Neutron Scattering. *Langmuir,* 29**,** 7607-7617.

POLLICE, A., LAERA, G. & BLONDA, M. 2004. Biomass growth and activity in a membrane bioreactor with complete sludge retention. *Water Research,* 38**,** 1799-1808.

PUZNAVA, N., PAYRAUDEAU, M. & THORNBERG, D. 2001. Simultaneous nitrification and denitrification in biofilters with real time aeration control. *Water Sci Technol,* 43**,** 269-76.

QIN, J.-J., KEKRE, K. A., TAO, G., OO, M. H., WAI, M. N., LEE, T. C., VISWANATH, B. & SEAH, H. 2006. New option of MBR-RO process for production of NEWater from domestic sewage. *Journal of Membrane Science,* 272**,** 70-77.

QIN, J. J., WAI, M. N., TAO, G., KEKRE, K. A. & SEAH, H. 2007. Membrane bioreactor study for reclamation of mixed sewage mostly from industrial sources. *Sep. Purif. Technol.,* 53**,** 296-300.

QIU, G., LAW, Y. M., DAS, S. & TING, Y. P. 2015. Direct and complete phosphorus recovery from municipal wastewater using a hybrid microfiltration-forward osmosis membrane bioreactor process with seawater brine as draw solution. *Environmental Science and Technology,* 49**,** 6156-6163.

QIU, G. & TING, Y.-P. 2013. Osmotic membrane bioreactor for wastewater treatment and the effect of salt accumulation on system performance and microbial community dynamics. *Bioresource Technology,* 150**,** 287-297.

QIU, G. & TING, Y.-P. 2014. Short-term fouling propensity and flux behavior in an osmotic membrane bioreactor for wastewater treatment. *Desalination,* 332**,** 91-99.

QIU, G., ZHANG, S., SRINIVASA RAGHAVAN, D. S., DAS, S. & TING, Y.-P. 2016. The potential of hybrid forward osmosis membrane bioreactor (FOMBR) processes in achieving high throughput treatment of municipal wastewater with enhanced phosphorus recovery. *Water Research,* 105**,** 370-382.

RADJENOVIĆ, J., PETROVIĆ, M. & BARCELÓ, D. 2009. Fate and distribution of pharmaceuticals in wastewater and sewage sludge of the conventional activated sludge (CAS) and advanced membrane bioreactor (MBR) treatment. *Water Research,* 43**,** 831-841.

RAJABZADEH, S., LIU, C., SHI, L. & WANG, R. 2014. Preparation of low-pressure water softening hollow fiber membranes by polyelectrolyte deposition with two bilayers. *Desalination,* 344**,** 64-70.

RATHINAM, K., OREN, Y., PETRY, W., SCHWAHN, D. & KASHER, R. 2018. Calcium phosphate scaling during wastewater desalination on oligoamide surfaces mimicking reverse osmosis and nanofiltration membranes. *Water Research,* 128**,** 217-225.

RAUTENBACH, R. & MELLIS, R. 1994. Waste water treatment by a combination of bioreactor and nanofiltration. *Desalination,* 95**,** 171-188.

REID, E., LIU, X. & JUDD, S. J. 2006. Effect of high salinity on activated sludge characteristics and membrane permeability in an immersed membrane bioreactor. *Journal of Membrane Science,* 283**,** 164-171.

RICE, G., BARBER, A. R., O'CONNOR, A. J., PIHLAJAMAKI, A., NYSTROM, M., STEVENS, G. W. & KENTISH, S. E. 2011. The influence of dairy salts on nanofiltration membrane charge. *Journal of Food Engineering,* 107**,** 164-172.

RIDGWAY, H. F., RIGBY, M. G. & ARGO, D. G. 1985. Bacterial adhesion and fouling of reverse osmosis membranes. *Journal / American Water Works Association,* 77**,** 97-106.

RITTMANN, B. & MCCARTY, L. P. 2003. *Environmental Biotechnology: Principles and Applications*.

ROSENBERGER, S., LAABS, C., LESJEAN, B., GNIRSS, R., AMY, G., JEKEL, M. & SCHROTTER, J. C. 2006. Impact of colloidal and soluble organic material on membrane performance in membrane bioreactors for municipal wastewater treatment. *Water Research,* 40**,** 710-720.

SADR GHAYENI, S. B., BEATSON, P. J., SCHNEIDER, R. P. & FANE, A. G. 1998. Adhesion of waste water bacteria to reverse osmosis membranes. *Journal of Membrane Science,* 138**,** 29-42.

SCHLÖGL, R. 1966. Membrane permeation in systems far from equilibrium. *Berichte der Bunsengesellschaft für physikalische Chemie,* 70**,** 400-414.

SCHOFIELD, R. W., FANE, A. G. & FELL, C. J. D. 1987. Heat and mass transfer in membrane distillation. *Journal of Membrane Science,* 33**,** 299-313.

SHAFFER, D. L., WERBER, J. R., JARAMILLO, H., LIN, S. & ELIMELECH, M. 2015. Forward osmosis: Where are we now? *Desalination,* 356**,** 271-284.

SHIMIZU, Y., SHIMODERA, K.-I. & WATANABE, A. 1993. Cross-flow microfiltration of bacterial cells. *Journal of Fermentation and Bioengineering,* 76**,** 493-500.

SIEW, W. E., LIVINGSTON, A. G., ATES, C. & MERSCHAERT, A. 2013. Molecular separation with an organic solvent nanofiltration cascade – augmenting membrane selectivity with process engineering. *Chemical Engineering Science,* 90**,** 299-310.

SIM, L. N., YE, Y., CHEN, V. & FANE, A. G. 2011. Investigations of the coupled effect of cake-enhanced osmotic pressure and colloidal fouling in RO using crossflow sampler-modified fouling index ultrafiltration. *Desalination,* 273**,** 184-196.

SOBECK, D. C. & HIGGINS, M. J. 2002. Examination of three theories for mechanisms of cation-induced bioflocculation. *Water Research,* 36**,** 527-538.

SONG, B. & LEFF, L. G. 2006. Influence of magnesium ions on biofilm formation by Pseudomonas fluorescens. *Microbiological Research,* 161**,** 355-361.

SRISURICHAN, S., JIRARATANANON, R. & FANE, A. G. 2006. Mass transfer mechanisms and transport resistances in direct contact membrane distillation process. *Journal of Membrane Science,* 277**,** 186-194.

STEINER, Z., RAPAPORT, H., OREN, Y. & KASHER, R. 2010. Effect of Surface-Exposed Chemical Groups on Calcium-Phosphate Mineralization in Water-Treatment Systems. *Environmental Science & Technology,* 44**,** 7937-7943.

SUBRAMANIAN, S. & SEERAM, R. 2013. New directions in nanofiltration applications — Are nanofibers the right materials as membranes in desalination? *Desalination,* 308**,** 198-208.

SUWARNO, S. R., HANADA, S., CHONG, T. H., GOTO, S., HENMI, M. & FANE, A. G. 2016. The effect of different surface conditioning layers on bacterial adhesion on reverse osmosis membranes. *Desalination,* 387**,** 1-13.

SZÉKELY, G., BANDARRA, J., HEGGIE, W., SELLERGREN, B. & FERREIRA, F. C. 2011. Organic solvent nanofiltration: A platform for removal of genotoxins from active pharmaceutical ingredients. *Journal of Membrane Science,* 381**,** 21-33.

TADKAEW, N., HAI, F. I., MCDONALD, J. A., KHAN, S. J. & NGHIEM, L. D. 2011. Removal of trace organics by MBR treatment: The role of molecular properties. *Water Research,* 45**,** 2439-2451.

TAKIMOTO, Y., HATAMOTO, M., ISHIDA, T., WATARI, T. & YAMAGUCHI, T. 2018. Fouling Development in A/O-MBR under Low Organic Loading Condition and Identification of Key Bacteria for Biofilm Formations. *Scientific Reports,* 8**,** 11427.

TAM, L. S., TANG, T. W., LAU, G. N., SHARMA, K. R. & CHEN, G. H. 2007. A pilot study for wastewater reclamation and reuse with MBR/RO and MF/RO systems. *Desalination,* 202**,** 106-113.

TANG, C. Y., CHONG, T. H. & FANE, A. G. 2011. Colloidal interactions and fouling of NF and RO membranes: A review. *Advances in Colloid and Interface Science,* 164**,** 126-143.

TAO, G., KEKRE, K., OO, M. H., VISWANATH, B., YUSOF, A. M. & SEAH, H. 2010. Energy Reduction and Optimisation in Membrane Bioreactor Systems. *Water Practice and Technology,* 5.

TAY, M. F., LIU, C., CORNELISSEN, E. R., WU, B. & CHONG, T. H. 2018. The feasibility of nanofiltration membrane bioreactor (NF-MBR)+reverse osmosis (RO) process for water reclamation: Comparison with ultrafiltration membrane bioreactor (UF-MBR)+RO process. *Water Research,* 129**,** 180-189.

TEYCHENE, B., GUIGUI, C. & CABASSUD, C. 2011. Engineering of an MBR supernatant fouling layer by fine particles addition: A possible way to control cake compressibility. *Water Research,* 45**,** 2060-2072.

THENG, B. K. G. 2012a. Chapter 12 - Humic Substances. *In:* THENG, B. K. G. (ed.) *Developments in Clay Science.* Elsevier.

THENG, B. K. G. 2012b. Chapter 12 - Humic Substances. *In:* THENG, B. K. G. (ed.) *Developments in Clay Science.* Elsevier.

TRIPATHI, C. S. & GRANT ALLEN, D. 1999. Comparison of mesophilic and thermophilic aerobic biological treatment in sequencing batch reactors treating bleached kraft pulp mill effluent. *Water Research,* 33**,** 836-846.

TSUNEDA, S., AIKAWA, H., HAYASHI, H., YUASA, A. & HIRATA, A. 2003. Extracellular polymeric substances responsible for bacterial adhesion onto solid surface. *FEMS microbiology letters,* 223**,** 287-292.

VAN DE LISDONK, C. A. C., RIETMAN, B. M., HEIJMAN, S. G. J., STERK, G. R. & SCHIPPERS, J. C. 2001. Prediction of supersaturation and monitoring of scaling in reverse osmosis and nanofiltration membrane systems. *Desalination,* 138**,** 259-270.

VAN DE LISDONK, C. A. C., VAN PAASSEN, J. A. M. & SCHIPPERS, J. C. 2000. Monitoring scaling in nanofiltration and reverse osmosis membrane systems. *Desalination,* 132**,** 101-108.

VAN DEN BROECK, R., VAN DIERDONCK, J., NIJSKENS, P., DOTREMONT, C., KRZEMINSKI, P., VAN DER GRAAF, J. H. J. M., VAN LIER, J. B., VAN IMPE, J. F. M. & SMETS, I. Y. 2012. The influence of solids retention time on activated sludge bioflocculation and membrane fouling in a membrane bioreactor (MBR). *Journal of Membrane Science,* 401-402**,** 48-55.

VAN OSS, C. J. 1993. Acid—base interfacial interactions in aqueous media. *Colloids and Surfaces A: Physicochemical and Engineering Aspects,* 78**,** 1-49.

VOGEL, D., SIMON, A., ALTURKI, A. A., BILITEWSKI, B., PRICE, W. E. & NGHIEM, L. D. 2010. Effects of fouling and scaling on the retention of trace organic contaminants by a nanofiltration membrane: The role of cake-enhanced concentration polarisation. *Separation and Purification Technology,* 73**,** 256-263.

WANG, B., WANG, W., HAN, H., HU, H. & ZHUANG, H. 2012. Nitrogen removal and simultaneous nitrification and denitrification in a fluidized bed step-feed process. *Journal of Environmental Sciences,* 24**,** 303-308.

WANG, G. H., FAN, Z., WU, D. X., QIN, L., ZHANG, G. L., GAO, C. J. & MENG, Q. 2014a. Anoxic/aerobic granular active carbon assisted MBR integrated with

nanofiltration and reverse osmosis for advanced treatment of municipal landfill leachate. *Desalination,* 349**,** 136-144.

WANG, S., GUILLEN, G. & HOEK, E. M. V. 2005. Direct observation of microbial adhesion to membranes. *Environmental Science and Technology,* 39**,** 6461-6469.

WANG, X., CHANG, V. W. C. & TANG, C. Y. 2016. Osmotic membrane bioreactor (OMBR) technology for wastewater treatment and reclamation: Advances, challenges, and prospects for the future. *Journal of Membrane Science,* 504**,** 113-132.

WANG, X., CHEN, Y., YUAN, B., LI, X. & REN, Y. 2014b. Impacts of sludge retention time on sludge characteristics and membrane fouling in a submerged osmotic membrane bioreactor. *Bioresource Technology,* 161**,** 340-347.

WETTERAU, G., LIU, P., CHALMERS, B., RICHARDSON, T. & VANMETER, H. B. 2011. Optimizing RO Design Criteria for Indirect Potable Reuse. *IDA Journal of Desalination and Water Reuse,* 3**,** 40-45.

WIBISONO, Y., CORNELISSEN, E. R., KEMPERMAN, A. J. B., VAN DER MEER, W. G. J. & NIJMEIJER, K. 2014. Two-phase flow in membrane processes: A technology with a future. *Journal of Membrane Science,* 453**,** 566-602.

WIJEKOON, K. C., HAI, F. I., KANG, J., PRICE, W. E., GUO, W., NGO, H. H., CATH, T. Y. & NGHIEM, L. D. 2014. A novel membrane distillation–thermophilic bioreactor system: Biological stability and trace organic compound removal. *Bioresource Technology,* 159**,** 334-341.

WIJEKOON, K. C., HAI, F. I., KANG, J., PRICE, W. E., GUO, W., NGO, H. H. & NGHIEM, L. D. 2013. The fate of pharmaceuticals, steroid hormones, phytoestrogens, UV-filters and pesticides during MBR treatment. *Bioresource Technology,* 144**,** 247-254.

WILF, M. & ALT, S. 2000. Application of low fouling RO membrane elements for reclamation of municipal wastewater. *Desalination,* 132**,** 11-19.

WOO, Y. C., LEE, J. J., SHIM, W.-G., SHON, H. K., TIJING, L. D., YAO, M. & KIM, H.-S. 2016. Effect of powdered activated carbon on integrated submerged membrane bioreactor–nanofiltration process for wastewater reclamation. *Bioresource Technology,* 210**,** 18-25.

WU, B., KITADE, T., CHONG, T. H., UEMURA, T. & FANE, A. G. 2012. Role of initially formed cake layers on limiting membrane fouling in membrane bioreactors. *Bioresource Technology,* 118**,** 589-593.

WU, B., KITADE, T., CHONG, T. H., UEMURA, T. & FANE, A. G. 2013. Impact of membrane bioreactor operating conditions on fouling behavior of reverse osmosis membranes in MBR–RO processes. *Desalination,* 311**,** 37-45.

WU, B., SUWARNO, S. R., TAN, H. S., KIM, L. H., HOCHSTRASSER, F., CHONG, T. H., BURKHARDT, M., PRONK, W. & FANE, A. G. 2017. Gravity-driven microfiltration pretreatment for reverse osmosis (RO) seawater desalination: Microbial community characterization and RO performance. *Desalination,* 418**,** 1-8.

WU, B., YI, S. & FANE, A. G. 2011. Microbial behaviors involved in cake fouling in membrane bioreactors under different solids retention times. *Bioresource Technology,* 102**,** 2511-2516.

WU, G., GUAN, Y. & ZHAN, X. 2008. Effect of salinity on the activity, settling and microbial community of activated sludge in sequencing batch reactors treating synthetic saline wastewater. *Water Science and Technology,* 58**,** 351-358.

XIA, S., JIA, R., FENG, F., XIE, K., LI, H., JING, D. & XU, X. 2012. Effect of solids retention time on antibiotics removal performance and microbial communities in an A/O-MBR process. *Bioresource Technology,* 106**,** 36-43.

XIA, S., LI, J., HE, S., XIE, K., WANG, X., ZHANG, Y., DUAN, L. & ZHANG, Z. 2010. The effect of organic loading on bacterial community composition of membrane biofilms in a submerged polyvinyl chloride membrane bioreactor. *Bioresource Technology,* 101**,** 6601-6609.

XIN, Y., BLIGH, M. W., KINSELA, A. S. & WAITE, T. D. 2016. Effect of iron on membrane fouling by alginate in the absence and presence of calcium. *Journal of Membrane Science,* 497**,** 289-299.

XU, P., BELLONA, C. & DREWES, J. E. 2010. Fouling of nanofiltration and reverse osmosis membranes during municipal wastewater reclamation: Membrane autopsy results from pilot-scale investigations. *Journal of Membrane Science,* 353**,** 111-121.

YAMAMOTO, K. 2001. Membrane bioreactor: An advanced wastewater treatment/reclamation technology and its function in excess-sludge minimization A2 - Matsuo, Tomonori. *In:* HANAKI, K., TAKIZAWA, S. & SATOH, H. (eds.) *Advances in Water and Wastewater Treatment Technology.* Amsterdam: Elsevier Science B.V.

YAMAMOTO, K., HIASA, M., MAHMOOD, T. & MATSUO, T. 1989. Direct solid-liquid separation using hollow fiber membrane in an activated sludge aeration tank. *Water Science and Technology,* 21**,** 43-54.

YANG, S., YANG, F., FU, Z. & LEI, R. 2009. Comparison between a moving bed membrane bioreactor and a conventional membrane bioreactor on organic carbon and nitrogen removal. *Bioresource Technology,* 100**,** 2369-2374.

YE, C., YANG, X., ZHAO, F.-J. & REN, L. 2016. The shift of the microbial community in activated sludge with calcium treatment and its implication to sludge settleability. *Bioresource Technology,* 207**,** 11-18.

YU, X.-C. & MARGOLIN, W. 1997. Ca2+-mediated GTP-dependent dynamic assembly of bacterial cell division protein FtsZ into asters and polymer networks in vitro. *The EMBO Journal,* 16**,** 5455-5463.

ZAVISKA, F., DROGUI, P., GRASMICK, A., AZAIS, A. & HÉRAN, M. 2013. Nanofiltration membrane bioreactor for removing pharmaceutical compounds. *Journal of Membrane Science,* 429**,** 121-129.

ZHANG, D., TRZCINSKI, A. P., KUNACHEVA, C., STUCKEY, D. C., LIU, Y., TAN, S. K. & NG, W. J. 2016. Characterization of soluble microbial products (SMPs) in a membrane bioreactor (MBR) treating synthetic wastewater containing pharmaceutical compounds. *Water Research,* 102**,** 594-606.

ZHANG, J., CHUA, H. C., ZHOU, J. & FANE, A. G. 2006. Factors affecting the membrane performance in submerged membrane bioreactors. *Journal of Membrane Science,* 284**,** 54-66.

ZHANG, J., ZHOU, J., LIU, Y. & FANE, A. G. 2010. A comparison of membrane fouling under constant and variable organic loadings in submerge membrane bioreactors. *Water Research,* 44**,** 5407-5413.

ZHAO, Y., SONG, L. & ONG, S. L. 2010. Fouling behavior and foulant characteristics of reverse osmosis membranes for treated secondary effluent reclamation. *Journal of Membrane Science,* 349**,** 65-74.

ZHU, A., CHRISTOFIDES, P. D. & COHEN, Y. 2009. On RO membrane and energy costs and associated incentives for future enhancements of membrane permeability. *Journal of Membrane Science,* 344**,** 1-5.

ZITA, A. & HERMANSSON, M. 1997. Determination of bacterial cell surface hydrophobicity of single cells in cultures and in wastewater in situ. *FEMS Microbiology Letters,* 152**,** 299-306.